

**Better spatial characterisation of evapotranspiration
and rainfall recharge estimates to groundwater using
remote sensing multispectral techniques at lysimeter
sites**

F Mourot
N Macdonald

R Westerhoff
S Cameron

**GNS Science Report 2019/17
August 2019**



DISCLAIMER

The Institute of Geological and Nuclear Sciences Limited (GNS Science) and its funders give no warranties of any kind concerning the accuracy, completeness, timeliness or fitness for purpose of the contents of this report. GNS Science accepts no responsibility for any actions taken based on, or reliance placed on the contents of this report and GNS Science and its funders exclude to the full extent permitted by law liability for any loss, damage or expense, direct or indirect, and however caused, whether through negligence or otherwise, resulting from any person's or organisation's use of, or reliance on, the contents of this report.

BIBLIOGRAPHIC REFERENCE

Mourot F, Westerhoff R, Macdonald N, Cameron S. 2019. Better spatial characterisation of evapotranspiration and rainfall recharge estimates to groundwater using remote sensing multispectral techniques at lysimeter sites. Lower Hutt (NZ): GNS Science. 82 p. (GNS Science report; 2019/17). doi:10.21420/Z3NQ-CE33.

CONTENTS

ABSTRACT	VI
KEYWORDS	VI
1.0 INTRODUCTION	1
2.0 RATIONALE AND UNDERPINNING THEORY	3
2.1 Evapotranspiration and Relations with Remotely-Sensed Vegetation Parameters	3
2.2 Evapotranspiration as Component of Rainfall Recharge	4
2.2.1 Rainfall Recharge Definition	4
2.2.2 Relation between Rainfall, Evapotranspiration and Rainfall Recharge	5
2.2.3 Uncertainty of Rainfall Recharge	5
3.0 SETTING OF THE STUDY	7
3.1 Location of the Study Sites	7
3.2 Climate and Surface Water	8
3.2.1 Climate	8
3.2.2 Surface Water	9
3.3 Geology and Hydrogeology	9
3.3.1 Substation Site	9
3.3.2 Collins Lane Site	11
3.4 Soils and Land Use	12
3.5 Site Monitoring Systems	15
3.6 Previous Rainfall Recharge Assessments and Allocations	17
3.6.1 Heretaunga Plains Aquifer	17
3.6.1 Kaituna-Pongakawa-Waitahanui Water Management Area	17
4.0 METHOD	18
4.1 Rainfall Recharge Lysimeter Data Analysis	18
4.2 Groundwater Elevation Data Analysis	18
4.3 Satellite Data and UAV Imagery Acquisition and Processing	18
4.3.1 UAV Material and Methodology	18
4.3.2 Satellite and UAV Input Data	19
4.3.3 Data Processing	19
4.4 Estimation of Recharge	21
5.0 RESULTS	22
5.1 Rainfall Recharge Lysimeter Data	22
5.1.1 Substation Site	22
5.1.2 Collins Lane Site	24
5.2 Groundwater Elevation Data	27
5.2.1 Substation Site	27
5.2.2 Collins Lane Site	29
5.3 Satellite Data and UAV Imagery Processing	29

5.3.1	Substation Site	29
5.3.2	Collins Lane Site.....	31
5.4	Estimated Recharge	34
6.0	DISCUSSION.....	36
6.1	Rainfall Recharge Lysimeter Data	36
6.1.1	Substation Site	36
6.1.2	Collins Lane Site.....	36
6.1.3	Inter-Site Comparison	36
6.2	Groundwater Elevation Data.....	37
6.2.1	Substation Site	37
6.2.2	Collins Lane Site.....	37
6.3	Satellite Data and UAV Imagery	38
6.3.1	Comparison of UAV and Satellite-Derived RET Values.....	38
6.3.2	RET Values Derived from UAV Data and Features Characterisation.....	39
6.3.3	RET Values Derived from UAV Data and Soil characterisation.....	41
6.4	Estimated Recharge	43
6.5	Comparison of Lysimeter and UAV Derived Recharge Estimates	43
6.6	Spatial Representativeness of Lysimeters in Context of Satellite and UAV Data and Further Research	44
6.7	Recommendations.....	45
7.0	CONCLUSION.....	47
8.0	ACKNOWLEDGEMENTS.....	48
9.0	REFERENCES	48

FIGURES

Figure 2.1	The relation between surface resistance and relative transpiration (=AET/PET) for two different landcover types	4
Figure 2.2	Model components for three random locations in New Zealand over a 15-year simulation period	5
Figure 3.1	Location of the Hawke’s Bay Substation study site.	7
Figure 3.2	Location of the Bay of Plenty Collins Lane study site.....	8
Figure 3.3	Main geological units and faults of Substation study site (Heron 2014).	10
Figure 3.4	NW SE geological cross-section through Omahu near Substation study site.....	10
Figure 3.5	Main geological units and faults of Collins Lane study area (Heron, 2014).	11
Figure 3.6	Cross-section retrieved from EBOF.....	12
Figure 3.7	Soil classification, medium profile available water value of 90 mm for the soils of the Substation site.....	13
Figure 3.8	Soil classification and medium profile available water values of the Collins Lane site.	13
Figure 3.9	Vineyards at Substation site, southern area (22/05/2019).....	14
Figure 3.10	Grazed grass land at Collins Lane site (09/04/2019).....	15
Figure 4.1	Schematic of the project workflow	20

Figure 5.1	Cumulative rainfall recharge measured at three lysimeters, Substation lysimeter site (Sept. 2012–May 2019).	22
Figure 5.2	Rainfall and rainfall recharge at Substation lysimeter site (1/04/2019–31/05/2019).	24
Figure 5.3	Cumulative rainfall recharge measured at three lysimeters, Collins Lane lysimeter site (June 2015–May 2019).	25
Figure 5.4	Rainfall and soil moisture at 10 cm depth, Collins Lane lysimeter site (1/04/2019–31/05/2019).	27
Figure 5.5	Daily average groundwater elevation in relation to rainfall and rainfall recharge data for Substation site (1/04/2019–31/05/2019).	28
Figure 5.6	Daily average groundwater elevation and river stage in relation to rainfall and rainfall recharge data for Substation site (1/04/2019–31/05/2019).	28
Figure 5.7	Daily average groundwater elevation and river stage in relation to rainfall and rainfall recharge data for the Collins Lane site (1/04/2019–31/05/2019).	29
Figure 5.8	Relative evapotranspiration (RET) from Sentinel-2 satellite data for the Substation site.....	30
Figure 5.9	Relative evapotranspiration (RET) estimates from UAV (top) and satellite data (middle) for the Substation site.....	31
Figure 5.10	Relative evapotranspiration (RET) from Sentinel-2 satellite data for the Collins lane site:	32
Figure 5.11	Relative evapotranspiration (RET) estimates from UAV (top) and satellite data (middle) for the Collins Lane location. Satellite data used is Sentinel-2 level 2 (surface reflectance).	33
Figure 5.12	Example of potential refinement of recharge model resolution from: typical existing model resolution (top) satellite data (middle) and UAV data (bottom) at the Substation site.....	34
Figure 5.13	Example of potential refinement of recharge model resolution from: typical existing model resolution (top) satellite data (middle) and UAV data (bottom) at the Collins Lane site.....	35
Figure 6.1	Overlay of UAV RET (high-resolution, 0.1 m x 0.1 m, in centre) on surrounding satellite (10 m x 10 m resolution) RET. The images are for the Substation southern area, surveyed with UAV on 3 May 2019.....	38
Figure 6.2	Overlay of UAV RET (high-resolution, 0.1 m x 0.1 m, in centre) on surrounding satellite (10 m x 10 m resolution) RET. The images are for the Collins lane area, surveyed with UAV on 17 May 2019.	39
Figure 6.3	UAV derived RET and vegetation state at the time of data collection, Substation Northern area (18/04/2019 and 03/05/2019).	40
Figure 6.4	UAV derived RET and vegetation state at the time of data collection, Collins Lane (09/04/2019 and 17/05/2019).	40
Figure 6.5	Relative evapotranspiration and soil classification, Substation Northern area (18/04/2019).	42
Figure 6.6	Relative evapotranspiration (RET) zoomed in on the lysimeter station at Collins Lane (left) and Substation south (right).	44
Figure 6.7	RET for Collins Lane UAV study area (9/04/2019), showing the location of the lysimeter station (red circle), roof of a shed (black arrow) and some examples of tracks (white arrows).	45

TABLES

Table 3.1	Average monthly rainfall, Penman PET, and air temperature data for 2000–2014.....	9
Table 4.1	Summary and characteristics of the input imagery data used for the project.	19
Table 5.1	Seasonal sum of rainfall and rainfall recharge recorded at Substation lysimeter site (Sept. 2012–May 2019).	23

Table 5.2	Seasonal sum of rainfall and rainfall recharge and average soil moisture recorded at Collins Lane lysimeter site (Sept. 2012–May 2019).	26
Table 6.1	Summary of the average rainfall and annual average rainfall recharge ratios at Substation and Collins Lane sites.	37

APPENDICES

APPENDIX 1	EXPLANATION OF EVAPOTRANSPIRATION AND THE RELATION TO SOIL WATER DEFICIT	53
A1.1	Relation between NDVI, LAI and FPAR Used in this Study.....	53
A1.2	Relation to Soil Water Deficit	53
APPENDIX 2	LOCATION OF SITE GEOLOGICAL CROSS-SECTIONS	55
A2.1	Substation Site	55
A2.2	Collins Lane Site.....	56
APPENDIX 3	SOIL REPORTS.....	57
A3.1	Substation Site	57
A3.2	Collins Lane Site.....	61
APPENDIX 4	LYSIMETER SITES PHOTOGRAPHS.....	69
A4.1	Substation Site	69
A4.2	Collins Lane Site.....	70
APPENDIX 5	BORE LITHOLOGICAL LOGS, BOREHEAD PHOTOGRAPHS AND BORE HYDROGRAPHS	71
A5.1	Substation Site	71
A5.2	Collins Lane Site.....	75
APPENDIX 6	PHOTOGRAPHS OF MATERIAL USED FOR THE UAV IMAGERY COLLECTION.....	78
A6.1	Altus LRX UAV and Ground Control Unit.....	78
A6.2	Micasense Rededge 3 Multispectral Camera, Attached to an Altus LRX UAV	79
A6.3	Workswell WIRIS 2nd Gen Thermal Camera, Attached to an Altus LRX UAV	80
APPENDIX 7	UAV FLIGHT LINES	81
A7.1	Substation Site	81
A7.2	Collins Lane Site.....	82

APPENDIX FIGURES

Figure A1.1	Relation between relative transpiration ($RT = AET/PET$) and fraction of transpirable soil water (FTSW) for 13 crop-soil combinations. Data from Verhoef and Egea (2014).	54
Figure A2.1	Location of the cross-section presented in the report for Substation site	55
Figure A2.2	Location of the cross-section presented in the report for Collins Lane site.....	56

Figure A3.1	Ashb_41 soil report–part 1 (Landcare Research, 2019).....	57
Figure A3.2	Ashb_41 soil report–part 2 (Landcare Research, 2019).....	58
Figure A3.3	Ashb_42 soil report–part 1 (Landcare Research, 2019).....	59
Figure A3.4	Ashb_42 soil report–part 2 (Landcare Research, 2019).....	60
Figure A3.5	Ohin_1 soil report–part 1 (Landcare Research, 2019).....	61
Figure A3.6	Ohin_1 soil report–part 2 (Landcare Research, 2019).....	62
Figure A3.7	Ails_3 soil report–part 1 (Landcare Research, 2019).....	63
Figure A3.8	Ails_3 soil report–part 2 (Landcare Research, 2019).....	64
Figure A3.9	Omeh_6 soil report–part 1 (Landcare Research, 2019).....	65
Figure A3.10	Omeh_6 soil report–part 2 (Landcare Research, 2019).....	66
Figure A3.11	Ngak_2 soil report–part 1 (Landcare Research, 2019).....	67
Figure A3.12	Ngak_2 soil report–part 2 (Landcare Research, 2019).....	68
Figure A4.1	Substation lysimeter site in 2013 (White et al. 2014).....	69
Figure A4.2	Substation lysimeter site in April 2019.....	69
Figure A4.3	Collins Lane lysimeter site on 09/04/2019.....	70
Figure A5.1	Photograph of Well 10371.....	73
Figure A5.2	Hydrograph of Well 10371.....	73
Figure A5.3	Hydrographs of Well 10371 and Ngaruroro River at Fernhill stage site.....	74
Figure A5.4	Photograph of Bore 1001284.....	76
Figure A5.5	Hydrograph of Bore 1001284.....	76
Figure A5.6	Hydrograph of Bore 1001284, Kaituna River at Te Matai stage site, rainfall and soil moisture at Te Puke lysimeter site.....	77

APPENDIX TABLES

Table A1.1	NDVI and Corresponding Values of LAI and FPAR (Myneni et al. 1999).....	53
------------	---	----

ABSTRACT

Regional councils have the responsibility to set up allocation limits to protect and ensure the sustainable use of their freshwater resources. An important part of allocation limit setting consists in assessing the amount of recharge to groundwater. Improvement of recharge models and assessments of sustainable allocation limits will become more important in the context of climate change, where more variable rainfall inputs are expected in the future.

This study, commissioned by Envirolink for Hawke's Bay and Bay of Plenty regional councils, aims to use two novel techniques, unmanned aerial vehicle (UAV) and satellite multispectral imagery interpretations, to enable better rainfall recharge estimates to groundwater through better estimates of actual evapotranspiration.

Therefore, UAV and satellite data have been acquired and processed in six surveys, three each at two sites, i.e., in the Hawke's Bay (Substation site) and the Bay of Plenty (Collins Lane site). The aim of these surveys was to explore the two novel techniques for their ability to improve spatial representation of evapotranspiration and recharge estimates near rainfall recharge lysimeters, i.e., to refine the understanding of how rainfall recharge, measured at lysimeter sites or modelled at a coarse resolution, can be better spatially represented over these aquifer recharge areas.

This study showed that inclusion of spatially detailed evapotranspiration data obtained from the UAV multispectral data can lead to significant improvements in recharge estimates. For this purpose, low resolution (10 m x 10 m) satellite data is used as a 'spatial interpolator' for the high resolution (0.1 m x 0.1 m) UAV data in combination with rainfall recharge time series measured at lysimeters and local hydrogeological information.

The study also found that UAV and satellite imagery data could be used to refine soil type mapping, to incorporate human-made features into recharge models, and optimise the location of new lysimeter sites. The use of cloud-computing services in data processing can significantly reduce the computational burden of using such high-resolution data and would be highly recommended for the development of dynamic recharge models.

This study has demonstrated proof of concept for improved parametrisation of rainfall recharge in regional numerical groundwater models (e.g., Heretaunga Plains Groundwater Flow model in Hawke's Bay and the Kaituna, Makatu and Pongakawa Water Management Area groundwater flow model in Bay of Plenty), which will ultimately benefit management of water resources through improved understanding and reduced uncertainty.

KEYWORDS

Rainfall recharge, groundwater, UAV, drone, multispectral, evapotranspiration, spatial representation, lysimeter.

1.0 INTRODUCTION

Under the Resource Management Act (RMA, New Zealand Government 1991), regional councils have the responsibility to manage their regional freshwater resources and to set up allocation limits to protect and ensure their sustainable use.

For this purpose, Hawke's Bay Regional Council (HBRC) and Bay of Plenty Regional Council (BoPRC) have developed tools, such as water budgets and groundwater models (e.g., Rakowski and Knowling, 2018; White et al. 2009), to assess allocation limits for the groundwater resources. The rainfall recharge input to aquifers is a crucial component of these tools and influences how much groundwater is allocated from an aquifer system. Rainfall recharge lysimeters provide one of the few physical measurements of the amount of rainfall recharge to aquifers. HBRC and BoPRC have installed four and nine lysimeter sites in each region, respectively, to quantify rainfall recharge locally (e.g., Lovett and Cameron, 2013).

As lysimeter measurements are local, the information that they provide needs to be up-scaled spatially over the recharge area to be fed into tools such as groundwater flow models. Much spatial variability information is lost or ignored if simple extrapolation procedures are used for up-scaling. Other approaches, such as modelling, provide estimates of rainfall recharge based on assumed physical or ecohydrological properties, such as soil permeability and evapotranspiration, which vary spatially and are not well constrained.

The current project therefore aims to use novel techniques (satellite and unmanned aerial vehicle (UAV) multispectral imagery processing) to enable better recharge estimates through better estimates of actual evapotranspiration, and to upscale local lysimeter observations over aquifer recharge areas. This is of particular relevance, since the incorporation of spatial diversity is expected to significantly improve reliability of lysimeter data and local recharge models that are currently used. Improvement of rainfall recharge models and assessments of sustainable allocation limits will become more important in the context of climate change, where more variable rainfall inputs are expected in the future.

GNS Science (GNS) owns an UAV with multispectral sensing equipment and has a track record in applying such information for characterising and modelling rainfall recharge over a wide range of scales (Westerhoff, 2015; Westerhoff et al. 2017; Westerhoff et al. 2018). Additionally, associated research has been completed by GNS to review, design, fabricate, and install lysimeters.

GNS was commissioned, within an Envirolink framework, by HBRC and BoPRC to undertake the aforementioned investigations, in order to refine their understanding and assessment of rainfall recharge variability to improve their management of regional water resources. This project is the first calibration/validation of the combined techniques. This study focuses on the improvement of spatial resolution of evapotranspiration of soil and vegetation, one of the dominant components of recharge, relatively easily observable by remote sensors.

Section 2.0 of this report explains the rationale of this study and elaborates on the theory underpinning this work. Section 3.0 describes the settings of two case study sites, i.e., climate, (hydro)geology, soils, and in-situ monitoring data available. Section 4.0 details the method undertaken to use remotely-sensed data of both UAV and satellites to estimate evapotranspiration ratios at the two study sites and explains how spatially improved evapotranspiration characterisation forms the basis of more spatially representative recharge

estimates. Sections 5.0 and 6.0 present and discuss the results of the available in-situ data in conjunction with the remotely-sensed measurements and provide recommendations for further work. Conclusions and acknowledgements are provided in Sections 7.0 and 8.0, respectively.

2.0 RATIONALE AND UNDERPINNING THEORY

2.1 Evapotranspiration and Relations with Remotely-Sensed Vegetation Parameters

Evapotranspiration is the “combined loss of water from a given area during a specified period of time, by evaporation from the soil surface and by transpiration from plants (Soil Science Society of America, 2008).

Vegetation information can be measured by satellites. For example, Mu et al. (2007, 2011) described satellite-derived data called MOD16 as: a global 1 km x 1 km resolution product of evapotranspiration derived from information on vegetation parameters from the MODIS satellite. The MOD16 evapotranspiration data was described and assessed by Westerhoff (2017) and tested in a national application in New Zealand (Westerhoff, 2015).

These studies rely on the normalised difference vegetation index (NDVI) as the basis for most vegetation properties:

$$NDVI = \frac{NIR - Red}{NIR + Red} \quad (\text{Eq. 1})$$

From NDVI, the following parameters can be estimated:

- FPAR is the fraction of absorbed photosynthetically active radiation and is used as a fraction of vegetation cover;
- LAI is the Leaf Area Index.

NDVI can be converted to LAI and FPAR using empirical relations in a look-up table (Myneni et al. 1999; Table A1.1 in Appendix 1). It should be noted, that these look-up tables are used as a back-up empirical relation by Myneni et al. (1999); their algorithms are far more complex than table values used in this report.

Surface resistance r_s is the main variable in evapotranspiration equations that links to water stress and is inversely proportional to LAI (e.g., Food and Agriculture Organization of the United Nations, 1998; Westerhoff, 2017):

$$r_s = \frac{c}{LAI} \quad (\text{Eq. 2})$$

where c is a constant. Assuming an average r_s value of 55 for unstressed grass (Hendriks, 2010), c gets a value of 363 (Figure 2.1). PET is the potential evapotranspiration: the evapotranspiration if ample moisture is available for plant growth. PET time series, e.g. daily, are available for all New Zealand climate stations (NIWA, 2014), as well as for ~5 km model pixels in the Virtual Climate Station (VCS) network (Tait et al., 2006). PET accounts for climatic drivers of evapotranspiration demand (e.g. temperature, wind, solar radiation, humidity), but not the ground processes that drive the actual supply of moisture (e.g. soil moisture, leaf area). Actual evapotranspiration (AET) equals PET when there are no limiting factors in water uptake from the plant. If there is a deficit of water, AET is lower than PET. AET is not provided in such consistent time series and is only available through satellite derived information (e.g. MOD16), or divergent approaches that derive AET from PET through incorporation of PET in a hydrological model (e.g., Anabalón and Sharma, 2017; Hong and White, 2015).

For a fully vegetation-covered area, the ratio between AET and PET is called relative transpiration (RT; Appendix 1):

$$RT = \frac{AET}{PET} \quad (\text{Eq. 3})$$

Mu et al. (2007, 2011) and Westerhoff (2017) demonstrated that RT can be calculated from r_s with an empirical relation (shown in Figure 2.1). That relation assumes that the area is fully covered with vegetation and that there is no evaporation from the soil.

If not fully covered, it is assumed that evaporation from the soil also occurs. Mu et al. (2011) sum up existing empirical relations of NDVI and soil heat flux for the proportion of area not covered with vegetation, e.g.:

$$A_{SOIL} = (-0.27 \times NDVI + 0.39) \times A \quad (\text{Eq. 4})$$

With A_{SOIL} the fraction of the total energy (A) available for evapotranspiration.

If evaporation from the soil is included, the ratio between AET and PET should be called Relative Evapotranspiration (RET). This study provides estimates of RET.

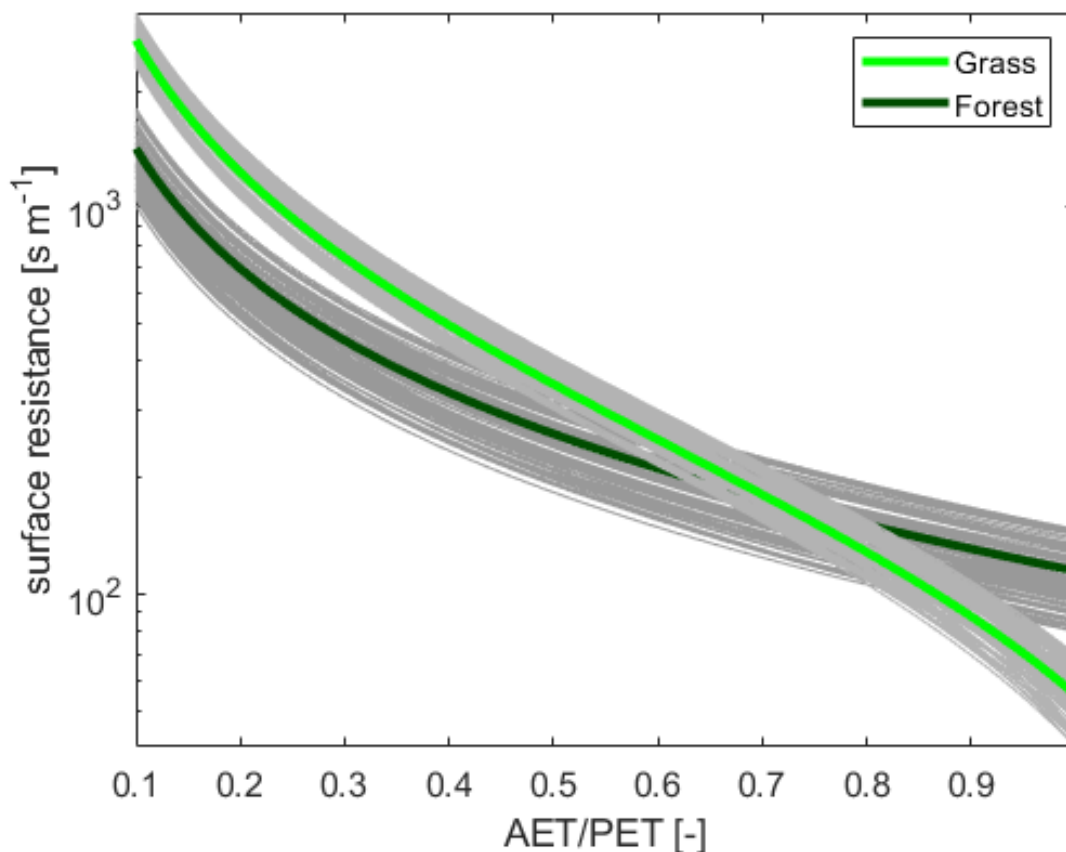


Figure 2.1 The relation between surface resistance and relative transpiration (=AET/PET) for two different landcover types (Westerhoff, 2017).

2.2 Evapotranspiration as Component of Rainfall Recharge

2.2.1 Rainfall Recharge Definition

Rainfall recharge (termed recharge for the purpose of this report) is the amount of rainfall that vertically drains from the soil to replenish the groundwater. A multitude of recharge models

exist (Rushton et al. 2006; Scott, 2004; Westenbroek et al. 2010; Westerhoff, 2017; White et al. 2014, 2003) all of which assume that recharge takes place by water draining through a soil when it reaches field capacity (i.e. near-saturation).

2.2.2 Relation between Rainfall, Evapotranspiration and Rainfall Recharge

Most models that estimate recharge to groundwater assume that recharge only takes place when the soil water deficit S is zero (Figure 2.2). The soil water deficit is dependent on the inflows and outflows of the soil and the soil type. For a flat terrestrial model cell within a recharge model, soil inflow is generally assumed equal to precipitation/rainfall (P), and soil outflow is the sum of actual evapotranspiration (AET) and recharge ($RRECH$). For areas that are not flat, runoff ($Roff$) and soil water flow between cells also plays a role in the recharge estimation.

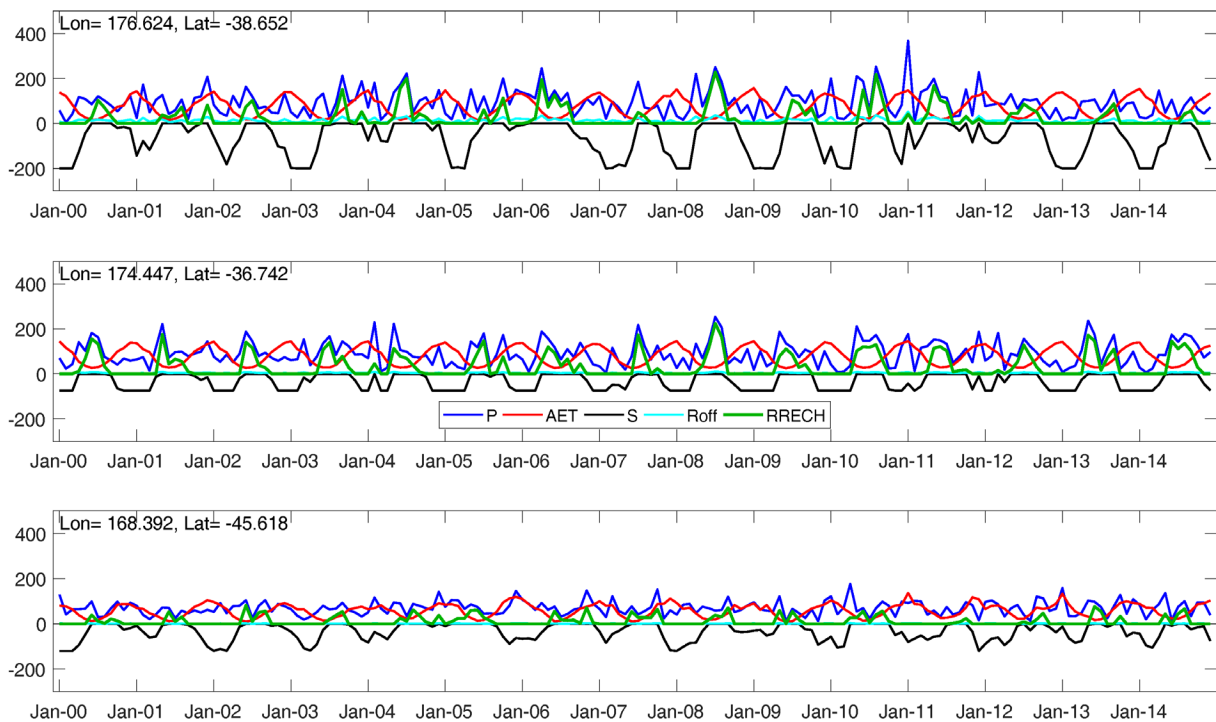


Figure 2.2 Model components for three random locations in New Zealand over a 15-year simulation period, with a monthly timestep: precipitation (P), actual evapotranspiration (AET), soil water deficit (S), runoff ($Roff$), and rainfall recharge ($RRECH$) in mm. (Westerhoff et al. 2018).

Long-term recharge can be estimated as (e.g., Freeze and Cherry, 1979):

$$RRECH = P - AET \quad (\text{Eq. 5})$$

With the assumptions that: (1) soil water deficit is constant over multiple years; (2) surface runoff for a model cell is zero in flat areas (plains). More background information on runoff estimations in recharge models are described in e.g., Cronshey (1986); Westenbroek et al. (2010); and Döll and Fiedler (2008); and Westerhoff (2017, 2018).

2.2.3 Uncertainty of Rainfall Recharge

An understanding of the uncertainty in estimating recharge is important. For example, the impact of recharge uncertainty was demonstrated by White et al. (2003), who used three rainfall recharge models for the Central Plains of Canterbury. They showed that estimated groundwater use as a percentage of rainfall recharge was highly (recharge) model-dependent

and, varied between 63% and 80% in a relative dry year (1997/1998). A detailed description of modelled recharge uncertainty was given by Westerhoff (2017) and Westerhoff et al. (2018). However, uncertainty of recharge estimates is typically not assessed in New Zealand, e.g.: uncertainty assessment for sub-regional models in New Zealand is uncommon; and uncertainty that is caused by the spatial heterogeneity of soil and vegetation is typically not taken into account.

Sources of uncertainty propagate through the estimation of major components in the recharge estimation process: rainfall, evapotranspiration, and soil properties (such as Profile of Available Water (PAW) or soil moisture properties). This current study focuses on the improved estimation of evapotranspiration as a potential means of improving recharge estimates. Mainly, it focuses on the usage of better spatially-explicit estimates of evapotranspiration through UAV and satellite imagery.

3.0 SETTING OF THE STUDY

3.1 Location of the Study Sites

One study site per region was selected after discussions with HBRC and BoPRC. These sites (Figure 3.1 and Figure 3.2) were selected because they are active lysimeter sites (recording rainfall and rainfall recharge data), in an area of particular relevance for groundwater allocation, and appropriate for the collection of UAV imagery (i.e., without excessive flight constraints).

For each site, one or two flight areas were delineated, considering the following criteria:

- flight area comprising a variety of soil types and allowing imagery to be collected in one day; and
- permission obtained to fly an UAV and collect ground control point measurements.

In the Hawke's Bay region, two areas were selected for the Fernhill Substation lysimeter site (called Substation onwards):

- the Northern area located northwest of Mere Road and State Highway 50 (SH 50) crossing, with an approximate area of 7.4 ha;
- the Southern area located south of Mere Road and SH 50 crossing, with an approximate area of 19.9 ha.

Both areas are located at an approximate altitude of 30 m above mean sea level (amsl).

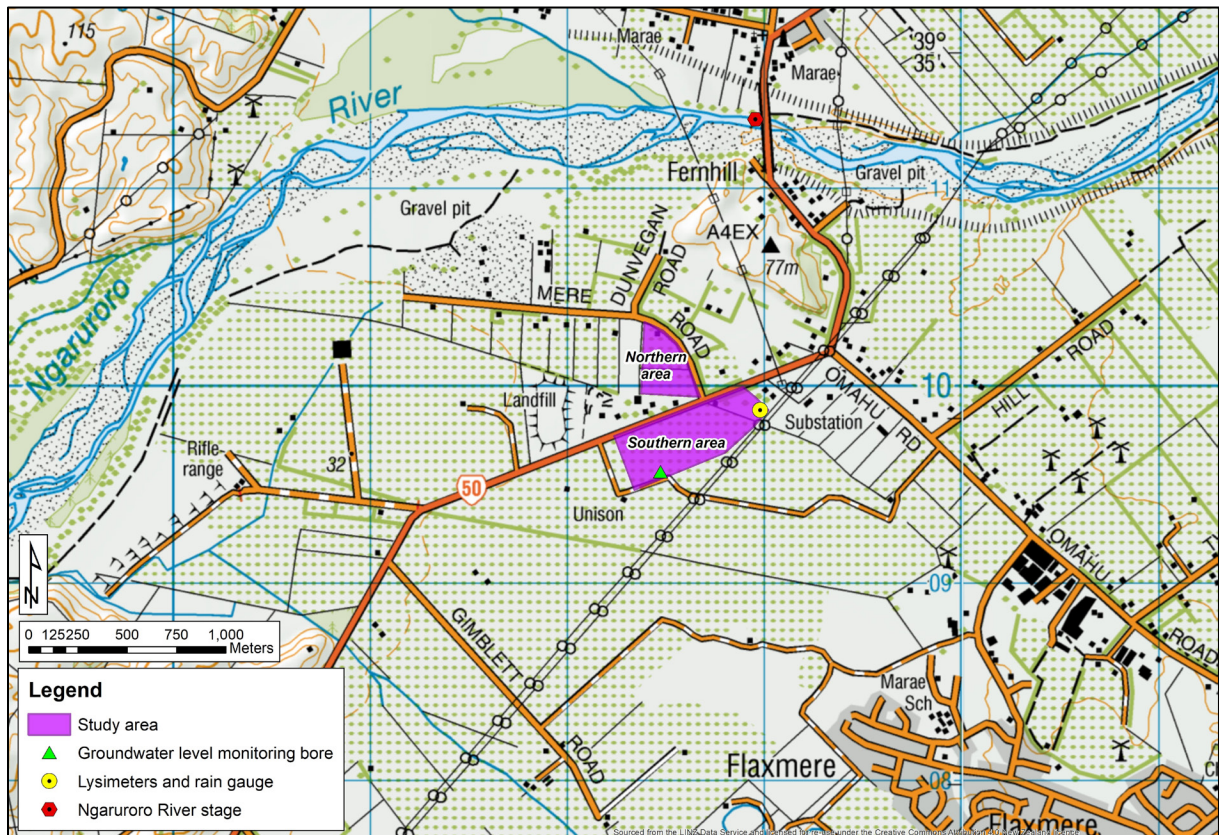


Figure 3.1 Location of the Hawke's Bay Substation study site.

In the Bay of Plenty region, one area was selected for the Te Puke Collins Lane lysimeter site (called Collins Lane onwards), north of Te Puke township, and south of Raparapahoe Canal, with an approximate area of 24 ha and at an approximate altitude of 3 m amsl.

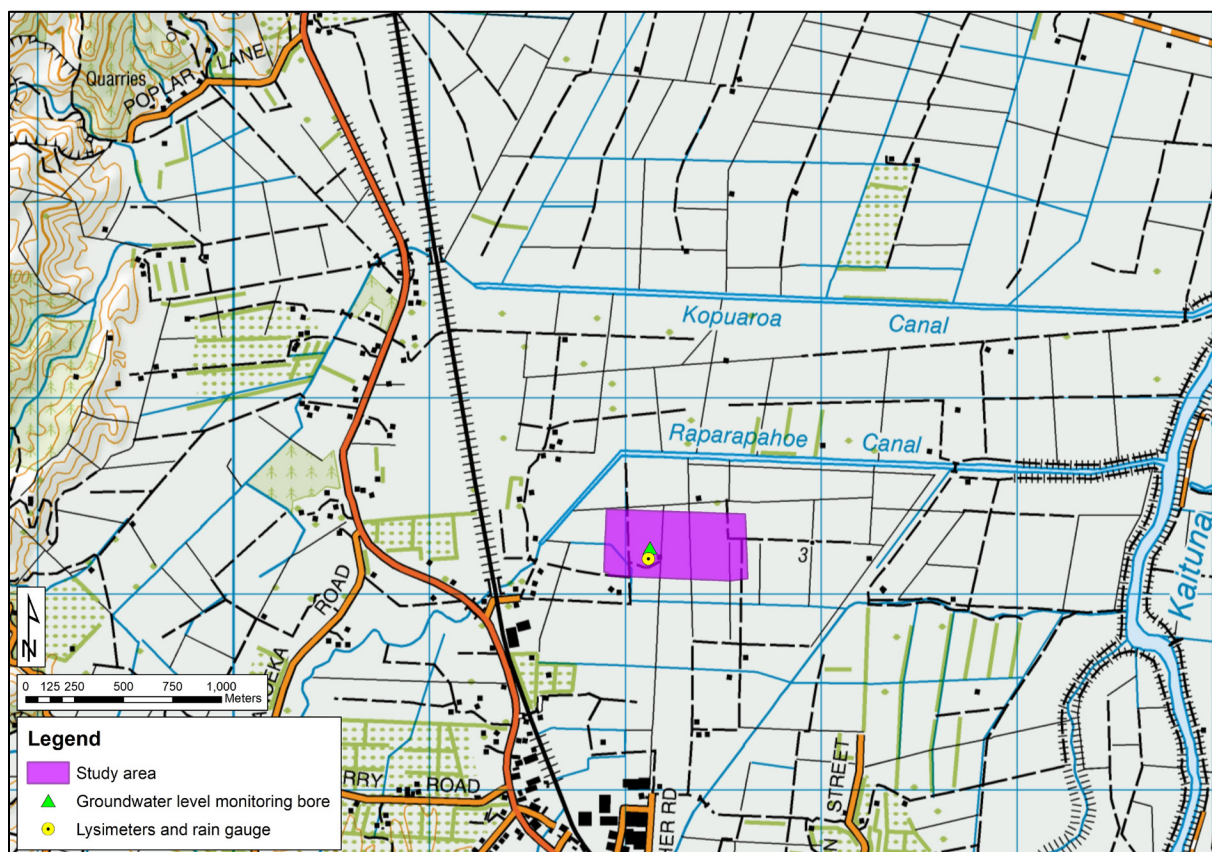


Figure 3.2 Location of the Bay of Plenty Collins Lane study site.

3.2 Climate and Surface Water

3.2.1 Climate

Daily precipitation, Penman potential evapotranspiration (PET), and temperature data from 1972 to the present day are available for New Zealand in a regular grid (0.05° of latitude and longitude, or approximately 5 km) from the VCS network (Tait et al., 2006). For the average climate values, the period covering 1 January 2000 to 31 December 2014 was used, since VCS data were readily available. A summary of the climate data is shown in Table 3.1.

Table 3.1 Average monthly rainfall, Penman PET, and air temperature data for 2000–2014. Source: Virtual Climate Station (VCS) Network (Tait et al. 2006).

Month	VCS cell covering Substation site			VCS cell covering Collins Lane site		
	Rainfall (mm)	PET (mm)	Mean air temperature (°C)	Rainfall (mm)	PET (mm)	Mean air temperature (°C)
Jan	69.2	157.0	18.3	102.9	155.1	19.1
Feb	47.4	117.4	18.3	115.6	121.3	19.6
Mar	54.7	96.5	16.6	124.1	104.3	17.9
Apr	85.8	55.9	14.0	181.6	61.7	15.6
May	70.8	37.6	11.7	179.5	38.3	13.2
Jun	94.2	27.5	9.4	164.9	25.9	10.8
Jul	128.8	28.9	8.7	162.0	30.8	10.1
Aug	66.4	44.5	9.6	146.1	44.4	10.8
Sep	54.5	72.3	11.5	102.0	67.4	12.4
Oct	68.3	108.4	13.1	122.2	100.5	13.8
Nov	39.1	130.7	14.7	66.5	128.4	15.6
Dec	71.4	148.5	17.4	155.6	138.7	18.0
Annual	850.0	1025.0	13.6	1623.1	1017.0	14.7

3.2.2 Surface Water

The Ngaruroro River, located approximately 1.3 km north of the Substation site (Figure 3.1), drains from the northeast flanks of the Kaimanawa Range and the southwest flanks of the Kaweka Range, and has a catchment area of 2500 km². The estimated mean annual low flow in the Ngaruroro River at Whanawhana is 8.3 m³/s (Waldron, 2017). Downstream of Whanawhana, more than 4 m³/s infiltrates into the aquifers of the Heretaunga Plains (Wilding, 2018), providing a significant source of groundwater recharge (Morgenstern et al. 2017).

The Kaituna River is located approximately 2.5 km east of the Collins Lane site (Figure 3.2). The Kaituna River has a catchment area of 587 km² (Brown, 2018). It flows north from Ōkere Falls, descending steeply through a number of gorges, travels west of Paengaroa and discharges into the sea at Te Tumu. The estimated mean annual low flow in the Kaituna River at Te Matai is 26 m³/s (Suren et al. 2016).

3.3 Geology and Hydrogeology

3.3.1 Substation Site

The Heretaunga Basin is a linear, fault-bounded subsiding basin. It has been repeatedly invaded by the sea as sea-level rises following cool, low sea-level stands through the middle and late Quaternary (Lee et al. 2014). Within the depositional sequence, river-channel gravels form one of New Zealand's most important aquifer systems, interconnecting unconfined and confined parts.

The surficial geology of the study area (Figure 3.3; Heron, 2014) consists of Holocene river deposits made of poorly consolidated alluvial gravel, sand and mud. The study site is located over the western unconfined area of the Heretaunga aquifer (Figure 3.4; after Morgenstern et

al. 2017; location of the cross-section provided in Appendix 2), and predominantly formed by river gravel fans, which allow for high rates of rainfall and river recharge.

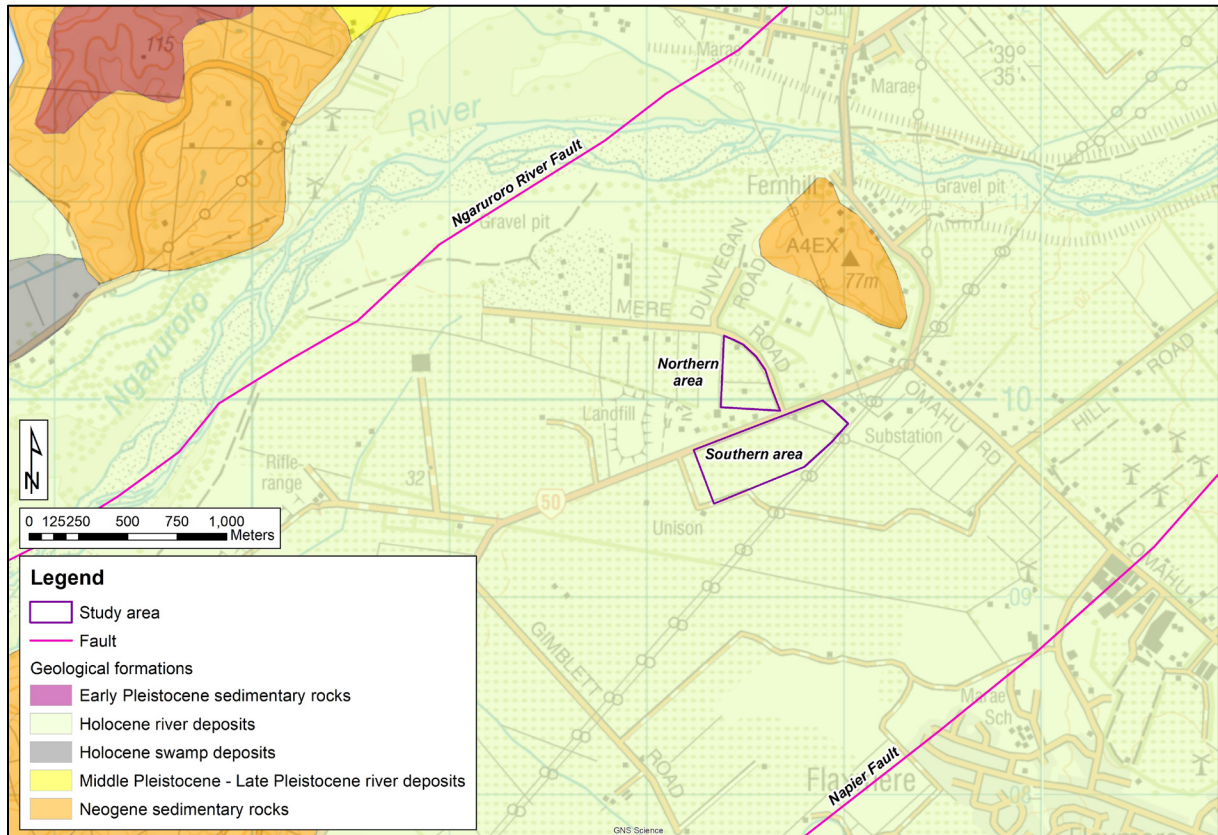


Figure 3.3 Main geological units and faults of Substation study site (Heron 2014).

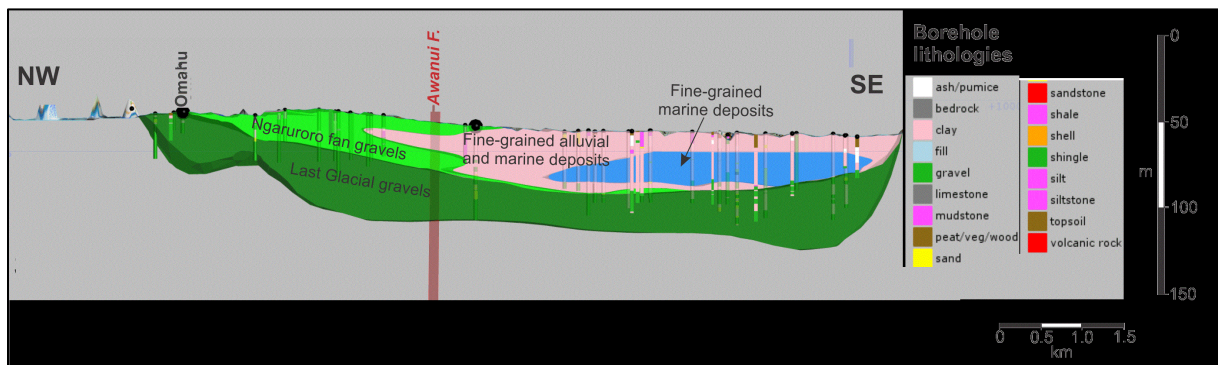


Figure 3.4 NW SE geological cross-section through Omahu near Substation study site (after Morgenstern et al. 2017). The location of the cross-section provided in Appendix 2.1.

3.3.2 Collins Lane Site

Geological development of the Western Bay of Plenty area began about 4 to 5.6 million years ago with volcanism and the formation of the Coromandel and Kaimai ranges. Since then, sequences of ignimbrites and rhyolite domes have been deposited in the area, with one ignimbrite sequence deposited by eruptions sourced from the Rotorua caldera. Deposition of currently preserved sediments began approximately 0.2 million years ago (White et al. 2009).

The surficial geology of the study area (Figure 3.5; Heron 2014) consists of:

- Holocene river deposits made of alluvial gravel, sand, silt, mud and clay with local peat;
- Holocene - Late Pleistocene river deposits made of moderately weathered, poorly to moderately sorted gravel with minor sand and silt underlying terraces.

The most important aquifers in the Western Bay of Plenty area (Figure 3.6; White et al. 2009; location of the cross-section provided in Appendix 2) on the basis of water storage volumes, groundwater use, and groundwater flow are:

- Tauranga Group Sediments;
- Waiteariki Ignimbrite—a volcanic unit erupted from near the Kaimai Range;
- Aongatete Ignimbrite—a volcanic unit that is not exposed at the ground surface and has a considerable thickness.

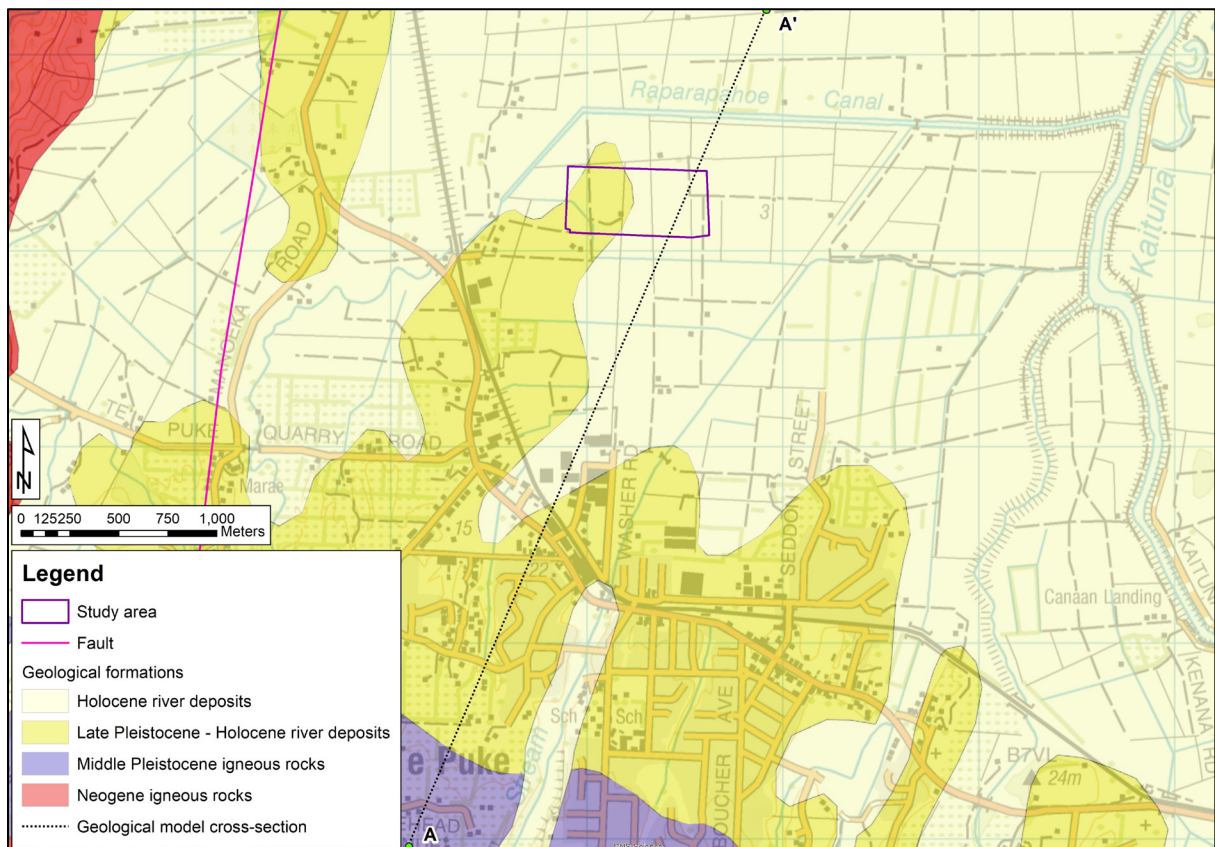


Figure 3.5 Main geological units and faults of Collins Lane study area (Heron, 2014).

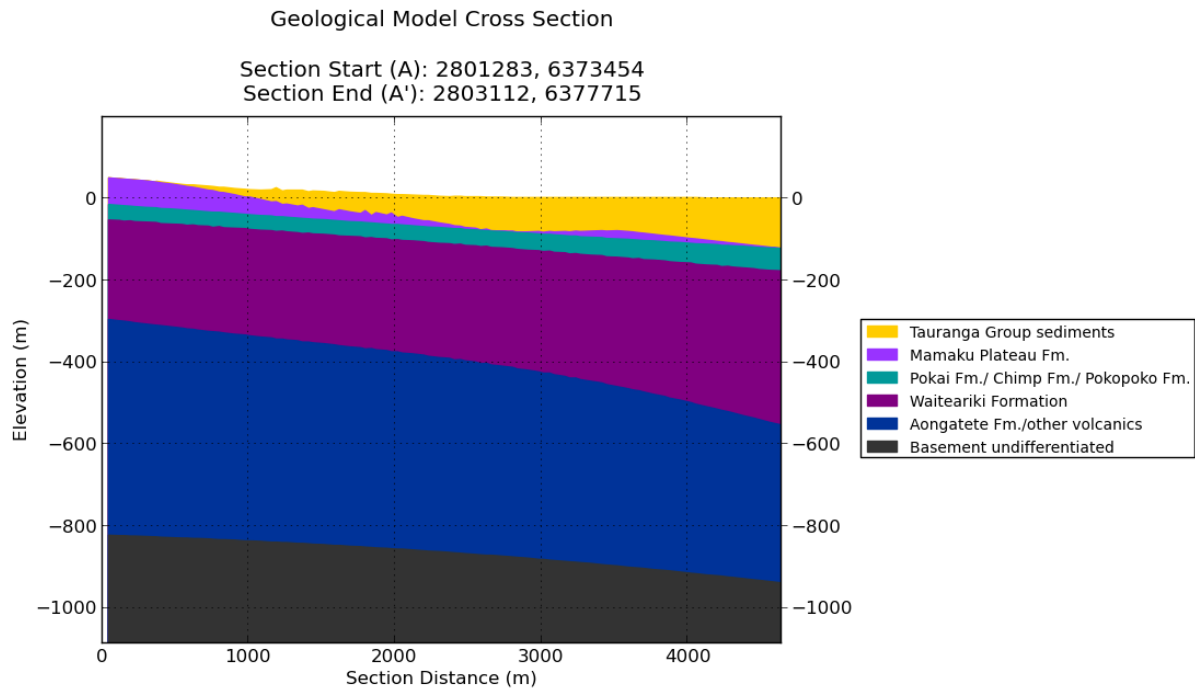


Figure 3.6 Cross-section retrieved from EBOF (<https://data.gns.cri.nz/ebof/>, based on Tschirter, et al. 2016). The location of the cross-section provided in Figure 3.5 and Appendix 2.2.

3.4 Soils and Land Use

Soils of the Substation site (Figure 3.7; Appendix 3) are classified by Landcare Research (2014, 2019) as fluvial raw soils (Ashb_41 and Ashb_42) from the Ashburton group. These soils are moderately well drained, have a low soil moisture, and a medium profile available water (PAW) value of 90 mm (Landcare Research 2014). However, White et al. (2017) indicated that due to previous calculations at the Substation lysimeter site (e.g., soil moisture balance), a PAW value of 20 mm is likely to be locally more realistic. Lovett and Cameron (2013) characterised the base sediments as a gravelly sand matrix for lysimeter 1 and 2, and as a medium textured sand for lysimeter 3.

Soils of the Collins Lane site (Figure 3.8; Appendix 3) are classified by Landcare Research (2014, 2019) as:

- acid mesic organic soils (Ails_3) from Ailsa group;
- typic orthic allophanic soils (Ngak_2) from Ngakura group;
- acidic orthic gley soils (Omeh_6) from Omeheu group;
- and typic acid gley soils (Ohin_1) from Ohineangaaga group.

Most of the soils located within the Collins Lane study area are poorly drained (i.e., Ails_3, Omeh_6, Ohin_1), at the exception of Ngak_2 soils that are characterised as well drained. Soils in the area have a high soil moisture, and medium PAW values between 60 and 105 mm (Landcare Research, 2014). No detailed characterisation of the lysimeter soil columns was available. According to the S-map Soil report (Appendix 3), the soils at this location have a loamy texture with a sandy fraction of 50–76 % and clay fraction of 8–17 %, varying with depth.

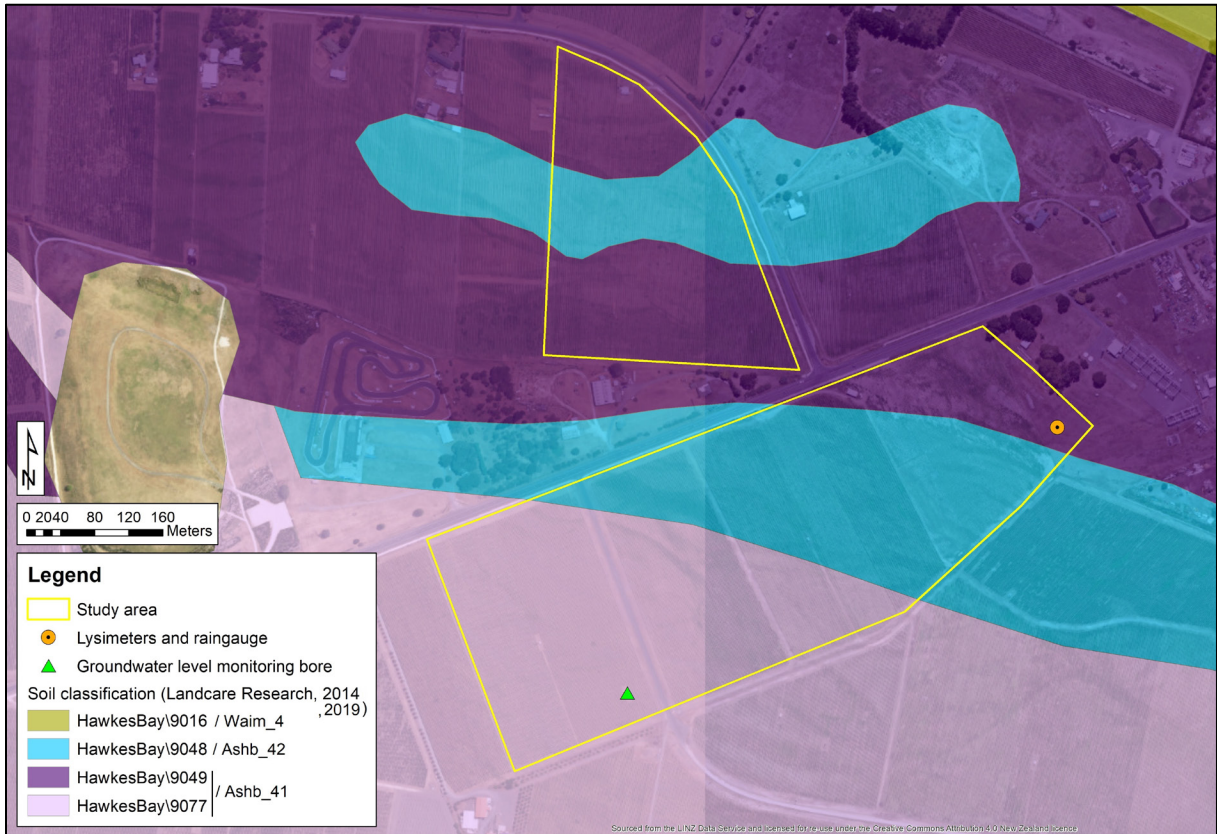


Figure 3.7 Soil classification, medium profile available water value of 90 mm for the soils of the Substation site.

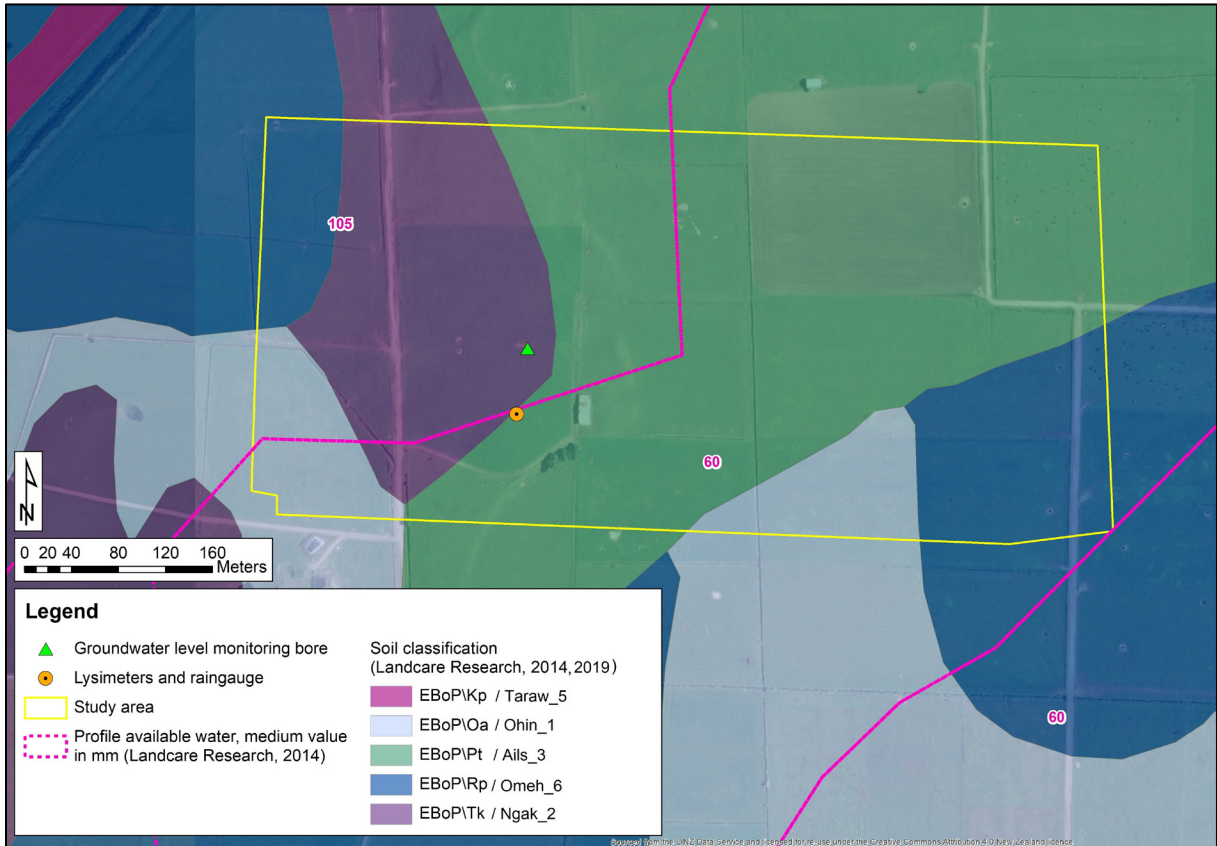


Figure 3.8 Soil classification and medium profile available water values of the Collins Lane site.

Land use in the Substation study areas mainly comprise vineyards, alternating rows of vines, and grass (Figure 3.9). The eastern margin of the Southern area is only covered by grass. Most of the vines had green and yellow leaves during flight 1 (18/04/19), yellow, dead or no leaves during flight 2 (3/05/19) and almost no leaves during flight 3 (22/05/19). The grass of the Northern area was grazed by sheep during flights 2 and 3, and a slight pugging of the soils was observed on the eastern margin on 22/05/19 during flight 3. A few trees and sealed roads (e.g., SH50 and Mere Road) are also located on the margins of the studied areas.



Figure 3.9 Vineyards at Substation site, southern area (22/05/2019).

Land use at the Collins Lane study area is dairy farm pasture (Figure 3.10). There were no cattle in the paddocks during the flights. A farm shed, water troughs, fences, unsealed farms tracks, several drains and a few trees are also located in the study area and are recognisable features on the imagery. Grass growth looked plentiful on most paddocks, except for the paddock where the lysimeter was placed, which looked substantially drier during flight 1 (09/04/19) compared to flights 2 and 3 (17/05/2019 and 27/05/2019, respectively).



Figure 3.10 Grazed grass land at Collins Lane site (09/04/2019).

3.5 Site Monitoring Systems

Each study site (Table 3.2, Appendix 4) includes a rainfall recharge monitoring system, consisting of:

- a rain gauge installed at ground level;
- three rainfall recharge lysimeters;
- an instrumentation enclosure;
- a telemetry system;
- soil moisture sensor¹.

The lysimeters are 500 mm in diameter and 700 mm deep and constructed of galvanised steel. Rainfall recharge is calculated from the volume of rainfall that infiltrates through the soil column, which is directed via pipes to an underground concrete enclosure housing three tipping-buckets rain gauges. Lovett and Cameron (2013) detailed the installation of the (Fernhill) Substation site, however no installation report was discoverable for the Collins Lane site.

Two groundwater level monitoring bores (Table 3.2, Appendix 5) are located approximately 590 m and 60 m from the Substation and Collins Lane rainfall recharge sites, respectively.

¹ For Substation site, the installation report mentions a neutron probe. However, no moisture data was discoverable.

Table 3.2 Summary of the monitoring sites and datasets utilised as part of this study.

Item	Substation			Collins Lane			
	Lysimeter	Rain gauge	Groundwater level monitoring bore	Lysimeter	Rain gauge	Soil moisture sensor	Groundwater level monitoring bore
Site id	(Fernhill) Substation Lysimeter		Well 10371 Substation	Raparapahoe at Collins Lane			Bore 1001284
Easting (NZTM)	1922974		1922469	1892114			1892123
Northing (NZTM)	5609878		5609566	5815182			5815238
Ground surface	Grass, non-grazed		Vineyards	Grass, grazed			
Start provided dataset	6/09/2012		21/10/1968	12/06/2015	13/06/2015		23/05/2016
End provided dataset	24/05/2019		28/05/2019	12/06/2019	13/06/2019		13/06/2019
Comments	3 lysimeters		Bore diameter: 150 mm Total depth: 13.4 m bgl*	3 lysimeters	Aquaflex Soil moisture dielectric ribbon sensor installed between 100–400 mm below ground level.		Bore diameter: 100 mm Total depth: 15.0 m bgl* Site includes 4 other deeper monitoring bores installed in deeper geological units.
Additional details	Photos in Appendix 4.		Lithological log, photos and hydrograph in Appendix 5.	Photos in Appendix 4.			Lithological log, photos and hydrograph in Appendix 5.

*bgl: below ground level

3.6 Previous Rainfall Recharge Assessments and Allocations

3.6.1 Heretaunga Plains Aquifer

The Substation site is located within the Tutaekuri, Ahuriri, Ngaruroro and Karamu (TANK) river catchments, which are currently subject to a plan change by HBRC, following the implementation of the National Policy Statement for Freshwater Management (NPS-FM) in the Hawke's Bay region. This catchment-wide approach to managing water and land includes groundwater resources underlying the Heretaunga Plains and is intended to ensure that appropriate limits are established for water resources within the management zones.

Rajanayaka & Fisk (2018) calculated land surface recharge as part of the development of the Heretaunga Aquifer groundwater model (Rakowski and Knowling 2018). The estimated rainfall recharge rates were primarily based on the daily soil moisture balance calculations (using the Irricalc model), depending on a number of factors, including rainfall, PET, and quick flow run-off threshold.

3.6.1 Kaituna-Pongakawa-Waitahanui Water Management Area

The Collins Lane site is located within the Kaituna-Pongakawa-Waitahanui Water Management Area, which is one of BoPRC's priority catchment areas to implement the NPS-FM in the Bay of Plenty region. Interim thresholds for groundwater allocation are set in Plan Change 9 (PC9) and have been calculated based on surface water catchment boundaries (to defined groundwater management zones) and a simple water balance model (Suren et al. 2016). White et al. (2009) estimated that rainfall recharge for the Lower Kaituna catchment was 30% of rainfall. This estimation integrated the sedimentary lithologies of the Tauranga Group Sediments, measurements through sedimentary deposits in Canterbury (White et al. 2003), and the fact that rainfall minus PET is 30% of rainfall at Tauranga (Bay of Plenty Regional Council 1990).

4.0 METHOD

4.1 Rainfall Recharge Lysimeter Data Analysis

For each lysimeter site, cumulative rainfall and rainfall recharge plots were prepared. A comparison was then undertaken between the rainfall and rainfall recharge curves, but also between the curves obtained for each of the three lysimeters.

Additionally, seasonal average rainfall and rainfall recharge values and ratios were calculated for the complete Substation and Collins Lane lysimeters datasets, in order to provide interannual context to the observations obtained during this project.

An inter-site comparison and intra-site comparisons with the rainfall, soil moisture (where available), and rainfall recharge data during the flight days were undertaken.

4.2 Groundwater Elevation Data Analysis

For both study sites, groundwater elevation data from a shallow bore, located in the vicinity of the lysimeters, were compared to the rainfall and rainfall recharge data over the investigation period.

Where available and in addition to groundwater elevation data, soil moisture and closest river stage data were plotted to provide insights on recharge source.

4.3 Satellite Data and UAV Imagery Acquisition and Processing

4.3.1 UAV Material and Methodology

4.3.1.1 UAV Aerial Photography

Multispectral imagery (MSI) and thermal infra-red imagery (TIR) were collected using a Micasense Rededge 3 Multispectral camera and a Workswell WIRIS 2nd Gen thermal camera, respectively, attached to an Altus LRX UAV (Appendix 6). Flight lines (Appendix 7) were created in Altus Planner for a flight-height of 120 m above ground level (agl) and flight speed of 8 m.s⁻¹. MSI images were collected with a minimum 75% end-lap and 75% side-lap² to improve stitching of the orthomosaics. TIR images were collected with a minimum 80% end-lap and 80% side-lap. Images were acquired in stable wind conditions and mainly within 2.5 hours of local solar noon to minimize the effects of sun angle on imagery³. The total images captured per flight at Collins Lane were 293, at Substation South 269, and at Substation North 124 images.

Prior to the UAV flights, ground control points (GCPs) were systematically surveyed across the study sites for georeferencing purposes. These included identifiable structures such as vineyard and farm posts and fences. GCPs were surveyed using a post processed kinematic global positioning system (GPS) Trimble GeoXH 3.5G Geoexplorer 6000, with an estimated horizontal and vertical error of 10 cm approximately. The number of GCPs surveyed at Collins Lane site were 11 GCPs, at Substation South area 9 GCPs, and at Substation North area 6 GCPs.

² End lap is the common image area on consecutive photographs along a flight strip and side lap encompasses the overlapping areas of photographs between adjacent flight lines.

³ For Substation North area, images were acquired outside 2.5 hours of solar noon due to flights occurring at Substation South within this timeframe.

4.3.1.2 UAV Imagery Processing

MSI orthomosaics for six flights were processed in Agisoft Metashape Professional (version 1.5.1) following the work flow and default parameters described in the Agisoft aerial data processing tutorial (Agisoft HelpDesk Portal, 2019). To ensure accurate alignment of images, GCP coordinates were imported and markers were placed on GCPs in images, after image alignment prior to the optimisation step of the workflow.

A technical issue with the Micasense camera meant that the extensible metadata platform (xmp) was not correctly tagged to most images for flights at Collins Lane on 17-05-19, and Substation South on 18-04-19 and 03-05-19. The few images that contained xmp were used to retroactively tag images without xmp using EXIFtool (version 11.57; Phil Harvey 2019). The MSI images from these flights were unable to be processed in Agisoft Metashape, therefore they were processed in Pix4D Mapper (version 4.3.4). Processing was undertaken following the default workflow and parameters described in the Micasense Rededge processing tutorial (Micasense Knowledge Base, 2019) and the Pix4D processing manual (Pix4D support, 2019). To ensure accurate alignment of images, GCP coordinates were imported and markers were placed on GCPs in images then re-optimized.

4.3.2 Satellite and UAV Input Data

Multispectral imagery (MSI) and thermal infrared imagery (TIR) were collected by an UAV for all the areas of the study sites at three different dates between early April and end of May 2019 (Table 4.1). Due to time restrictions, only the Near infrared (NIR) and Red bands of the MSI were processed, which covers the main scope of this project.

MSI from the Sentinel-2 satellite was processed for the two study sites. Both Sentinel-2 products (top of atmosphere 'Level 1C' and atmospherically corrected 'Level 2A' data) are available from the European Space Agency and were further processed, for the period June 2018 to May 2019. Level 2 (atmospherically corrected) data were not available for the period June 2018–November 2018, hence Level 1 data (top of atmosphere) data were used. This is because Level 2 has only been made available for New Zealand since December 2018 (Table 4.1).

Table 4.1 Summary and characteristics of the input imagery data used for the project.

Vehicle	Instrument	Multispectral bands used	Spatial resolution	Study sites	Study area	Data collected or selected for processing
UAV	Mica-sense Red-Edge	Red: 668 nm NIR: 840 nm	8 cm (flight at 120 m agl*)	Substation	Northern	18/04/2019
					Southern	03/05/2019 22/05/2019
				Collins Lane		09/04/2019 17/05/2019 27/05/2019
Sentinel-2 satellite	MSI	Red: 665 nm NIR: 833– 835 nm	Red band: 10m. NIR band: 20m.	Substation	Northern	Level 1: Jun. 2018–May 2019; Level 2 data: January 2019–May 2019
					Southern	
				Collins Lane		

* agl: above ground level

4.3.3 Data Processing

UAV and satellite data were both processed in the Google Earth Engine (GEE) cloud-computing platform (Gorelick et al. 2017). Since the GEE platform allows for satellite data processing in the Cloud, the huge burden of downloading satellite data, or processing large datasets, is removed, which facilitates fast processing and easy sharing of results. Imports and exports of other datasets, such as shapefiles, geotiff files, etc is also possible. The satellite data is freely available in GEE, and mosaicked UAV MSI data (geotiff files) was imported into GEE for processing.

Figure 4.1 depicts the workflow that was followed to process relative evapotranspiration (RET) for both UAV and satellite data, with subsequent processing steps explained in more detail in the following sub-sections. Source code for the scripts is available in GEE:

Substation site:

<https://code.earthengine.google.com/ba7dee8da2c6072db61be7faeca93dd>

Collins Lane site:

<https://code.earthengine.google.com/29fdca6180b43a9665494514d11c28d1>

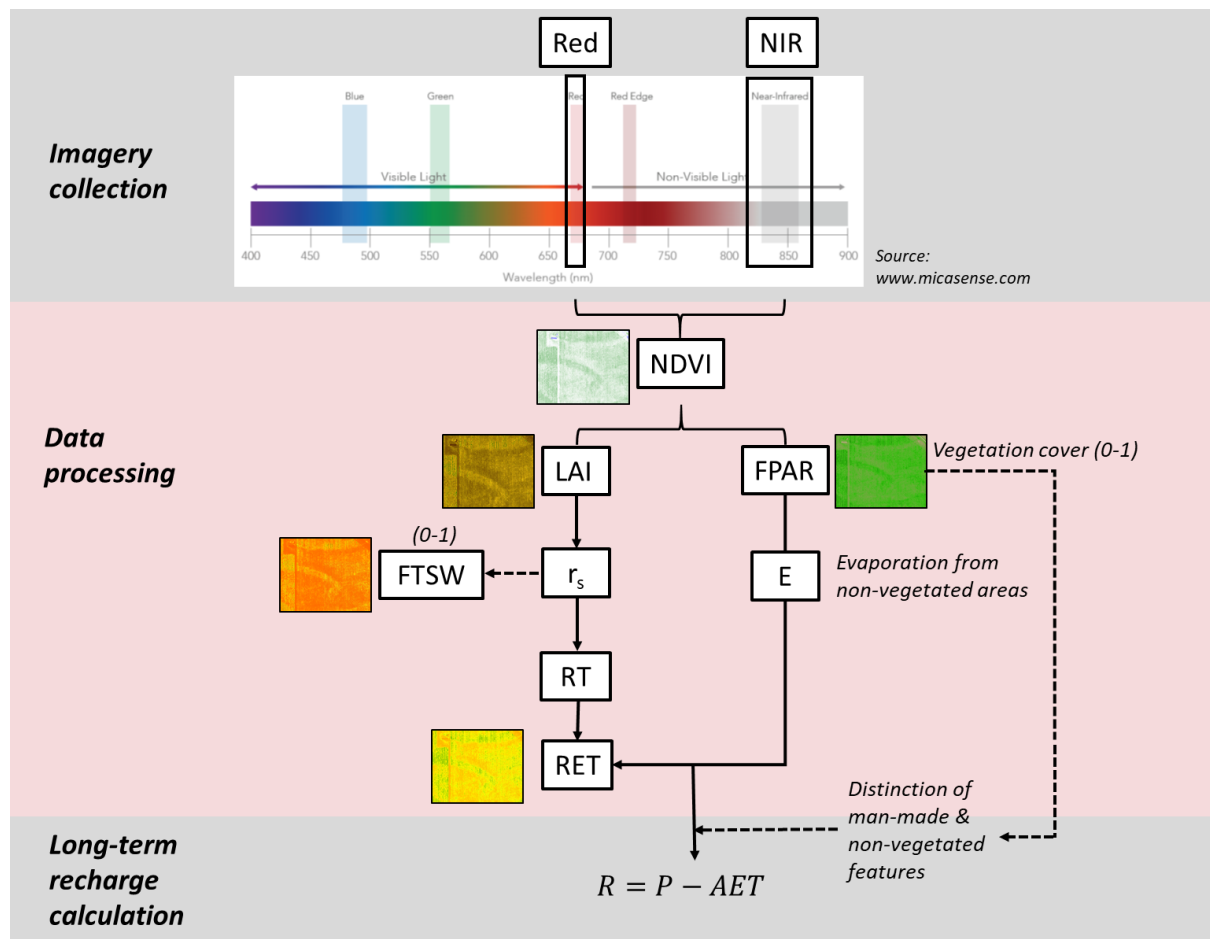


Figure 4.1 Schematic of the project workflow (NIR: Near Infrared, NDVI: Normalised Difference Vegetation Index, LAI: Leaf Area Index, FPAR: Fraction of Photosynthetically Active Radiation, r_s : surface resistance, FTSW: Fraction of Transpirable Soil Water, RT: Relative Transpiration, RET: Relative evapotranspiration; R: Recharge, P: Precipitation, AET: Actual Evapotranspiration; dashed lines=task out of project scope).

4.3.3.1 Estimation of Normalised Difference Vegetation Index (NDVI)

NDVI for both UAV and satellite data was estimated (Equation 1). As a pre-processing step, the red and NIR bands of the UAV were scaled, so the mean values of UAV and satellite over the case study area were equal. This was done by scaling the UAV data values for the red and near-infrared bands to the same bands from the satellite data. Scaling was completed by addition of the region mean value of the satellite data and subsequent subtraction of the UAV mean value for the survey area for each UAV pixel value.

4.3.3.2 Estimation of LAI and FPAR from Multispectral UAV and Satellite Data

NDVI was converted to LAI and FPAR using the values provided by Myneni et al. (1999; Table A1.1 in Appendix 1). For the sake of the experiment, only the value of grass was used. However, the method can be relatively easily expanded to incorporate multiple types of landcover.

4.3.3.3 Estimation of Relative Transpiration from Multispectral UAV and Satellite Data

For the area with vegetation cover, surface resistance r_s was estimated from LAI values with Equation 2, assuming a grass surface. Subsequently, relative transpiration was calculated from r_s using the empirical relation provided in Figure 2.1.

For the non-vegetated features (estimated by FPAR) the relative amount of soil evaporation was estimated with Equation 4.

4.4 Estimation of Recharge

To show the benefits of inputting the relative evapotranspiration layers derived from this study into recharge models, a hypothetical case of long-term recharge was developed for both sites. These recharge estimations were based on UAV and satellite datasets related to the investigation period (April - May 2019) and are “hypothetical” because we assumed data from the short data coverage period to represent a long-term average value; collection of more UAV data was not feasible within the project budget constraints.

For these hypothetical cases, the average recharge for a model grid cell of approximately 1 km x 1 km (e.g., such as in Westerhoff et al. 2018) was based on average rainfall and Penman PET values for the VCS cell covering the site.

For the geometry of the model pixel, Sentinel-2 Level 2A satellite data was obtained for the period December 2018–May 2019 and averaged into a ‘mean NDVI’, which was then used to derive relative evapotranspiration as described in the above sections. This was assumed to represent a long-term average value of NDVI.

One of the three sets of UAV images at each site was then processed and assumed to represent a hypothetical average value of NDVI at the resolution of the UAV for the same period.

Both satellite data and UAV-derived NDVI were then used in the derivation of relative evapotranspiration values. AET was estimated as relative evapotranspiration multiplied by PET (Equation 3).

Long-term recharge was then estimated with Equation 5.

5.0 RESULTS

5.1 Rainfall Recharge Lysimeter Data

5.1.1 Substation Site

5.1.1.1 Lysimeter Datasets

The Substation lysimeter site has been collecting rainfall and rainfall recharge data since early September 2012 (Figure 5.1).

The largest rainfall recharge ratios (Table 5.1) were usually observed in winter (e.g., 0.9 in 2016; 0.8 in 2013, 2017 and 2018) and the lowest ratios in summer (e.g., 0.0 in 2012–2013, 2013–2014, 2015–2016 and 2017–2018).

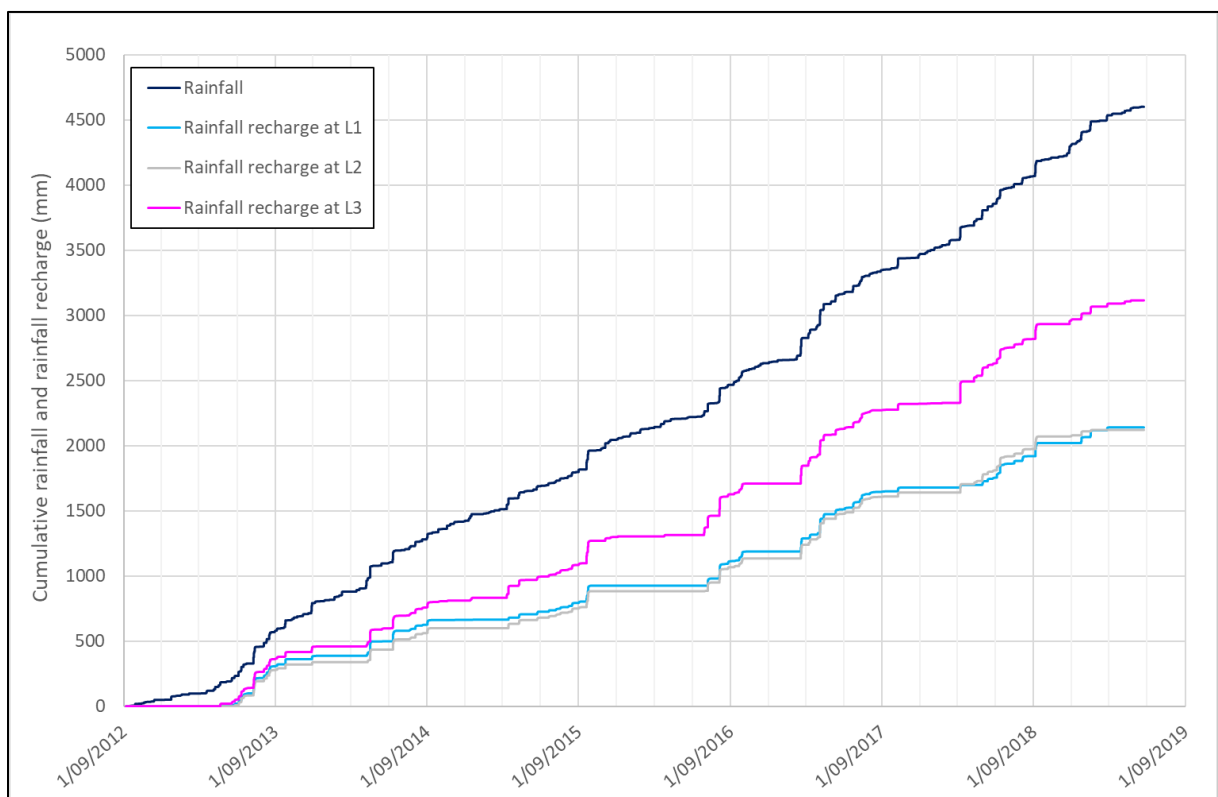


Figure 5.1 Cumulative rainfall recharge measured at three lysimeters, Substation lysimeter site (Sept. 2012–May 2019).

Table 5.1 Seasonal sum of rainfall and rainfall recharge recorded at Substation lysimeter site (Sept. 2012–May 2019).

		Sum of rainfall (mm)	Sum of rainfall recharge (mm)			Rainfall recharge ratio			Average rainfall recharge (mm)	Average rainfall recharge ratio
			L1	L2	L3	L1	L2	L3		
2012	Spring	49.6	0.576	0.288	0.064	0.0	0.0	0.0	0.3	0.0
	Summer	49.2	0.1	0.0	0.0	0.0	0.0	0.0	0.0	0.0
2013	Autumn	134.8	20.2	8.6	51.9	0.1	0.1	0.4	26.9	0.2
	Winter	345.6	286.7	268.8	311.6	0.8	0.8	0.9	289.0	0.8
	Spring	213.4	78.0	61.3	94.1	0.4	0.3	0.4	77.8	0.4
2014	Summer	88.4	2.5	0.3	2.3	0.0	0.0	0.0	1.7	0.0
	Autumn	218.8	111.9	96.1	138.8	0.5	0.4	0.6	115.6	0.5
	Winter	189.2	127.0	126.7	160.5	0.7	0.7	0.8	138.1	0.7
	Spring	130.6	36.4	38.4	53.1	0.3	0.3	0.4	42.6	0.3
2015	Summer	93.6	1.7	0.0	21.0	0.0	0.0	0.2	7.6	0.1
	Autumn	177.4	61.6	79.7	162.3	0.3	0.4	0.9	101.2	0.6
	Winter	108.2	66.6	70.4	89.5	0.6	0.7	0.8	75.5	0.7
	Spring	247.2	132.9	133.2	214.1	0.5	0.5	0.9	160.1	0.6
2016	Summer	90.6	0.0	0.0	5.6	0.0	0.0	0.1	1.9	0.0
	Autumn	84.2	0.0	0.0	11.0	0.0	0.0	0.1	3.7	0.0
	Winter	247.0	187.9	184.7	312.1	0.8	0.7	1.3	228.2	0.9
	Spring	166.0		66.4	82.1	0.0	0.4	0.5	74.2	0.3
2017	Summer	193.6	101.6	105.2	137.7	0.5	0.5	0.7	114.8	0.6
	Autumn	340.0	223.4	237.7	282.8	0.7	0.7	0.8	247.9	0.7
	Winter	181.2	134.5	130.8	143.4	0.7	0.7	0.8	136.2	0.8
	Spring	123.6	31.3	32.4	49.1	0.3	0.3	0.4	37.6	0.3
2018	Summer	108.6	0.0	0.0	6.4	0.0	0.0	0.1	2.1	0.0
	Autumn	278.4	76.7	171.1	304.3	0.3	0.6	1.1	184.0	0.7
	Winter	211.8	164.9	162.6	186.2	0.8	0.8	0.9	171.2	0.8
	Spring	240.8	101.3	102.5	147.5	0.4	0.4	0.6	117.1	0.5
2019	Summer	226.0	119.2	44.3	123.7	0.5	0.2	0.5	95.7	0.4
	Autumn	64.4	0.0	0.0	25.7	0.0	0.0	0.4	8.6	0.1

5.1.1.2 Rainfall and Rainfall Recharge Data during the Investigation Period

During the April–May 2019 period (Figure 5.2), a few rainfall events were recorded on the lysimeter rainfall rain gauge (e.g., 8/04/2019 and 22/04/2019). Rainfall recharge was only observed at lysimeter L3, with the main rainfall recharge events on the same days (8/04/19 and 22/04/19).

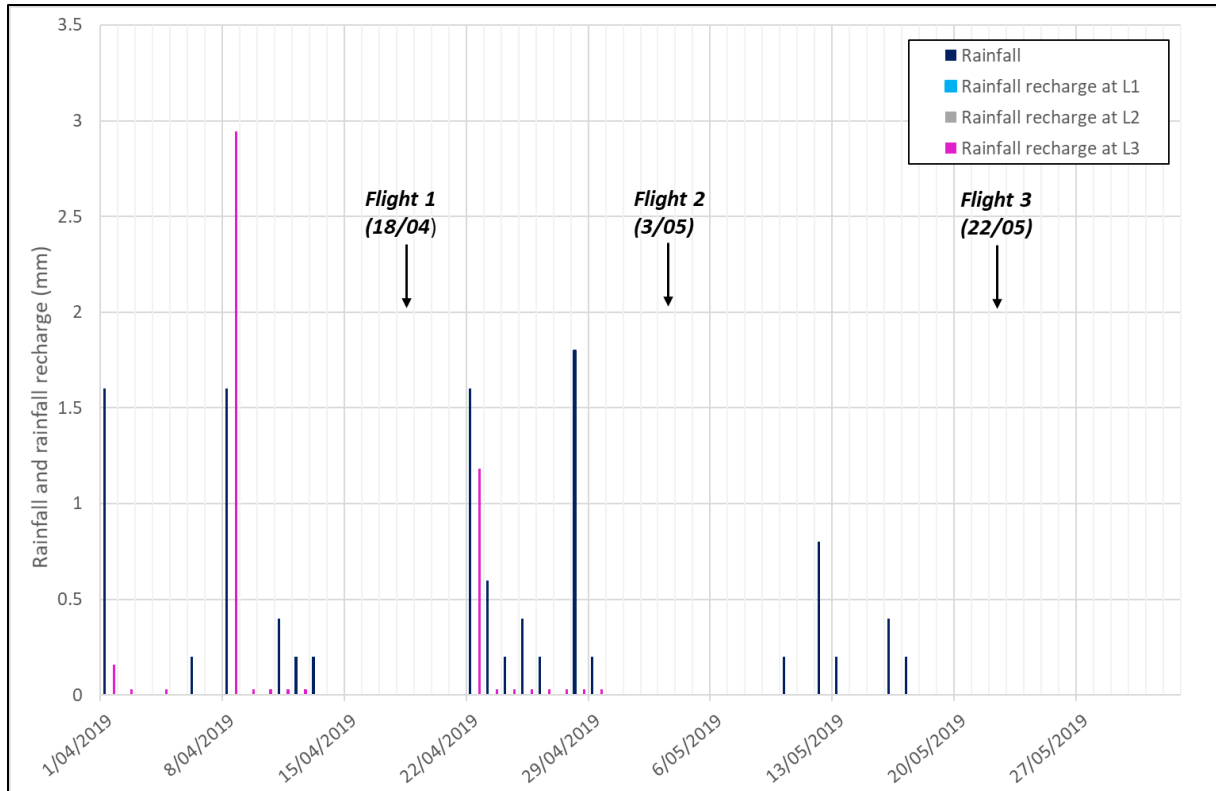


Figure 5.2 Rainfall and rainfall recharge at Substation lysimeter site (1/04/2019–31/05/2019).

5.1.2 Collins Lane Site

5.1.2.1 Lysimeter Datasets

The Collins Lane lysimeter site has been collecting rainfall and rainfall recharge data since mid-June 2015 (Figure 5.3, Table 5.2). The largest rainfall recharge ratios are usually observed in winter (e.g., 0.7 in 2016; 0.6 in 2018) and the lowest ratios in summer (e.g., 0.0 in 2015–2016 and 2016–2017).

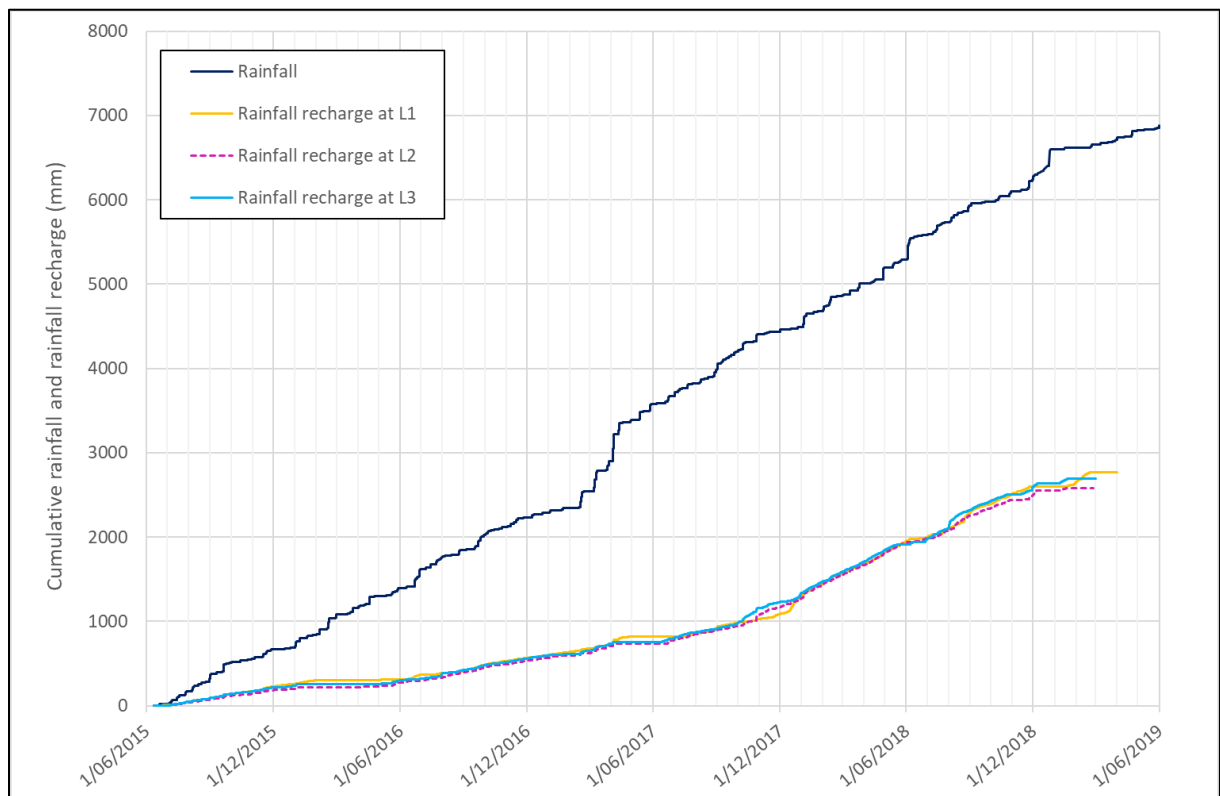


Figure 5.3 Cumulative rainfall recharge measured at three lysimeters, Collins Lane lysimeter site (June 2015–May 2019).

Table 5.2 Seasonal sum of rainfall and rainfall recharge and average soil moisture recorded at Collins Lane lysimeter site (Sept. 2012–May 2019).

		Sum of rainfall (mm)	Average soil moisture (%)	Sum of rainfall recharge (mm)			Rainfall recharge ratio			Average rainfall recharge (mm)	Average rainfall recharge ratio
				L1	L2	L3	L1	L2	L3		
2015	Winter	318.1	29	170.6	137.2	160.4	0.5	0.4	0.5	156.1	0.5
	Spring	347.6	25	132.8	84.1	96.2	0.4	0.2	0.3	104.4	0.3
	Summer	396.7	19	3.8	2.0	0.1	0.0	0.0	0.0	2.0	0.0
2016	Autumn	329.2	28	81.5	94.0	71.4	0.2	0.3	0.2	82.3	0.3
	Winter	453.9	31	297.2	300.5	288.3	0.7	0.7	0.6	295.3	0.7
	Spring	385.2	29	133.8	115.0	134.4	0.3	0.3	0.3	127.7	0.3
2017	Summer	308.2	16	3.2	5.4	1.4	0.0	0.0	0.0	3.3	0.0
	Autumn	1040.8	30	716.8	742.6	726.7	0.7	0.7	0.7	728.7	0.7
	Winter	409.9	32	218.7	240.3	241.8	0.5	0.6	0.6	233.6	0.6
	Spring	447.8	30	223.6	222.7	187.2	0.5	0.5	0.4	211.2	0.5
2018	Summer	431.6	22	50.5	42.6	29.7	0.1	0.1	0.1	40.9	0.1
	Autumn	420.8	27	140.2	121.0	153.3	0.3	0.3	0.4	138.2	0.3
	Winter	645.1	32	406.4	312.4	396.3	0.6	0.5	0.6	371.7	0.6
	Spring	305.7	25	19.2	19.7	19.0	0.1	0.1	0.1	19.3	0.1
2019	Summer	410.8	21	166.3	136.1	182.9	0.4	0.3	0.4	161.8	0.4
	Autumn	229.0	19	2.2	2.2	2.0	0.0	0.0	0.0	2.1	0.0

5.1.2.2 Rainfall and Soil Moisture Data during the Investigation Period

Soil moisture data recorded at an approximate depth of 10 cm varied between 16 % and 29 % between April and May 2019 and increased rapidly after each rainfall event (Figure 5.4). Soil moisture values measured at 10 cm depth at mid-day during the UAV imagery collection were around 19 %, 22 % and 21% for flights 1, 2 and 3, respectively. No recharge was measured at the three lysimeters over this period.

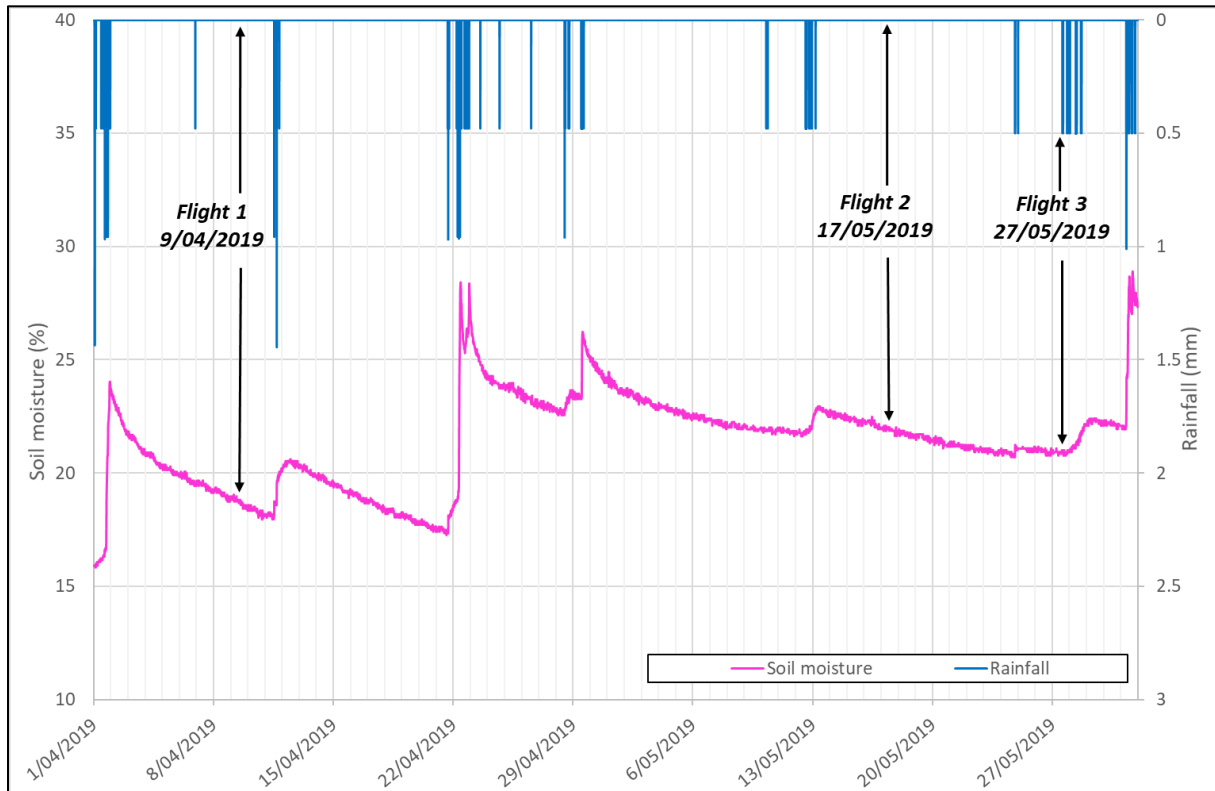


Figure 5.4 Rainfall and soil moisture at 10 cm depth, Collins Lane lysimeter site (1/04/2019–31/05/2019).

5.2 Groundwater Elevation Data

5.2.1 Substation Site

During the investigation period (April–May 2019) the groundwater elevation at Well 10371, located approximately 590 m from the lysimeter site (Figure 3.1), was relatively stable (variation of 0.13 m; Figure 5.5) in comparison to the January 2016–May 2019 period (Appendix 5). The Ngaruroro River hydrograph at Fernhill stage site (located approximately 1.9 km north-east of Well 10371; Figure 3.1) shows larger variations (amplitude of 0.57 m between April–May 2019; Figure 5.6).

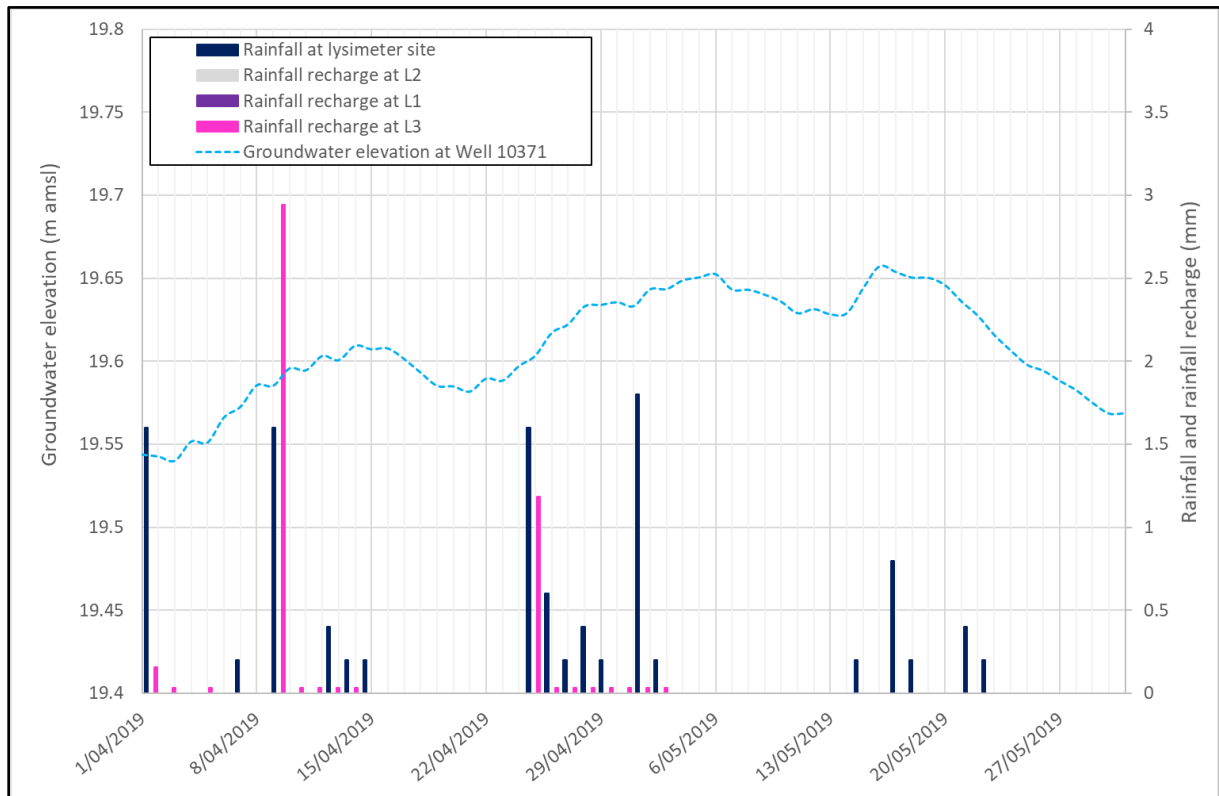


Figure 5.5 Daily average groundwater elevation in relation to rainfall and rainfall recharge data for Substation site (1/04/2019–31/05/2019).

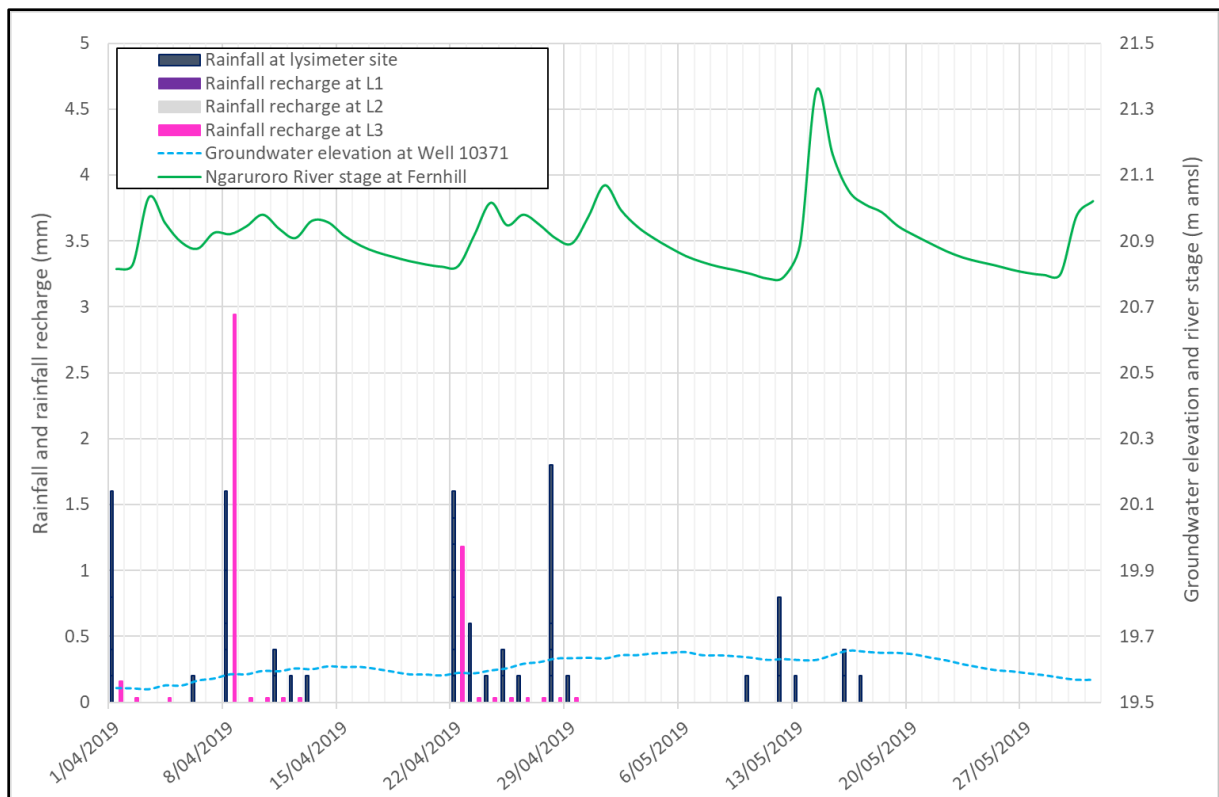


Figure 5.6 Daily average groundwater elevation and river stage in relation to rainfall and rainfall recharge data for Substation site (1/04/2019–31/05/2019).

5.2.2 Collins Lane Site

The groundwater elevation at the Collins Lane site (Bore 1001284, located approximately 60 m from the lysimeter site, Figure 3.2) is below sea level and was relatively stable between April and May 2019 (variation of 0.09 m, Figure 5.7) in comparison to the June 2016–May 2019 period (Appendix 5). The Kaituna River hydrograph at Te Matai river flow monitoring site (located 5.3 km from the lysimeter site) indicates levels above sea level, with larger variations (0.47 m between April–May 2019).

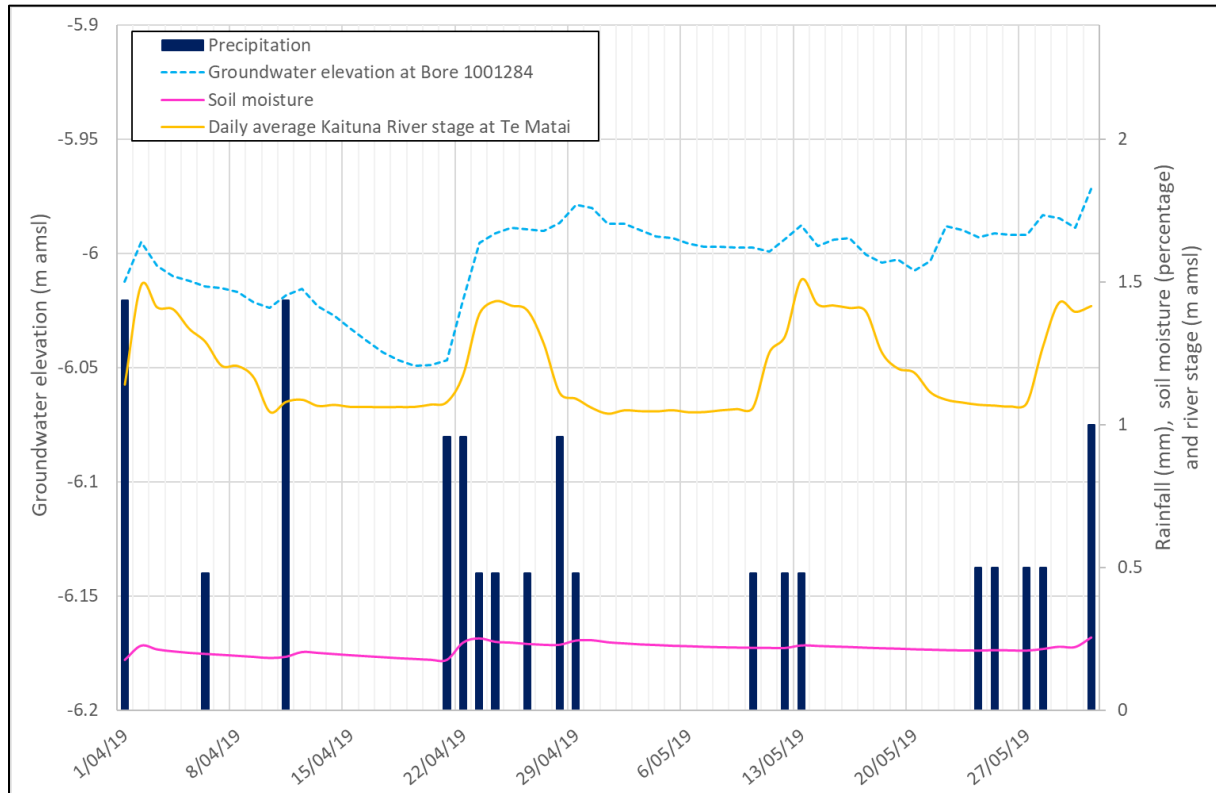


Figure 5.7 Daily average groundwater elevation and river stage in relation to rainfall and rainfall recharge data for the Collins Lane site (1/04/2019–31/05/2019).

5.3 Satellite Data and UAV Imagery Processing

5.3.1 Substation Site

Sentinel-2 data was processed for the period June 2018 to May 2019. Level 1 data, although available for the entire period, can only be used for relative comparison of vegetation. For example, the Level 1 data showed that vegetation was generally less healthy (e.g., sprayed, cut, or drier) in the September–October–November (SON) period than in the December–January–February (DJF) period (Figure 5.8). Level 2A was not available for the period June 2018–November 2018. However, it covers the period of UAV data acquisition and was used for comparisons with the UAV data.

RET from both UAV (Figure 5.9, top) and satellite (Figure 5.9, middle) were used to calculate AET from PET (Equation 3), of which the mean monthly value Penman PET for the Substation site is shown in Figure 5.9 (bottom).

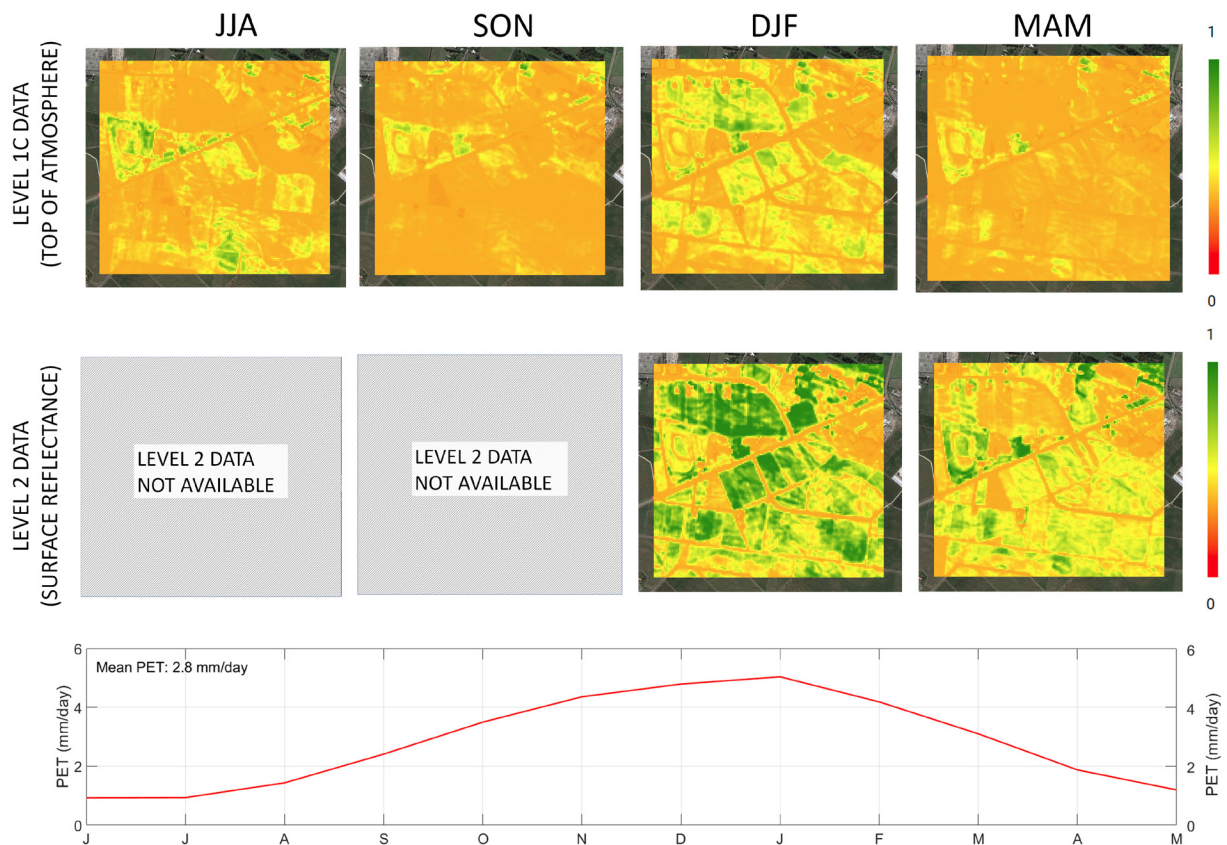


Figure 5.8 Relative evapotranspiration (RET) from Sentinel-2 satellite data for the Substation site: Top: level 1C (top of atmosphere); Middle: Level 2 surface reflectance. To derive AET, RET is multiplied by PET, plotted at the bottom as mean monthly Penman PET (NIWA, 2014) for the nearest virtual climate station (VCS) cell. JJA = June-July-August, SON = September-October-November, DJF = December-January-February, MAM = March-April-May.

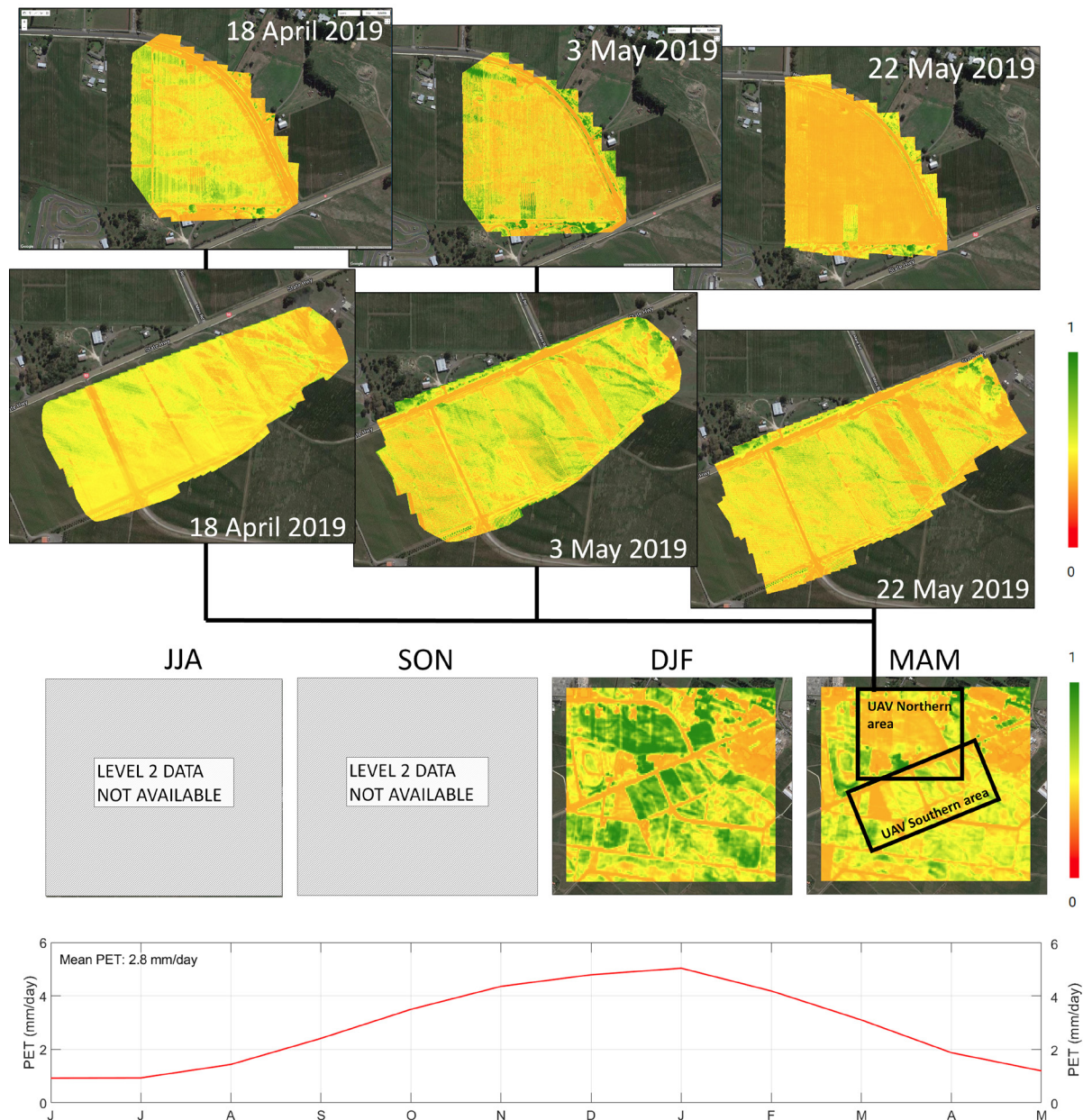


Figure 5.9 Relative evapotranspiration (RET) estimates from UAV (top) and satellite data (middle) for the Substation site. The satellite data is Sentinel-2 level 2 (surface reflectance). To derive AET, RET is multiplied by PET, plotted at the bottom as mean monthly Penman PET (NIWA, 2014) for the nearest virtual climate station (VCS) cell. JJA = June-July-August, SON = September-October-November, DJF = December-January-February, MAM = March-April-May.

5.3.2 Collins Lane Site

Similar to the Substation site, Sentinel-2 data was processed for the time period from June 2018 to May 2019 (Figure 5.10) for Collins Lane. Level 2A was not available for the period June 2018–November 2018 but does cover the period of UAV data acquisition and was thus used for comparisons with the UAV data.

RET from both UAV (Figure 5.11, top) and satellite (Figure 5.11, middle) were used to calculate AET from PET (Equation 3), of which the mean monthly value Penman PET for the Collins Lane site is shown in Figure 5.11 (bottom).

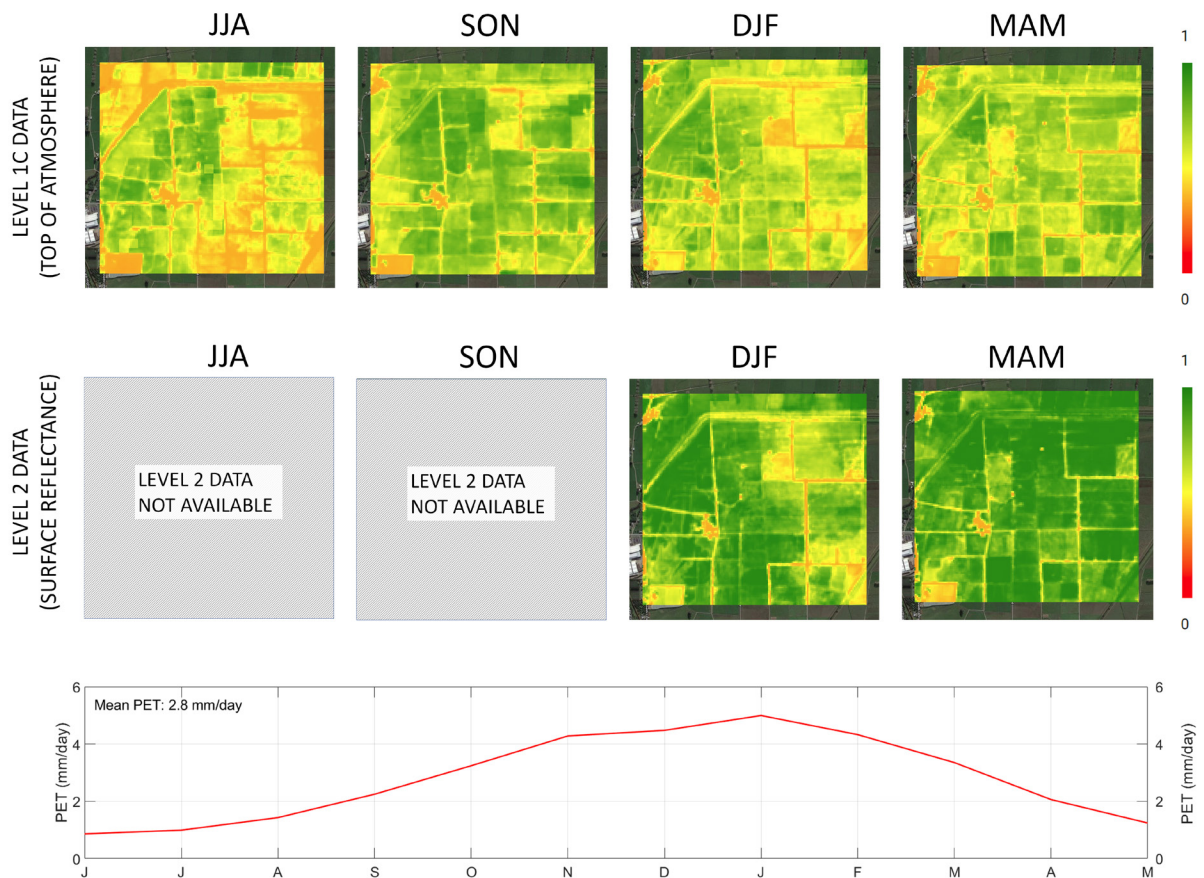


Figure 5.10 Relative evapotranspiration (RET) from Sentinel-2 satellite data for the Collins lane site: Top: level 1C (top of atmosphere); Middle: Level 2 surface reflectance (middle) To derive AET, RET is multiplied by PET, plotted at the bottom as mean monthly Penman PET (NIWA, 2014) for the nearest virtual climate station (VCS) cell. JJA = June-July-August, SON = September-October-November.

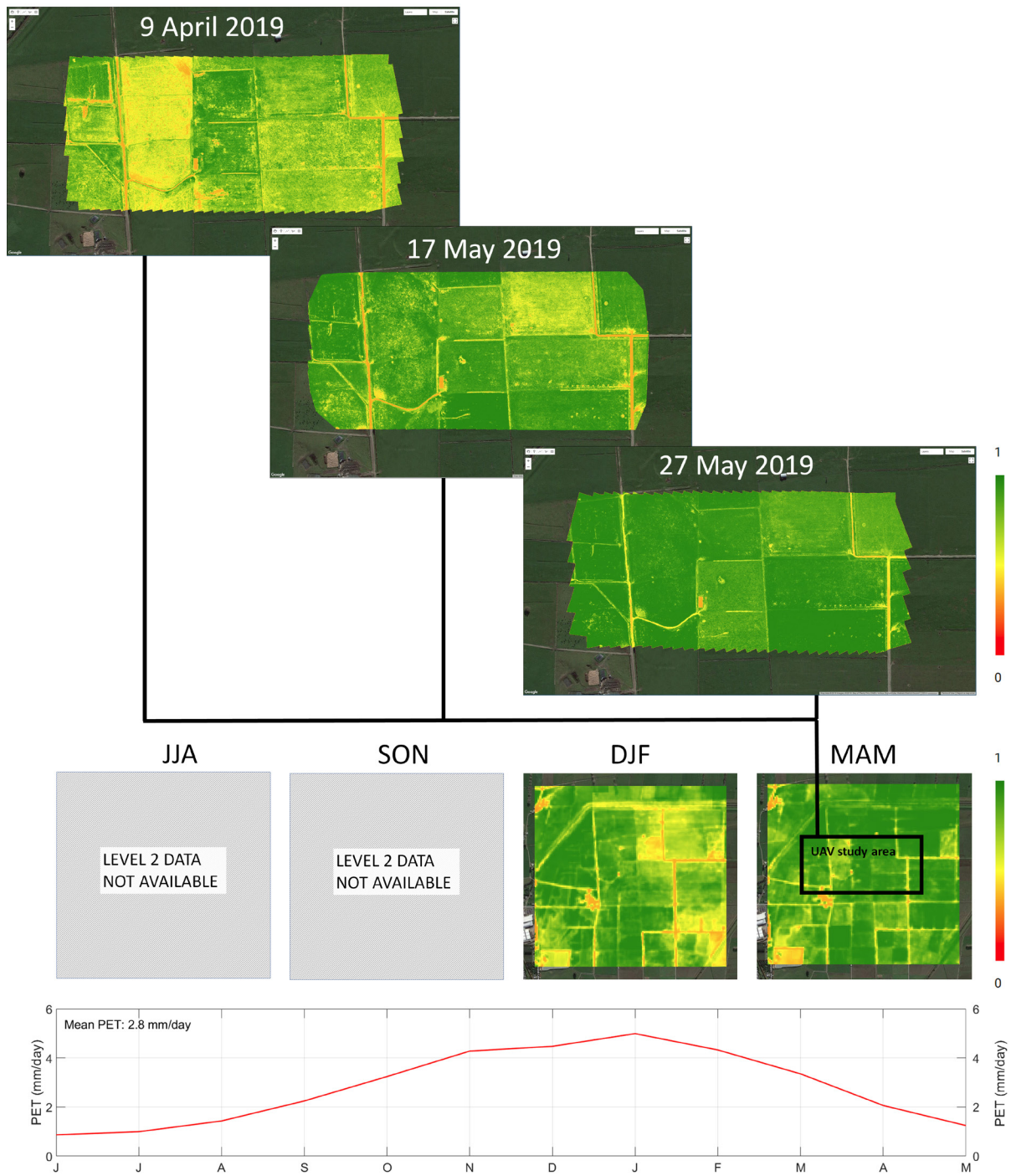


Figure 5.11 Relative evapotranspiration (RET) estimates from UAV (top) and satellite data (middle) for the Collins Lane location. Satellite data used is Sentinel-2 level 2 (surface reflectance). To get AET, RET should be multiplied by PET, plotted at the bottom as mean monthly Penman PET (NIWA 2014) for the nearest virtual climate station (VCS) cell. JJA = June-July-August, SON = September-October-November, DJF = December-January-February, MAM = March-April-May.

5.4 Estimated Recharge

Recharge estimates were assessed from diverse sources and at different scales (Figure 5.12 for Substation and Figure 5.13 for Collins Lane), using the method described in Section 4.4:

- from a recharge model, with a 1 km x 1 km pixel size;
- from satellite MSI data, with a 10 m x 10 m pixel size;
- from the UAV MSI data, with a 10 cm x 10 cm pixel size.

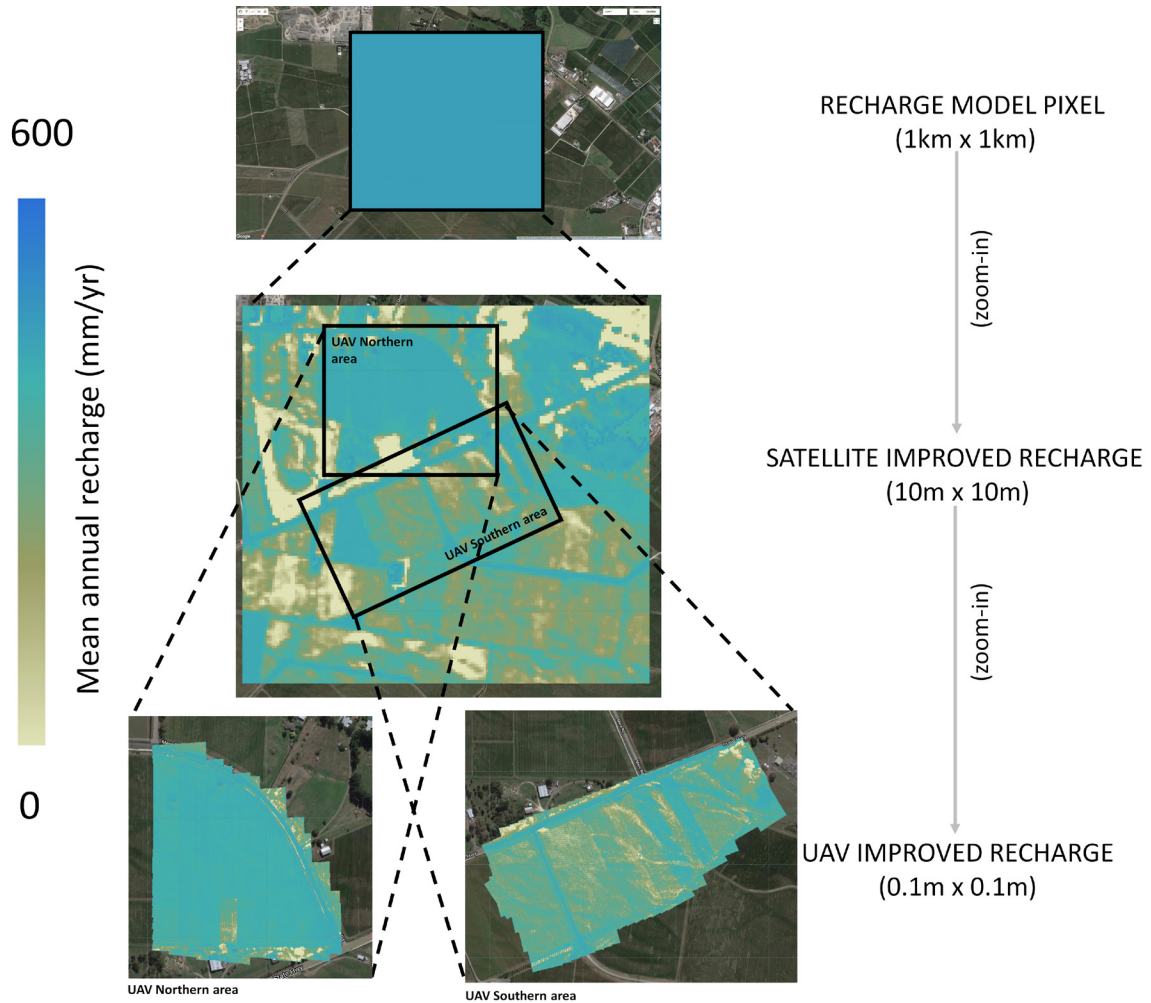


Figure 5.12 Example of potential refinement of recharge model resolution from: typical existing model resolution (top) satellite data (middle) and UAV data (bottom) at the Substation site.

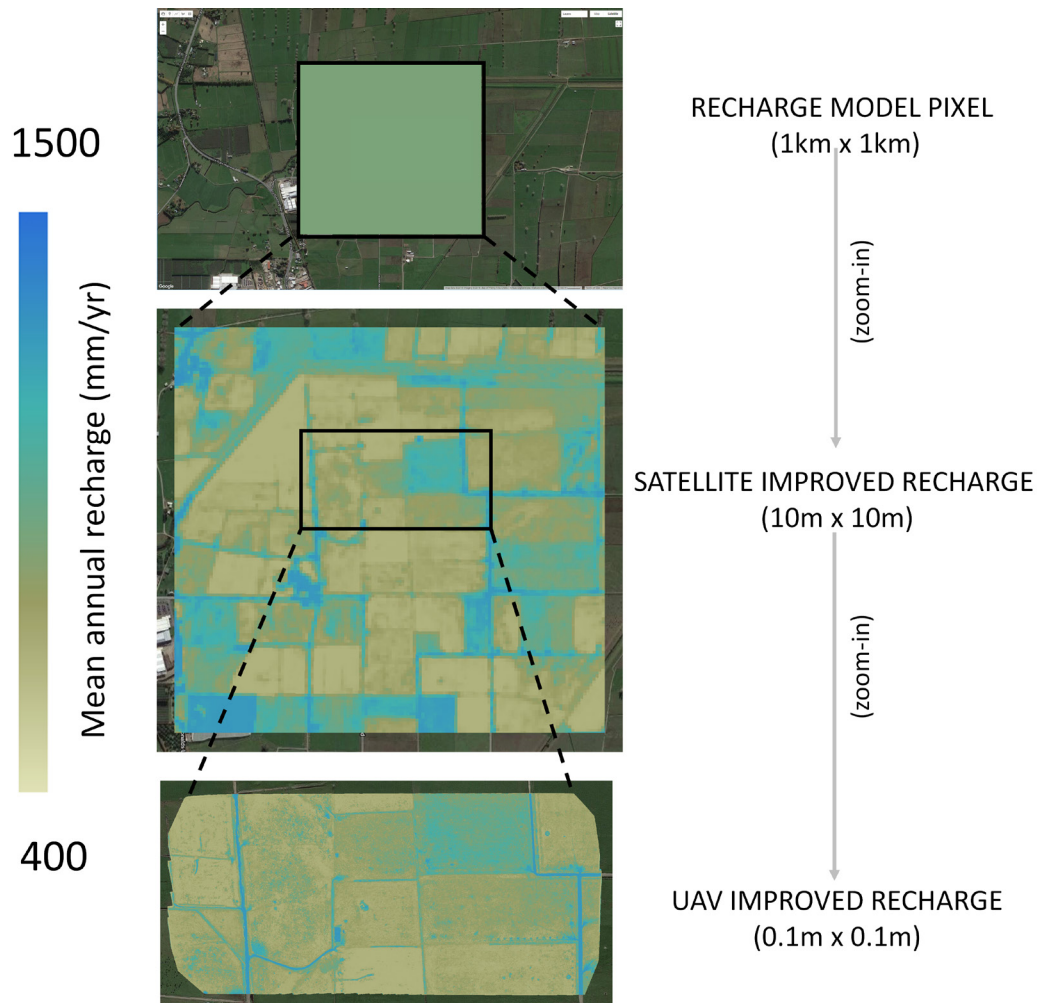


Figure 5.13 Example of potential refinement of recharge model resolution from: typical existing model resolution (top) satellite data (middle) and UAV data (bottom) at the Collins Lane site.

6.0 DISCUSSION

6.1 Rainfall Recharge Lysimeter Data

6.1.1 Substation Site

The cumulative curves of each lysimeter (Figure 5.1) have similar trends, with a divergence for the lysimeter L3, in comparison to lysimeters L1 and L2. Lysimeter L3 records more rainfall recharge than lysimeters L1 and L2. This is likely due to the difference in soil type, as identified during the lysimeter installation (Section 3.4); and a reflection of such alluvial river deposits being relatively heterogeneous and varying over small distances and depths.

The highest seasonal rainfall recharge average (289.0 mm) was observed in winter 2013, with a seasonal rainfall of 345.6 mm (Table 5.1).

6.1.2 Collins Lane Site

In contrast, the cumulative rainfall recharge curves (Figure 5.3) of the three lysimeters are very comparable, which is inferred to be due to relatively similar lysimeter soil columns.

The highest seasonal rainfall recharge average (728.7 mm) was observed in autumn 2017 and associated with a very large seasonal rainfall (1040.8 mm) for this period (Table 5.2).

Soil moisture data were below 30% during the investigation period, which indicates unsaturated soil conditions, and explains the absence of recharge at the three lysimeters (Figure 5.4)

6.1.3 Inter-Site Comparison

Measured rainfall recharge (Table 6.1) was less at the Substation site than at Collins Lane site, with annual averages of 453.2 mm and 751.4 mm from 2016 to 2018, respectively. However, the Substation site had a larger average rainfall recharge ratio (0.6) compared to Collins Lane site (0.4) over the same period. The difference in rainfall recharge between the Substation and Collins Lane sites is likely due to the difference in both rainfall (i.e., annual average of 755.3 mm at Substation and 1858.4 mm at Collins Lane, from 2016 to 2018) and soil properties at the two sites. The Substation site has coarse gravely soils, which is likely to result in greater infiltration than at the Collins site, which has finer grained loamy soils. Differences in rainfall recharge due to variation in soil type was noted by White et al. (2017) for lysimeters located in the Heretaunga Plains.

Table 6.1 Summary of the average rainfall and annual average rainfall recharge ratios at Substation and Collins Lane sites.

Period	Substation			Collins Lane		
	Rainfall (mm)	Average rainfall recharge (mm)	Average rainfall recharge ratio	Rainfall (mm)	Average rainfall recharge (mm)	Average rainfall recharge ratio
2013	737.4	395.4	0.5	NA	NA	NA
2014	627	303.9	0.5	NA	NA	NA
2015	626.4	338.7	0.6	NA	NA	NA
2016	587.8	306.2	0.5	1565.0	507.3	0.3
2017	838.4	537.4	0.6	2206.8	1176.8	0.5
2018	839.6	515.9	0.6	1803.3	570.1	0.3
Annual average (2016–2018)	755.3	453.2	0.6	1858.4	751.4	0.4

Note: Annual average calculations are not applicable (NA) for the years with incomplete datasets. Rainfall is as recorded at lysimeter sites.

6.2 Groundwater Elevation Data

6.2.1 Substation Site

Increase in groundwater elevation at well 10371 corresponds to measured recharge at lysimeter L3 after rainfall events and/or increase in Ngaruroro River stage (Figure 5.5 and Figure 5.6). For example, increases in groundwater elevation followed the recharge events measured on 8/04/2019 and 22/04/2019. Rakowski and Knowling (2018) analysed groundwater level responses to flood events in the Ngaruroro River for bores located near or even at significant distance from the River. They assessed that a typical stage-increase of 1.5 m in the Ngaruroro River resulted in a lagged and dampened approximately 0.07 m increase in groundwater level in Well 10371.

6.2.2 Collins Lane Site

As noted previously, the Collins Lane lysimeters did not record any rainfall recharge during the study period. However, groundwater level and soil moisture at the site (Figure 5.7) had similar trend indicating a correlation to the rainfall events during the investigation period (April 2019–May 2019) and suggest that rainfall recharge might have occurred upgradient in the catchment and/or locally by another mechanism than rainfall infiltration. The Kaituna at Te Matai river flow monitoring site (located 5.3 km from the lysimeter) is subject to fluctuations from management of Lake Rotoiti water levels and tidal influences (Bay of Plenty Regional Council, 2019; Figure 5.7). The tidal influence is clearly visible on the 5-minute time step series and also noticeable on the bore hydrograph (Figure A5.6 in Appendix 5).

6.3 Satellite Data and UAV Imagery

6.3.1 Comparison of UAV and Satellite-Derived RET Values

UAV and satellite-derived RET correlate very well, both spatially and in absolute values (Figure 6.1 and Figure 6.2), meaning the higher resolution UAV data can be used to complement the lower resolution but more abundant satellite-derived data.

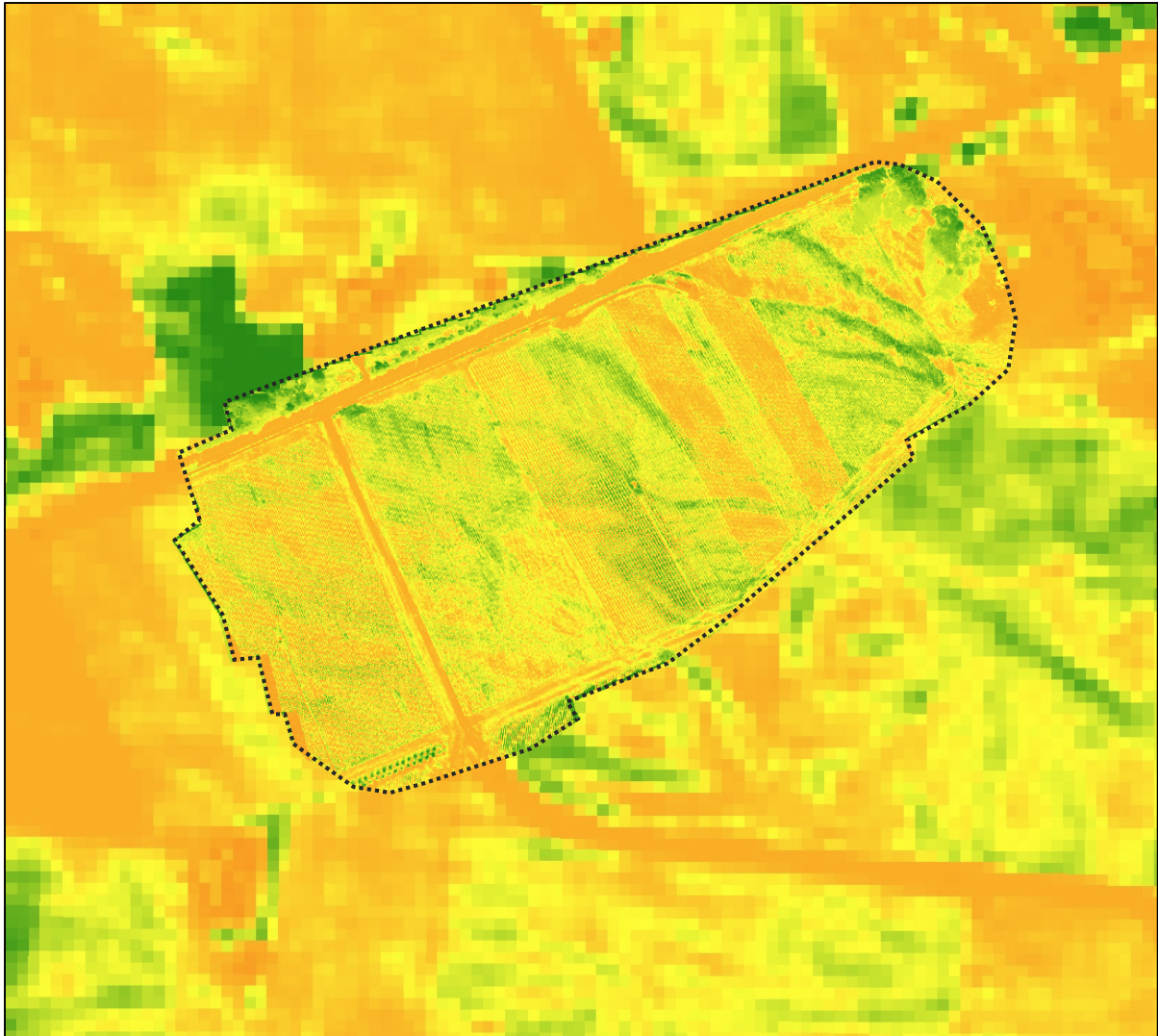


Figure 6.1 Overlay of UAV RET (high-resolution, 0.1 m x 0.1 m, in centre) on surrounding satellite (10 m x 10 m resolution) RET. The images are for the Substation southern area, surveyed with UAV on 3 May 2019.

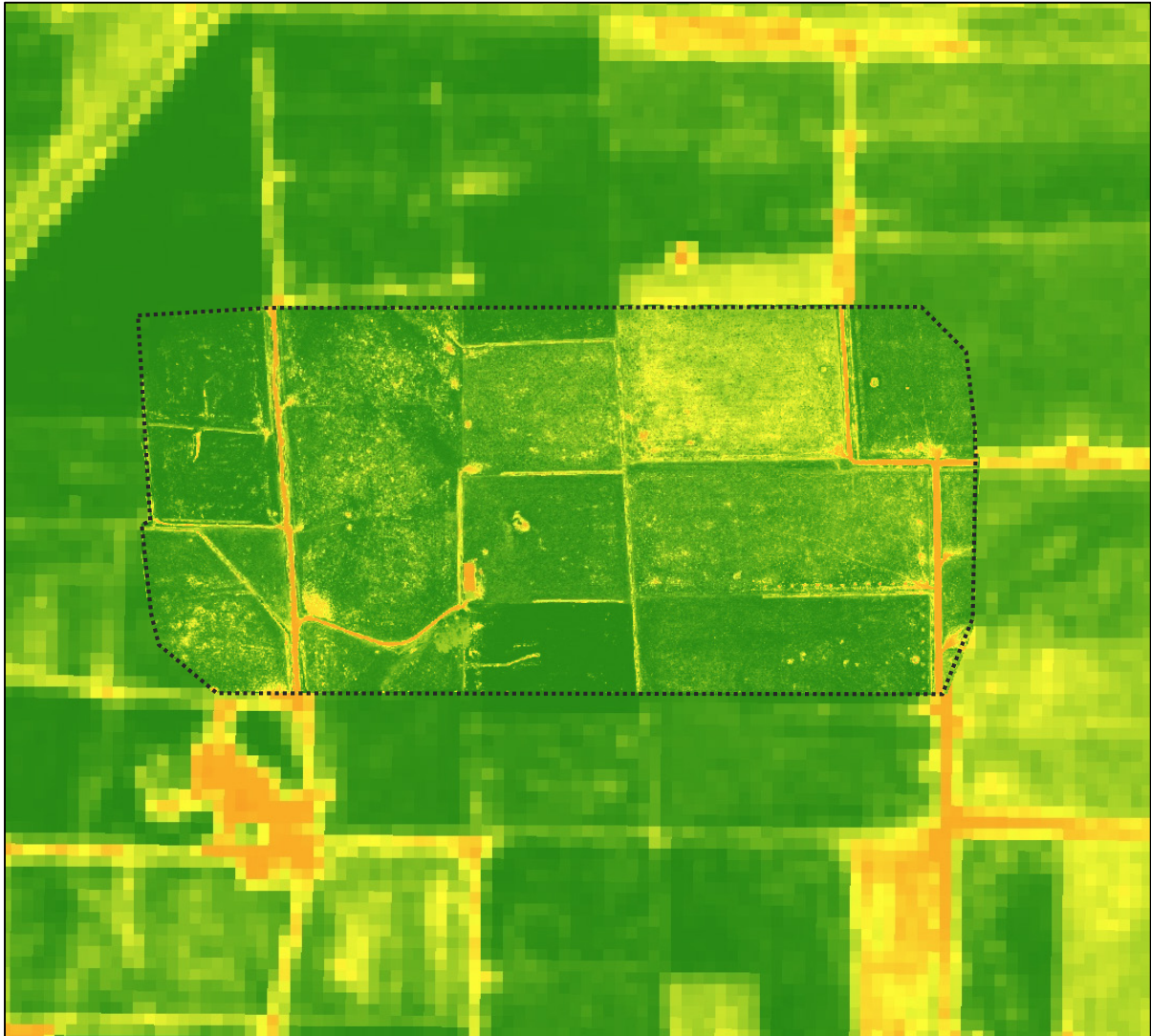


Figure 6.2 Overlay of UAV RET (high-resolution, 0.1 m x 0.1 m, in centre) on surrounding satellite (10 m x 10 m resolution) RET. The images are for the Collins lane area, surveyed with UAV on 17 May 2019.

6.3.2 RET Values Derived from UAV Data and Features Characterisation

Features such as roads, rooftops, bare land or dry vegetation show low values of RET (i.e., low AET). Highly vegetated areas have higher RET.

For the Substation site, UAV data show individual vines (Figure 6.3) and indicate that from May for the Northern area and from April for the Southern area the higher RET values observed were from the grass underlying the vines, as most of the vines had withered leaves or were leafless. Vegetation features underlying the vines show distinct patterns, which are likely due to variation in soil type (more discussion on this in Section 6.3.3).

For the Collins Lane site, UAV data attest of the evolution of the vegetation state and health over the investigation period, with healthier and greener vegetation in May compared to April 2019 (Figure 6.4).

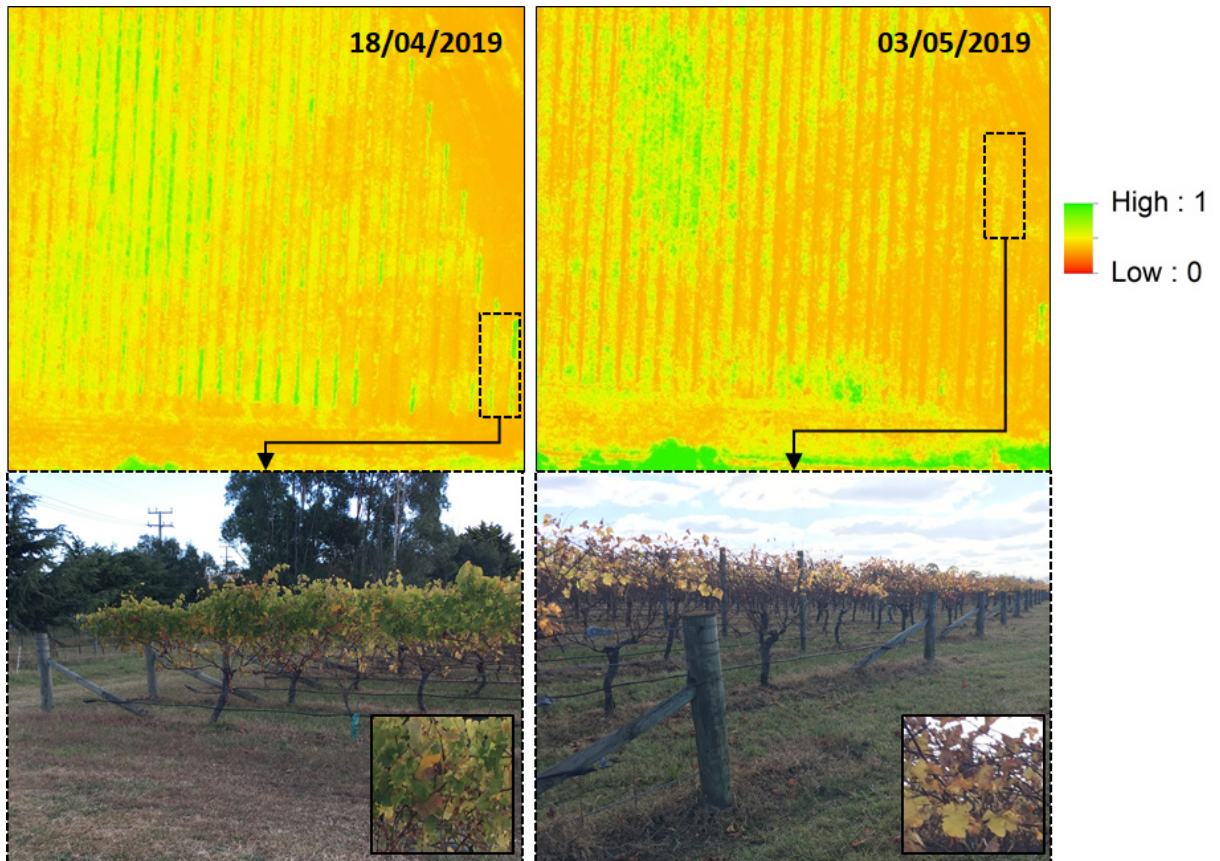


Figure 6.3 UAV derived RET and vegetation state at the time of data collection, Substation Northern area (18/04/2019 and 03/05/2019).

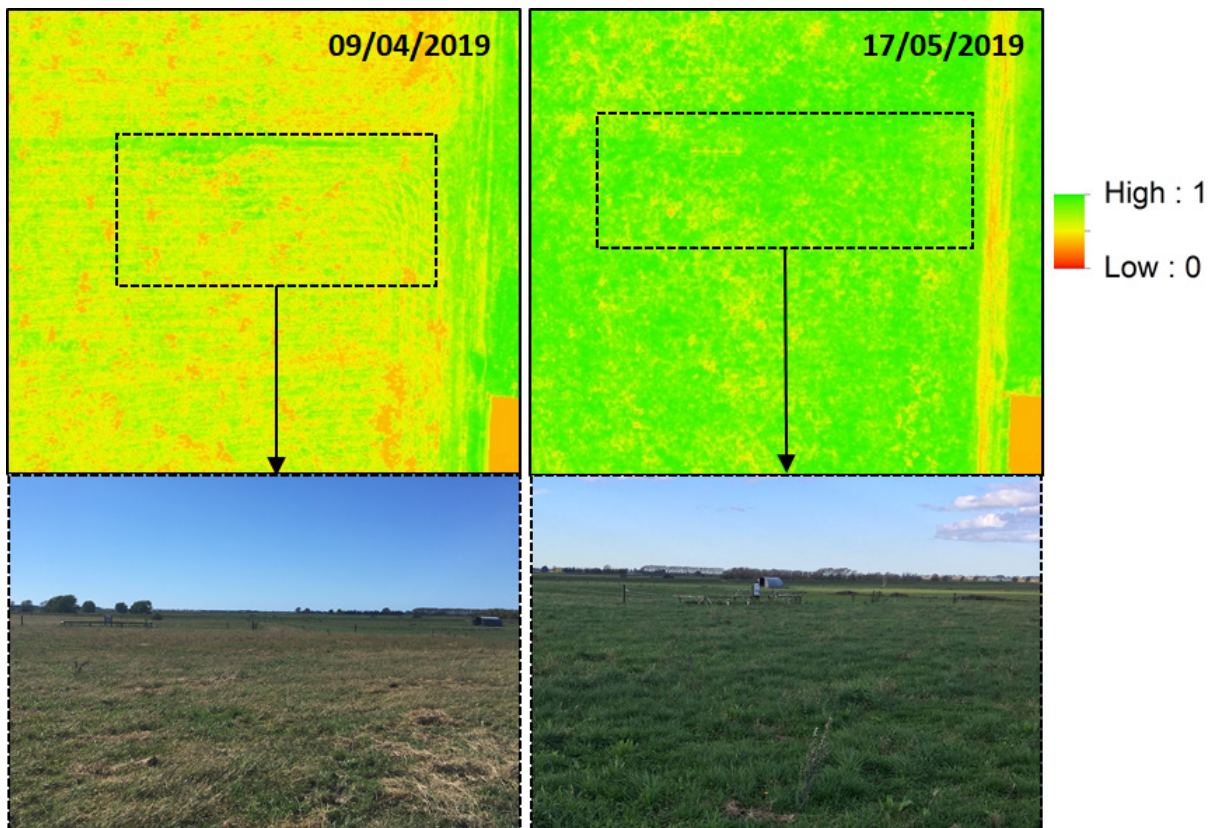


Figure 6.4 UAV derived RET and vegetation state at the time of data collection, Collins Lane (09/04/2019 and 17/05/2019).

6.3.3 RET Values Derived from UAV Data and Soil characterisation

More abundant or healthier vegetation has higher RET values, which can clearly be seen in some of the UAV images (e.g., Figure 6.5, left of the bottom image). NDVI also clearly distinguishes different vegetation health status, which are likely to be (partially) linked to differences in soil types (Figure 6.5, top image). The soil heterogeneity observed on the Substation UAV imagery (and also discernible on the aerial photograph) seems to correspond to former river meander channels. These features are known to introduce considerable variability in the sediment distribution (gravel, sand and clay) of the area, with coarser sediment prevailing within the paleochannels. The current soil classification in the area appears to be of much lower spatial resolution and reliability than the UAV multispectral-derived images shown in this example.

Hence, multispectral imagery, such as the UAV derived data presented in this study, can help to improve soil characterisation and could be a valuable addition to existing remote sensing methodologies (such as aerial imagery and LiDAR) for soil mapping studies.

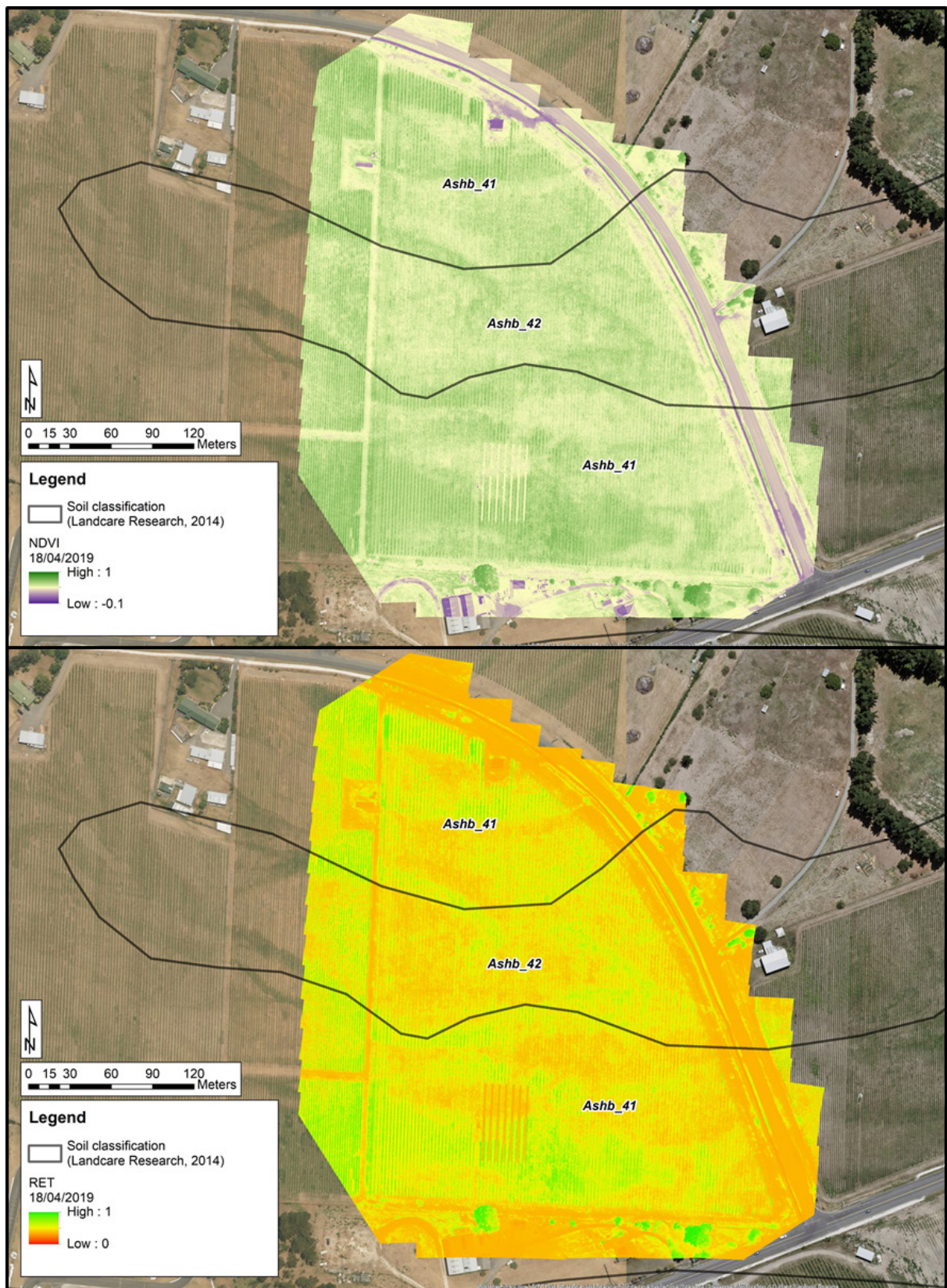


Figure 6.5 Relative evapotranspiration and soil classification, Substation Northern area (18/04/2019).

6.4 Estimated Recharge

The superior spatial resolution of UAV and satellite data, compared to coarser model estimates (e.g., a 1 km x 1 km model pixel), provides a substantial improvement to the spatial resolution of the long-term recharge model estimates (Figure 5.12 and Figure 5.13).

Similarly, satellite or UAV derived RET data are beneficial for dynamic recharge models, e.g. in a recharge model with daily, weekly or monthly time steps. In addition, UAV and satellite imagery are well-suited to capture seasonal changes in vegetation. However, the incorporation of a dynamic recharge model was not in the scope of this study and would require further development. If such a dynamic recharge model incorporating satellite data was developed it would involve large input and output datasets. For example, Sentinel-2 data has 10 m resolution and is currently acquired every 6 to 12 days over various areas of New Zealand. Assuming most current recharge models have a raster size of 100 m–100 m with a daily time step, the associated satellite datasets could easily be 100 times larger than a model cell, with a corresponding extensive computational resource required to rasterise the satellite data at the same temporal resolution (i.e., satellite data with 6–12 days resolution would need to be interpolated to daily values), and associated uncertainty. The use of cloud processing services is then highly recommended to avoid time consuming and excessive computational efforts on local computers if such an approach was developed.

6.5 Comparison of Lysimeter and UAV Derived Recharge Estimates

The project examined whether recharge measurements at individual lysimeter columns were discernible with the high-resolution UAV imagery of RET and recharge. For this purpose, RET and long-term recharge estimates (from Sections 5.3 and 5.4) are shown with lysimeter locations for the Collins Lane and Substation south sites (Figure 6.6). Differences in RET and recharge values can be seen for individual lysimeters (the lysimeter sites consist of three individual lysimeters, see Section 3.5). Spatial differences in RET and recharge in the UAV derived data are clearly visible at finer resolution than the diameter of the lysimeter column, meaning that the UAV data identify variations in recharge at the individual lysimeter scale. These variations may be associated with different evapotranspiration behaviours or with the mechanics of individual lysimeters. Other potential contributing factors are: the uncertainty of the exact location of each lysimeters column in the UAV image (sub-metre at Substation, but uncertain at Collins Lane); or artefacts of the installation procedure affecting the soil hydrology at individual lysimeters).

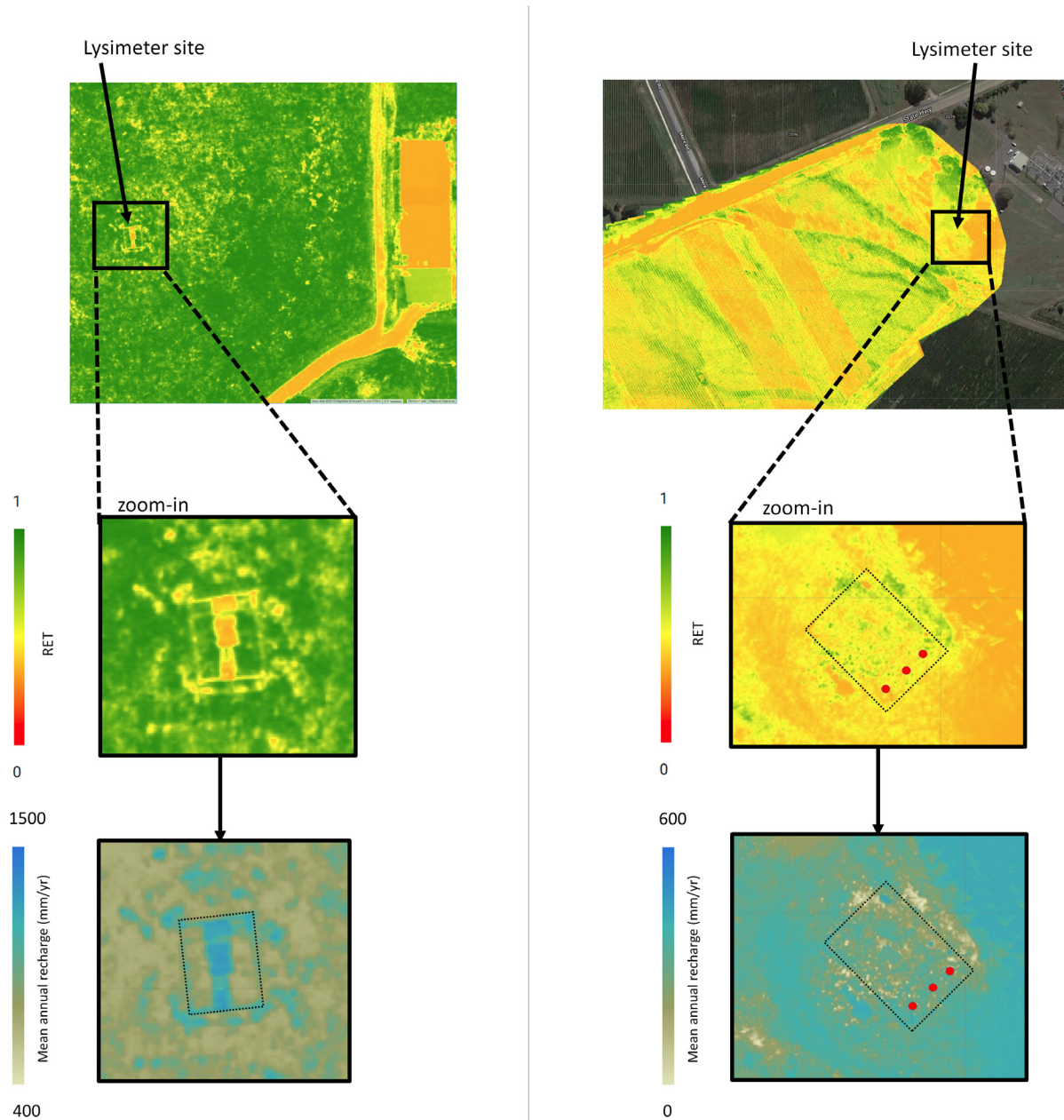


Figure 6.6 Relative evapotranspiration (RET) zoomed in on the lysimeter station at Collins Lane (left) and Substation south (right). Top and middle are RET, a (hypothetical long-term) recharge estimate is shown at the bottom. The locations of the individual lysimeters at lysimeter stations are indicated by red circles where they are known (not known for Collins Lane).

6.6 Spatial Representativeness of Lysimeters in Context of Satellite and UAV Data and Further Research

At the Collins Lane site, the paddock in which the lysimeters are located (Figure 6.7, red circle) was drier during the UAV data acquisition on 9 April 2019 compared to surrounding paddocks. These surrounding paddocks, were “greener”, indicating more abundant and healthier vegetation, i.e. higher soil moisture available for vegetation. Recharge would be expected to be different at these “green areas” due to this difference in soil moisture availability and vegetation. Reasons for those differences include: (1) different (higher) soil moisture availability causes more evapotranspiration; (2) different farm management practices (cattle grazing regimes, fertiliser inputs) cause different soil drainage patterns and vegetation growth;

(3) rainfall falling on less dense and or less healthy vegetation will have less uptake by plants, and rainfall would therefore infiltrate faster, or a larger fraction of rainfall is removed as runoff. The differences in soil moisture are also supported by the soil types (Section 3.4; Appendix 3). In the “drier area near the lysimeter”, Ngak_2 soils are characterised as “well drained”, with a smaller clay fraction and probably have a lower soil moisture in comparison to some of the soils underlying the “greener areas”, e.g., Ails_3 soils, characterised as “poorly drained”, with a larger clay fraction. More research is required on all mentioned processes, where recharge is influenced by vegetation.

As mentioned in Section 6.3.2 human-made features, such as roofs or roads can be easily distinguished in the UAV RET imagery (Figure 6.7). No transpiration occurs on these areas, and evaporation depends on the properties of the material (the most important property being a reflection property called ‘albedo’). Defining the difference in evaporation properties for human-made features was not an objective of this study: all these features were processed with the assumption of behaving as bare soil (Equation 4). Although evaporation differences might not vary greatly with slightly varying albedo, further research is required to quantify these differences.

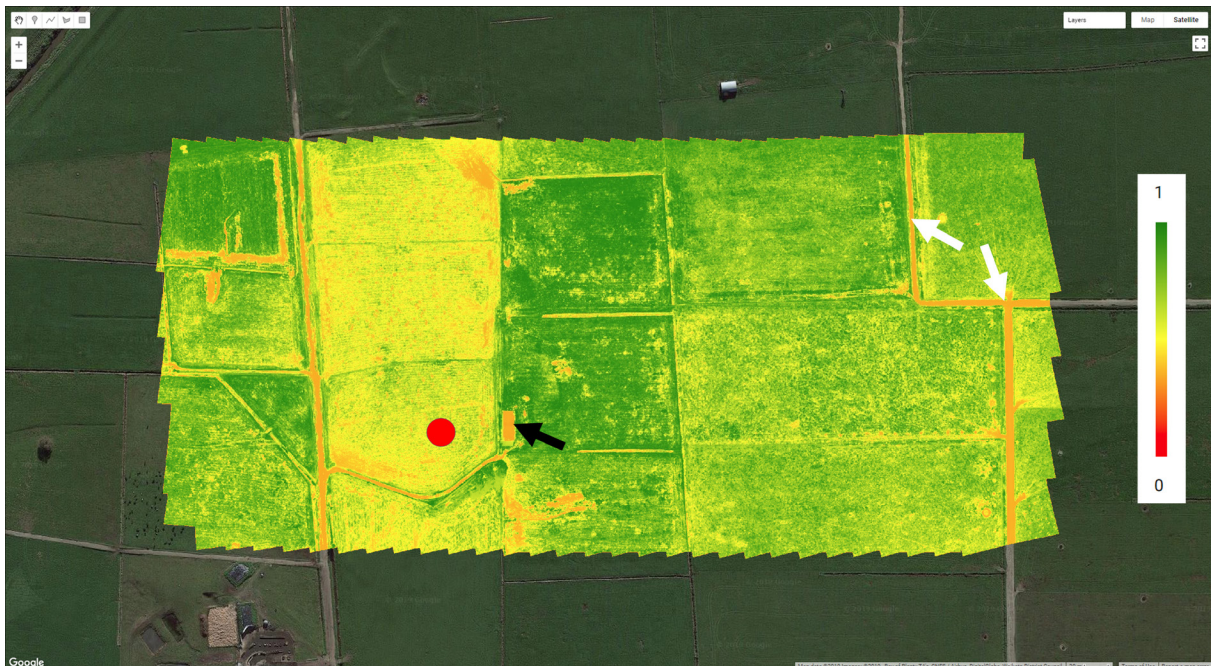


Figure 6.7 RET for Collins Lane UAV study area (9/04/2019), showing the location of the lysimeter station (red circle), roof of a shed (black arrow) and some examples of tracks (white arrows).

6.7 Recommendations

This study illustrates how remotely-sensed multispectral data can improve the spatial estimates of recharge, and factors involved in recharge estimation, such as the placement of lysimeters; the understanding of the role of human-made features (e.g., roads and roofs); and the characterisation of soil type and/or properties. Additional work is required on how to appropriately incorporate such high-resolution recharge information into existing or future recharge models.

Despite its good spatial representation, the remotely-sensed data provides a relatively poor temporal representation, which is the opposite of the lysimeter data, which provides good temporal data, but poor spatial representation.

The development of machine learning techniques, enabling the fusion of all available relevant data sets (i.e., rainfall, AET, groundwater elevation, soil types/properties and multispectral imagery) could provide improvements to both the spatial and temporal coverage.

Other improvements that were outside the scope of this study, but are recommended for follow-on work include:

- Improvements in the spatial resolution of rainfall data. As rainfall is the most dominant component of rainfall recharge, similar approaches to improve rainfall data resolution could be devised with remotely-sensed devices, e.g., using high-resolution rainfall from ground-based rainfall radar stations or using remotely-sensed surface soil moisture which can provide information on recent rainfall;
- Currently, it was assumed that non-vegetated features were all soil. However, for open water bodies, evaporation can be substantially higher. Therefore, identification of open water bodies and subsequent techniques to estimate of open water evaporation needs to be developed;
- This study identified different recharge characteristics at the Substation and Collins Lane sites (Section 6.1) and temporal variations within the same site, that highlight the influence of differences in soil properties at the local scale (e.g., water holding capacity of the soils) and recent climate conditions on recharge. However, this study did not characterise soil parameters, such as profile of available water (PAW) or fraction of transpirable soil (FTSW) water, and the influence of vegetation cover and soil type on these parameters – these aspects require research.

7.0 CONCLUSION

UAV and satellite derived multispectral data have been acquired and processed from a total of six surveys, three each at two sites, in the Hawke's Bay (Substation site) and Bay of Plenty (Collins Lane site) regions. The aim of these surveys was to provide proof of concept that multispectral data can be used to improve spatial representation of evapotranspiration and estimates of rainfall recharge to groundwater in the vicinity of the lysimeter sites.

Results showed that the combined use of UAV and satellite data can enhance the understanding of the spatial distribution of evapotranspiration and lead to improved recharge estimates. Relative evapotranspiration data (RET), derived by remotely-sensed spectral signals of vegetation and soil, can be used to scale PET to AET, which is one of the critical inputs in recharge estimation. As part of this work, RET values were input into a static (long-term and hypothetical) recharge estimate model of the study sites. Incorporation of satellite data provided estimates at 10 m resolution; UAV data provided estimates at 10 cm resolution.

Such datasets can contribute to the refinement of important factors involved in recharge estimation, such as: the placement of lysimeters; the understanding of the role of human-made features (e.g., roads and roofs); and improved characterisation of soil type and/or properties.

Results from the project also highlight the need to develop approaches that address how high-resolution recharge information can be appropriately incorporated into transient recharge models.

This study brings valuable insights for improved parametrisation in regional and local numerical models (e.g., Heretaunga Plains Groundwater Flow model in Hawke's Bay and the Kaituna, Makatu and Pongakawa Water Management Area groundwater flow model in Bay of Plenty), which will ultimately benefit water resource management practices (e.g., allocation limits, land use restrictions).

8.0 ACKNOWLEDGEMENTS

Our thanks go to the following regional council staff who provided a significant support and involvement in this project: Hawke's Bay Regional Council (Simon Harper, Senior Scientist - Groundwater; Thomas Wilding, Senior Scientist - Hydrology; Jeff Smith, Team Leader - Principal Scientist Hydrology - Hydrogeology; and Kim Coulson, Senior Resource Analyst - Hydrology); Bay of Plenty Regional Council : (Mitch Green, Environmental Scientist - Water Quantity and Raoul Fernandes, Science Team Leader - Hydrogeology, Hydrology and Geothermal).

The authors of this report would also like to acknowledge the landowners who gave permission to collect UAV imagery and access to their properties and the managers who helped us to organise the flights: Steve Wheeler (Mission Estate), Sandy Mowat (Delegats), Tony Smith (Babich Wines), David Verwey, David Marshall and Neil Bromley (Transpower Ltd).

Andrew Tait (NIWA) kindly provided the VCS climate data of rainfall and PET for this research.

Lastly, thanks to Conny Tschritter for reviewing this report.

9.0 REFERENCES

- Agisoft HelpDesk Portal. 2019. [accessed 2019 Jun 1].
<https://agisoft.freshdesk.com/support/solutions/articles/31000148381-micasense-altum-processing-workflow-including-reflectance-calibration-in-agisoft-metashape-professi>
- Anabalón, A., Sharma, A. 2017. On the divergence of potential and actual evapotranspiration trends: An assessment across alternate global datasets: *Earths Future* 5, 905–917.
<https://doi.org/10.1002/2016EF000499>
- Bay of Plenty Regional Council. 1990. Te Puke-Maketu Groundwater Resource Evaluation. Technical Publication No. 1. 52p + appendix.
- Brown, S. 2018. The Science Story Environmental Summary Report, Kaituna - Pongakawa– Waitahanui Water Management Area, WSP Opus report for Bay of Plenty Regional Council, 28 p.
- Cronshey, R., 1986. Urban hydrology for small watersheds. Technical Report TR-55, 164p., US Dept. of Agriculture, Soil Conservation Service, Engineering Division.
- Döll, P., Fiedler, K., 2008. Global-scale modeling of groundwater recharge. *Hydrology and Earth System Sciences* 12 (3), 863-885.
- Exiftool by Phil Harvey. 2019. [accessed 2019 Jun 1]. <https://www.sno.phy.queensu.ca/~phil/exiftool/>
- Food and Agriculture Organization of the United Nations. 1998. Crop evapotranspiration: guidelines for computing crop water requirements, FAO irrigation and drainage paper. Food and Agriculture Organization of the United Nations, Rome.
- Freeze, R., Cherry, J. 1979. *Groundwater*. Prentice-Hall, Inc., Englewood Cliffs, NJ.
- Gorelick, N., Hancher, M., Dixon, M., Ilyushchenko, S., Thau, D., Moore, R. 2017. Google Earth Engine: Planetary-scale geospatial analysis for everyone. *Remote Sens. Environ.*
<https://doi.org/10.1016/j.rse.2017.06.031>
- Hendriks, M.R. 2010. *Introduction to physical hydrology*. Oxford University Press, Oxford ; New York.
- Heron, D.W. (custodian). 2014. Geological Map of New Zealand 1:250 000. Lower Hutt (NZ):GNS Science. 1 DVD containing digital GIS vector data + all 21 QMAP texts as PDFs.

- Hong, T., White, P.A. 2015. Rainfall recharge estimation based on a nonlinear Bayesian technique with a dynamic state-space formulation in the Canterbury Plains (No. GNS Science Report 2014/37, 44p).
- Bay of Plenty Regional Council. 2019. Environmental data - Live monitoring for Kaituna at Te Matai site. [accessed 2019 Aug 28]. <https://monitoring.boprc.govt.nz/MonitoredSites/cgi-bin/hydwebservice/cgi/sites/details?site=187&treecatchment=22>
- Landcare Research. 2014. S-map - a new soil spatial information system for New Zealand. Lincoln (NZ): Landcare Research.
- Landcare Research. 2019. S-map—The digital soil map for New Zealand. Lincoln (NZ): Landcare Research. [accessed 2019 Jun 12]. <https://smap.landcareresearch.co.nz/app/>
- Lee, J. M.; Tschirter, C.; Begg, J. G. 2014. A 3D geological model of the greater Heretaunga/Ahuriri Groundwater Management Zone, Hawke's Bay. GNS Science Consultancy Report 2014/89. 31 p.
- Lovett, A.; and Cameron, S. 2013. Installation of rainfall recharge recording sites: Bridge Pa, Maraekakaho and Fernhill, Heretaunga Plains, Hawke's Bay. GNS Science Consultancy report CR 2013/05 51p.
- Micasense Knowledge Base. 2019. [accessed 2019 Jun 1]. <https://support.micasense.com/hc/en-us/articles/115000831714-How-to-Process-MicaSense-Sensor-Data-in-Pix4D>
- Morgenstern, U., Begg, J.G., van der Raaij, R.W., Moreau, M., Martindale, H., Daughney, C., Franzblau, R., Stewart, M., Knowling, M.J., Toews, M., Trompetter, V., Kaiser, J., Gordon, D. 2017. Heretaunga Plains Aquifers: Groundwater Dynamics, Source and Hydrochemical Processes as Inferred from Age and Chemistry Tracer Data. Lower Hutt (NZ): GNS Science. 82 p. (GNS Science report 2017/33). doi:10.21420/G2Q92G.
- Mu, Q., Heinsch, F.A., Zhao, M., Running, S.W. 2007. Development of a global evapotranspiration algorithm based on MODIS and global meteorology data. Remote Sens. Environ. 111, 519–536.
- Mu, Q., Zhao, M., Running, S.W. 2011. Improvements to a MODIS global terrestrial evapotranspiration algorithm. Remote Sens. Environ. 115, 1781–1800. <https://doi.org/10.1016/j.rse.2011.02.019>
- Myneni, R.B., Knyazikhin, Y., Zhang, Y., Tian, Y., Wang, Y., Lotsch, A., Privette, J.L., Morisette, J.T., Running, S.W., Nemani, R., Glassy, J., Votava, P., 1999. MODIS Leaf Area Index (LAI) And Fraction Of Photosynthetically Active Radiation Absorbed By Vegetation (FPAR) Product (MOD15) (No. Algorithm Theoretical Basis Document Version 4.0), <http://eospsso.gsfc.nasa.gov/atbd/modistables.html>).
- New Zealand Government. 1991, Resource Management Act, Author, Wellington, N.Z.
- NIWA. 2014. CliFlo: the national climate database. [accessed 2019 May 21]. <http://cliflo.niwa.co.nz>.
- Pix4D support. 2019. [accessed 2019 Jun 1]. <https://support.pix4d.com/hc/en-us/articles/202557759-Menu-Process-Processing-Options-1-Initial-Processing-General>
- Rajanayaka C., Fisk L. 2018. Irrigation water demand and land surface assessment for Heretaunga Plains. Aqualinc, 28 p.
- Rakowski, P., and Knowling, M. 2018. Heretaunga Aquifer Groundwater Model - Development Report. Hawke's Bay Regional Council, 182 p.
- Rushton, K.R., Eilers, V.H.M., Carter, R.C. 2006. Improved soil moisture balance methodology for recharge estimation. J. Hydrol. 318, 379–399. <https://doi.org/10.1016/j.jhydrol.2005.06.022>

- Scott, D.M. 2004. Groundwater Allocation Limits: land-based recharge estimates. No. Environment Canterbury Report U04/97.
- Soil Science Society of America. 2008. Glossary of soil science terms. Madison (WI): Soil Science Society of America. 93 p.
- Suren, A., Park, S., Carter, R., Fernandes R., Bloor, M., Barber, J., Dean, S. 2016. Kaituna-Maketū and Pongakawa-Waitahanui WMA: Current State and Gap Analysis, Bay of Plenty Regional Council Environmental Publication 2016/01, 155 p.
- Tait, A.; Henderson, R.; Turner, R.; Zheng, X. 2006. Thin plate smoothing spline interpolation of daily rainfall for New Zealand using a climatological rainfall surface. *Int. J. Climatol.*, 26, 2097–2115.
- Tschirter, C., Rawlinson, Z., White, P.A., Schaller, K. 2016. Update of the 3D geological models for the Western Bay of Plenty and Paengaroa-Matata area, GNS Science Consultancy Report 2015/196.
- Verhoef, A., Egea, G. 2014. Modeling plant transpiration under limited soil water: Comparison of different plant and soil hydraulic parameterizations and preliminary implications for their use in land surface models. *Agric. For. Meteorol.* 191, 22–32.
<https://doi.org/10.1016/j.agrformet.2014.02.009>.
- Waldron, R., Kozyniak K. 2017. Hawke's Bay hydrological data 2008-2014 - State of the Environment technical report (draft). Hawke's Bay Regional Council.
- Wilding, T.K. 2018. Heretaunga Springs: Gains and losses of stream flow to groundwater on the Heretaunga Plains. HBRC Report No. RM18-13 – 4996, Hawke's Bay Regional Council. 92 p.
- Westenbroek, S.M., Kelson, V.A., Dripps, W.R., Hunt, R.J., Bradbury, K.R. 2010. SWB - A Modified Thornthwaite-Mather Soil-Water-Balance Code for Estimating Groundwater Recharge. No. U.S. Geological Survey Techniques and Methods 6-A31, 60 p.
- Westerhoff, R., White, P., Rawlinson, Z. 2018. Incorporation of Satellite Data and Uncertainty in a Nationwide Groundwater Recharge Model in New Zealand. *Remote Sens.* 10, 58 p.
<https://doi.org/10.3390/rs10010058>
- Westerhoff, R.S. 2017. Satellite remote sensing for improvement of groundwater characterisation (PhD thesis). University of Waikato, Hamilton, New Zealand.
- Westerhoff, R.S. 2015. Using uncertainty of Penman and Penman–Monteith methods in combined satellite and ground-based evapotranspiration estimates. *Remote Sens. Environ.* 169, 102–112. <https://doi.org/10.1016/j.rse.2015.07.021>
- White, P.A., Hong, Y.-S., Murray, D.L., Scott, D.M., Thorpe, H.R. 2003. Evaluation of regional models of rainfall recharge to groundwater by comparison with lysimeter measurements, Canterbury, New Zealand. *J. Hydrol. NZ* 42, 39–64.
- White, P.A.; Lovett, A.P.; Gordon, D. 2017. Quality control and quality assurance of Hawke's Bay rainfall recharge measurements: 2011-2014. Lower Hutt, N.Z.: GNS Science. GNS Science report 2016/16. 21 p.; doi: 10.21420/G28G6P.
- White, P.A.; Meilhac, C.; Zemansky, G.M.; Kilgour, G.N. 2009. Groundwater resource investigations of the western Bay of Plenty area stage 1: conceptual geological and hydrological models and preliminary allocation assessment. GNS Science consultancy report 2008/240. 221 p.
- White, P.A., Tschirter, C., Westerhoff, R., Lovett, A. 2014. Rainfall recharge models of the Heretaunga Plains, GNS Science Report 2013/50, 48 p.

APPENDICES

This page left intentionally blank.

APPENDIX 1 EXPLANATION OF EVAPOTRANSPIRATION AND THE RELATION TO SOIL WATER DEFICIT

A1.1 Relation between NDVI, LAI and FPAR Used in this Study

Table A1.1 NDVI and Corresponding Values of LAI and FPAR (Myneni et al. 1999).

NDVI	Grassland / cereal crops		Shrubland		Broadleaf crop		Savannah		Broadleaf forest		Needle lead forest	
	LAI	FPAR	LAI	FPAR	LAI	FPAR	LAI	FPAR	LAI	FPAR	LAI	FPAR
0.025	0	0	0	0	0	0	0	0	0	0	0	0
0.075	0	0	0	0	0	0	0	0	0	0	0	0
0.125	0.3199	0.1552	0.2663	0.1389	0.2452	0.132	0.2246	0.1179	0.1516	0.07028	0.1579	0.08407
0.175	0.431	0.2028	0.3456	0.1741	0.3432	0.1774	0.3035	0.1554	0.1973	0.08922	0.2239	0.1159
0.225	0.5437	0.2457	0.4357	0.2103	0.4451	0.2192	0.4452	0.218	0.2686	0.1187	0.324	0.1618
0.275	0.6574	0.2855	0.5213	0.2453	0.5463	0.2606	0.574	0.2731	0.3732	0.1619	0.4393	0.2121
0.325	0.7827	0.3283	0.6057	0.2795	0.6621	0.3091	0.7378	0.3395	0.5034	0.2141	0.5629	0.2624
0.375	0.931	0.3758	0.6951	0.3166	0.7813	0.3574	0.878	0.393	0.6475	0.2714	0.664	0.3028
0.425	1.084	0.419	0.8028	0.3609	0.8868	0.3977	1.015	0.4425	0.7641	0.32	0.7218	0.333
0.475	1.229	0.4578	0.9313	0.4133	0.9978	0.4357	1.148	0.4839	0.9166	0.3842	0.8812	0.393
0.525	1.43	0.5045	1.102	0.4735	1.124	0.4754	1.338	0.5315	1.091	0.4402	1.086	0.4599
0.575	1.825	0.571	1.31	0.535	1.268	0.5163	1.575	0.5846	1.305	0.4922	1.381	0.5407
0.625	2.692	0.6718	1.598	0.6039	1.474	0.566	1.956	0.6437	1.683	0.568	1.899	0.6458
0.675	4.299	0.8022	1.932	0.666	1.739	0.6157	2.535	0.6991	2.636	0.702	2.575	0.7398
0.725	5.362	0.8601	2.466	0.7388	2.738	0.7197	4.483	0.8336	3.557	0.7852	3.298	0.8107
0.775	5.903	0.8785	3.426	0.822	5.349	0.8852	5.605	0.8913	4.761	0.8431	4.042	0.8566
0.825	6.606	0.9	4.638	0.8722	6.062	0.9081	5.777	0.8972	5.52	0.8697	5.303	0.8964
0.875	6.606	0.9	6.328	0.9074	6.543	0.9196	6.494	0.9169	6.091	0.8853	6.501	0.9195
0.925	6.606	0.9	6.328	0.9074	6.543	0.9196	6.494	0.9169	6.091	0.8853	6.501	0.9195
0.975	6.606	0.9	6.328	0.9074	6.543	0.9196	6.494	0.9169	6.091	0.8853	6.501	0.9195

A1.2 Relation to Soil Water Deficit

Although this study did not estimate soil water properties, initial research was undertaken towards this possibility. This section details that research.

Relative transpiration is the ratio between actual evapotranspiration (AET) and potential evapotranspiration (PET) and is an indicator of soil water deficit. Many empirical relations between RT and soil water deficit exist, the most comprehensive being the study of Verhoef and Egea (2014), who assessed relative transpiration as function of the fraction of transpirable soil water (FTSW). FTSW is independent of soil type, because it is calculated as a normalised index:

$$FTSW = \frac{\theta - \theta_{WP}}{\theta_{FC} - \theta_{WP}}$$

with θ the soil moisture, WP the wilting point and FC the field capacity. For 13 different crops of vegetation, they assessed RT and FTSW and their relation (Figure A1.1). Other relations between RT and soil water are described by e.g., Food and Agriculture Organization of the United Nations (1998) and Rushton et al. (2006).

Figure A1.1 can be used to convert RT to FTSW. For example, if the Leaf Area Index is known, we can estimate water stress r_s . However, to translate RT to FTSW it should be noted that it is assumed that the whole area measured with satellite data is fully covered with vegetation. If this is not the case, corrections to this algorithm should be made.

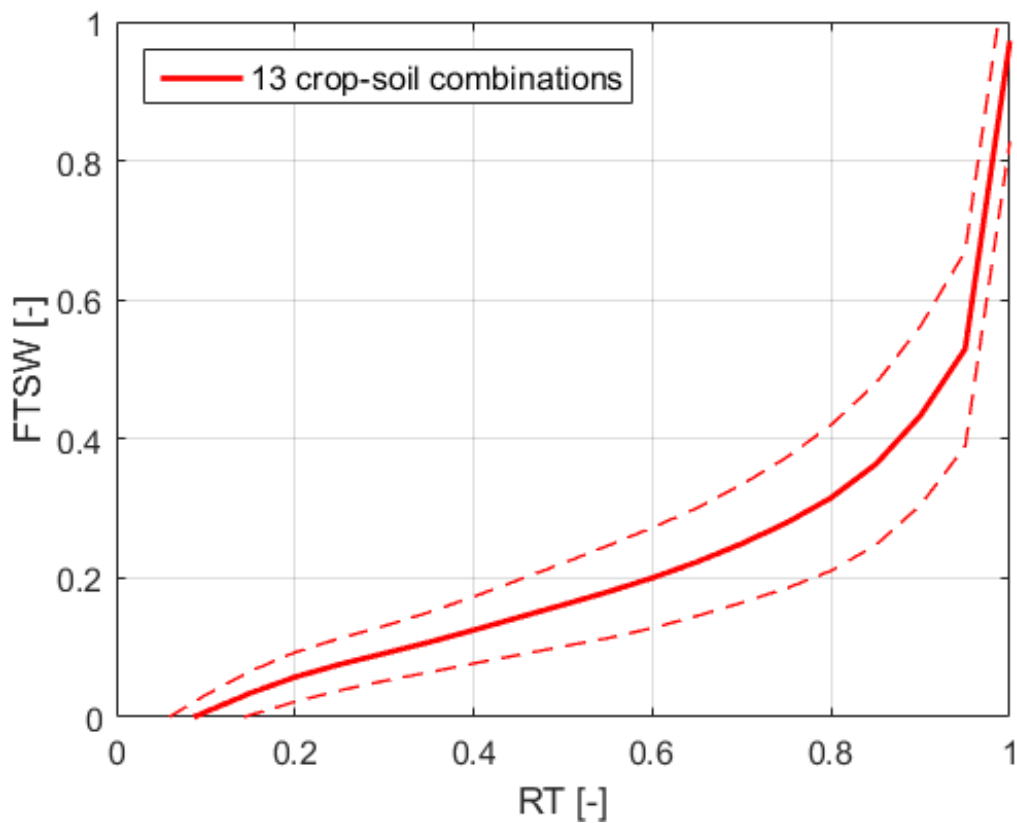


Figure A1.1 Relation between relative transpiration (RT = AET/PET) and fraction of transpirable soil water (FTSW) for 13 crop-soil combinations. Data from Verhoef and Egea (2014).

APPENDIX 2 LOCATION OF SITE GEOLOGICAL CROSS-SECTIONS

A2.1 Substation Site

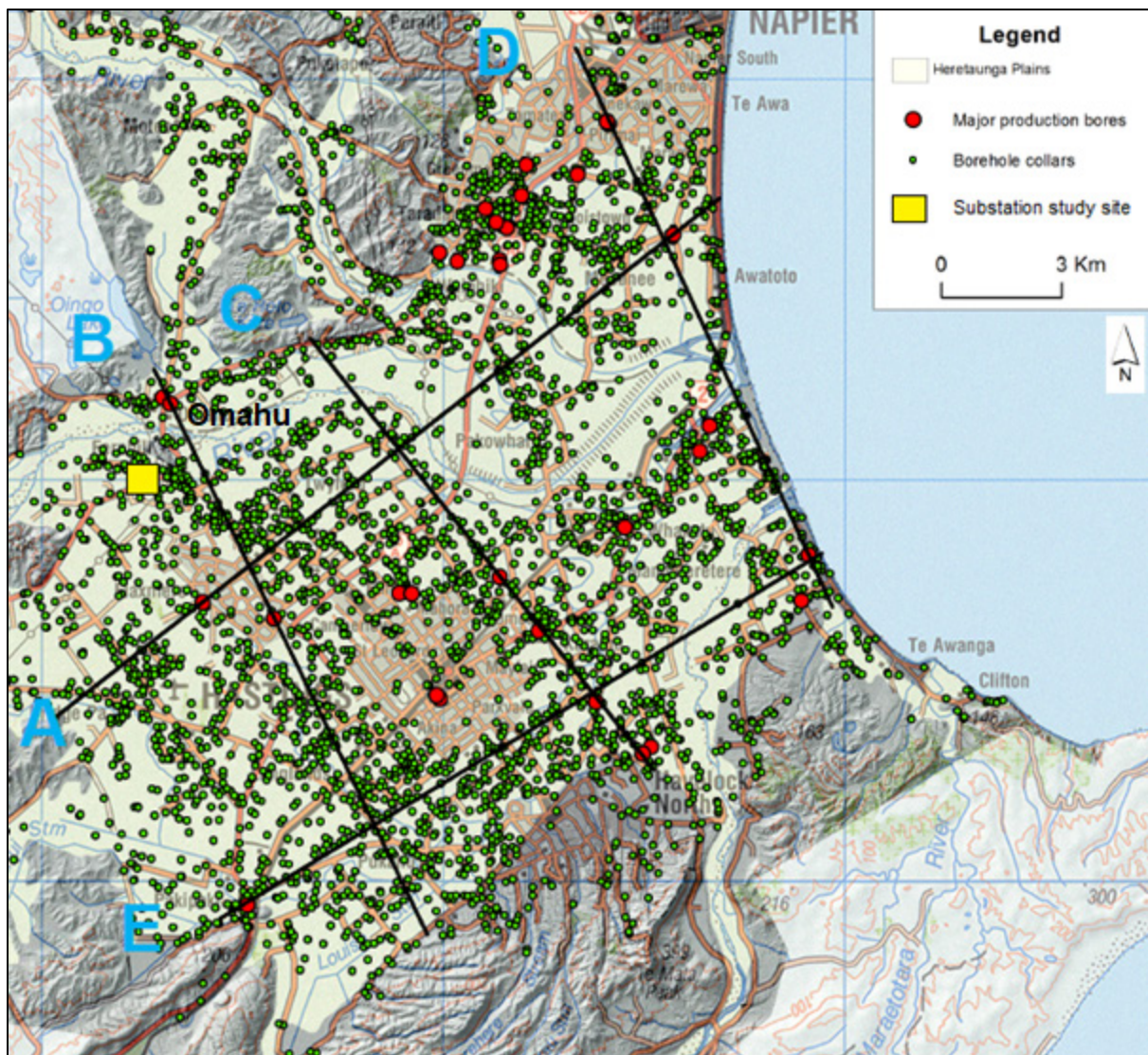


Figure A2.1 Location of the cross-section presented in the report for Substation site (Section 3.3.1). The cross-section is cross-section B through Omahu near Substation study site (after Morgenstern et al. 2017).

A2.2 Collins Lane Site

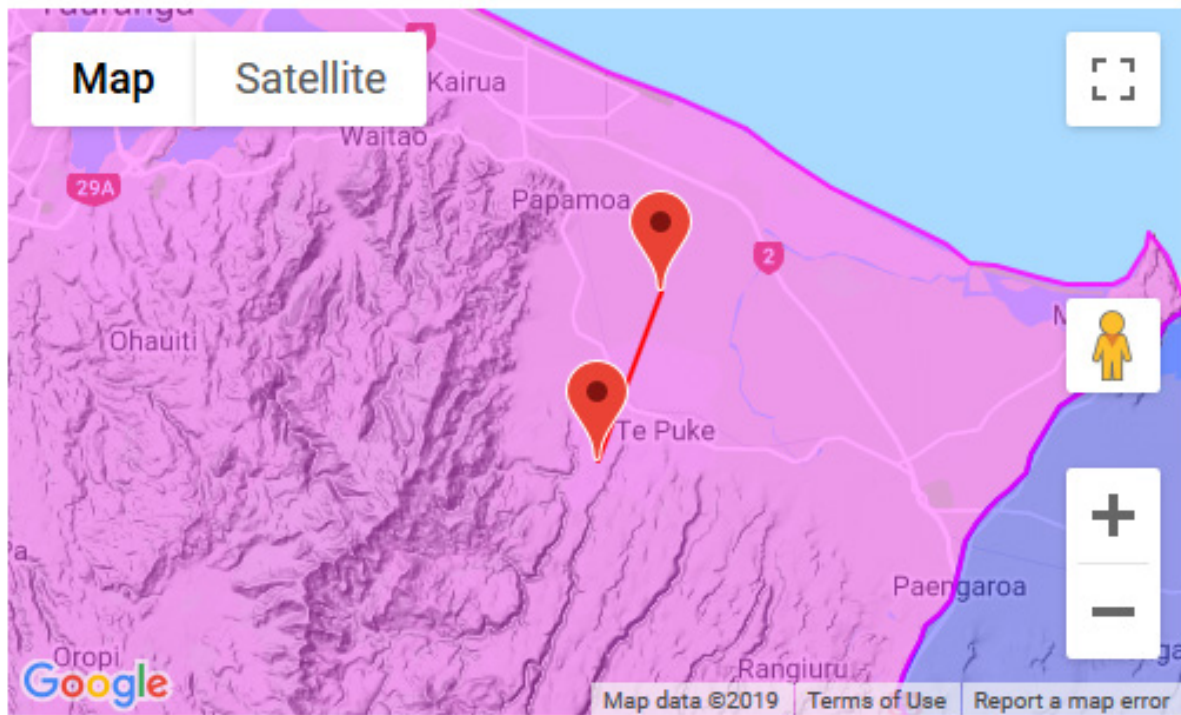


Figure A2.2 Location of the cross-section presented in the report for Collins Lane site (Section 3.3.2). Cross-section retrieved from EBOF (<https://data.gns.cri.nz/ebof/>) (based on Tschritter et al. 2016).

APPENDIX 3 SOIL REPORTS

A3.1 Substation Site



SOIL REPORT

Hawke's Bay Regional Council

Report generated: 12-Jun-2019 from <https://smap.landcareresearch.co.nz>

This information sheet describes the typical average properties of the specified soil to a depth of 1 metre, and should not be the primary source of data when making land use decisions on individual farms and paddocks.

S-map correlates soils across New Zealand. Both the old soil name and the new correlated (soil family) name are listed below.

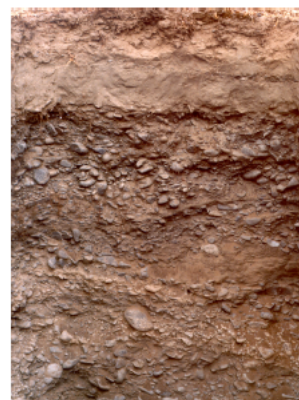
Family: Ashburtonf

Smapp ref: Ashb_41a.1

Omahu (Ashburton_41a.1)

Key physical properties

Depth class (diggability)	Very shallow (5 - 15 cm)
Texture profile	Sandy loam
Potential rooting depth	Unlimited
Rooting barrier	No significant barrier within 1 m
Topsoil stoniness	Moderately stony
Topsoil clay range	0 - 2 %
Drainage class	Moderately well drained
Aeration in root zone	Unlimited
Permeability profile	Rapid
Depth to slowly permeable horizon	No slowly permeable horizon
Permeability of slowest horizon	Rapid (> 72 mm/h)
Profile available water	Low (59 mm)
	(0 - 100cm or root barrier)
	Low (38 mm)
	(0 - 60cm or root barrier)
	Low (21 mm)
	(0 - 30cm or root barrier)
Dry bulk density, topsoil	1.18 g/cm ³
Dry bulk density, subsoil	1.42 g/cm ³
Depth to hard rock	No hard rock within 1 m
Depth to soft rock	No soft rock within 1 m
Depth to stony layer class	Shallow



Key chemical properties

Topsoil P retention Very Low (3%)

About this publication

- This information sheet describes the *typical average properties* of the specified soil.
- For further information on individual soils, contact Landcare Research New Zealand Ltd: www.landcareresearch.co.nz
- Advice should be sought from soil and land use experts before making decisions on individual farms and paddocks.
- The information has been derived from numerous sources. It may not be complete, correct or up to date.
- This information sheet is licensed by Landcare Research on an "as is" and "as available" basis and without any warranty of any kind, either express or implied.
- Landcare Research shall not be liable on any legal basis (including without limitation negligence) and expressly excludes all liability for loss or damage howsoever and whenever caused to a user of this factsheet.



© Landcare Research New Zealand Limited 2019. Licensed under Creative Commons Attribution - NonCommercial - No Derivative Works 3.0 New Zealand License (BY-NC-ND)



Figure A3.1 Ashb_41 soil report-part 1 (Landcare Research 2019).

Family: Ashburtonf

Smop ref: Ashb_41a.1

Omahu (Ashburton_41a.1)

Additional factors to consider in choice of management practices

Vulnerability classes relate to soil properties only and do not take into account climate or management

Soil structure integrity

Structural vulnerability	Very high (1.00)
Pugging vulnerability	not available yet

Water management

Water logging vulnerability	Very low
Drought vulnerability - if not irrigated	High
Bypass flow	High
Hydrological soil group	A

Contaminant management

N leaching vulnerability	Very high
P leaching vulnerability	not available yet
Bypass flow	High
Dairy effluent (FDE) risk category	C if slope > 7 deg otherwise E

Relative Runoff Potential	Slope	0-3°	4-7°	8-15°	16-25°	>25°
	Risk	VL	VL	VL	VL	L

Additional information

Soil classification	Fluvial Raw Soils (WF)
Family	Ashburtonf
Sibling number	41
Profile texture group	Sandy
Soil profile material	Rounded stony soil
Rock class of stones/rocks	From hard sandstone rock
Rock origin of fine earth	From hard sandstone rock
Parent material origin	Alluvium

Characteristics of functional horizons in order from top to base of profile:

Functional Horizon	Thickness	Stones	Clay*	Sand*
Stony Sandy Weak	0 - 5 cm	15 - 30 %	0 - 2 %	85 - 95 %
Stony Sandy Loose	5 - 15 cm	15 - 30 %	0 - 2 %	85 - 95 %
Very Stony Sandy Loose	80 - 95 cm	40 - 65 %	0 - 2 %	85 - 95 %

* clay and sand percent values are for the mineral fines (excludes stones). Silt = 100 - (clay + sand)



© Landcare Research New Zealand Limited 2019. Licensed under Creative Commons Attribution - NonCommercial - No Derivative Works 3.0 New Zealand License (BY-NC-ND)



Figure A3.2 Ashb_41 soil report–part 2 (Landcare Research 2019).

Report generated: 12-Jun-2019 from <https://smap.landcareresearch.co.nz>

This information sheet describes the typical average properties of the specified soil to a depth of 1 metre, and should not be the primary source of data when making land use decisions on individual farms and paddocks.

S-map correlates soils across New Zealand. Both the old soil name and the new correlated (soil family) name are listed below.

Family: Ashburtonf

Smmap ref: Ashb_42a.1

Omahu (Ashburton_42a.1)

Key physical properties

Depth class (diggability)	Shallow (15 - 35 cm)
Texture profile	Sandy loam
Potential rooting depth	Unlimited
Rooting barrier	No significant barrier within 1 m
Topsoil stoniness	Moderately stony
Topsoil clay range	0 - 2 %
Drainage class	Moderately well drained
Aeration in root zone	Unlimited
Permeability profile	Rapid
Depth to slowly permeable horizon	No slowly permeable horizon
Permeability of slowest horizon	Rapid (> 72 mm/h)
Profile available water	Moderate to low (69 mm)
	(0 - 100cm or root barrier)
	(0 - 60cm or root barrier) Low (44 mm)
	(0 - 30cm or root barrier) Low (25 mm)
Dry bulk density, topsoil	1.18 g/cm ³
Dry bulk density, subsoil	1.42 g/cm ³
Depth to hard rock	No hard rock within 1 m
Depth to soft rock	No soft rock within 1 m
Depth to stony layer class	Shallow



Key chemical properties

Topsoil P retention Very Low (3%)

About this publication

- This information sheet describes the *typical average properties* of the specified soil.
- For further information on individual soils, contact Landcare Research New Zealand Ltd: www.landcareresearch.co.nz
- Advice should be sought from soil and land use experts before making decisions on individual farms and paddocks.
- The information has been derived from numerous sources. It may not be complete, correct or up to date.
- This information sheet is licensed by Landcare Research on an "as is" and "as available" basis and without any warranty of any kind, either express or implied.
- Landcare Research shall not be liable on any legal basis (including without limitation negligence) and expressly excludes all liability for loss or damage howsoever and whenever caused to a user of this factsheet.

Omahu (Ashburton_42a.1)

Additional factors to consider in choice of management practices

Vulnerability classes relate to soil properties only and do not take into account climate or management

Soil structure integrity

Structural vulnerability Very high (1.00)
 Pugging vulnerability not available yet

Water management

Water logging vulnerability Very low
 Drought vulnerability - if not irrigated Moderate
 Bypass flow High
 Hydrological soil group A

Contaminant management

N leaching vulnerability Very high
 P leaching vulnerability not available yet
 Bypass flow High
 Dairy effluent (FDE) risk category C if slope > 7 deg otherwise E

Relative Runoff Potential

Slope	0-3°	4-7°	8-15°	16-25°	>25°
Risk	VL	VL	VL	VL	L

Additional information

Soil classification Fluvial Raw Soils (WF)
 Family Ashburtonf
 Sibling number 42
 Profile texture group Sandy
 Soil profile material Rounded stony soil
 Rock class of stones/rocks From hard sandstone rock
 Rock origin of fine earth From hard sandstone rock
 Parent material origin Alluvium

Characteristics of functional horizons in order from top to base of profile:

Functional Horizon	Thickness	Stones	Clay*	Sand*
Stony Sandy Weak	0 - 5 cm	20 - 30 %	0 - 2 %	85 - 95 %
Stony Sandy Loose	15 - 30 cm	20 - 30 %	0 - 2 %	85 - 95 %
Very Stony Sandy Loose	65 - 85 cm	40 - 50 %	0 - 2 %	85 - 95 %

* clay and sand percent values are for the mineral fines (excludes stones). Silt = 100 - (clay + sand)



© Landcare Research New Zealand Limited 2019. Licensed under Creative Commons Attribution - NonCommercial - No Derivative Works 3.0 New Zealand License (BY-NC-ND)



Figure A3.4 Ashb_42 soil report–part 2 (Landcare Research 2019).

A3.2 Collins Lane Site



S-map Soil Report

Environment Bay of Plenty

Report generated: 12-Jun-2019 from <https://smap.landcareresearch.co.nz>

S-map maps soils at a nominal scale of 1:50,000. At this scale it is common to identify two or more soil siblings that are likely to be present at the selected location. A more detailed resolution is needed to produce map units comprising a single soil sibling. Therefore, it is recommended that users consider the characteristics of each of the identified siblings, the expected proportion of each, and select the S-map sibling that best matches their field observations of the paddock. If no local information is available then it is common practice to select the dominant S-map sibling, i.e. the first listed sibling.

This information sheet describes the typical average properties of the specified soil to a depth of 1 metre, and should not be the primary source of data when making land use decisions on individual farms and paddocks.

Ohineangaagaf

Typic Acid Gley Soil

Ohin_1a.1 (100% of the mapunit at location (1891928, 5815172), Confidence: High)

Key physical properties

Depth class (diggability)	Deep (> 1 m)
Texture profile	Loam
Potential rooting depth	Unlimited
Rooting barrier	No significant barrier within 1 m
Topsoil stoniness	Stoneless
Topsoil clay range	20 - 30 %
Drainage class	Poorly drained
Aeration in root zone	Very limited
Permeability profile	Moderate Over Slow
Depth to slowly permeable horizon	15 - 80 (cm)
Permeability of slowest horizon	Slow (< 4 mm/h)
Profile available water	(0 - 100cm or root barrier) Very high (265 mm) (0 - 60cm or root barrier) Very high (157 mm) (0 - 30cm or root barrier) Very high (84 mm)
Dry bulk density, topsoil	0.94 g/cm ³
Dry bulk density, subsoil	1.22 g/cm ³
Depth to hard rock	No hard rock within 1 m
Depth to soft rock	No soft rock within 1 m
Depth to stony layer class	No significant stony layer within 1 m

Key chemical properties

Topsoil P retention Medium (52%)

About this publication

- This information sheet describes the typical average properties of the specified soil to a depth of 1 metre.
- For further information on individual soils, contact Landcare Research New Zealand Ltd: www.landcareresearch.co.nz
- Advice should be sought from soil and land use experts before making decisions on individual farms and paddocks.
- The information has been derived from numerous sources. It may not be complete, correct or up to date.
- This information sheet is licensed by Landcare Research on an "as is" and "as available" basis and without any warranty of any kind, either express or implied.
- Landcare Research shall not be liable on any legal basis (including without limitation negligence) and expressly excludes all liability for loss or damage howsoever and whenever caused to a user of this factsheet.



© Landcare Research New Zealand Limited 2019. Licensed under Creative Commons Attribution - NonCommercial - No Derivative Works 3.0 New Zealand License (BY-NC-ND)



Figure A3.5 Ohin_1 soil report–part 1 (Landcare Research 2019).

Ohineangaagaf

S-map ref: Ohin_1a.1

Ohin_1a.1 (100% of the mapunit at location (1891928, 5815172), Confidence: High)

Additional factors to consider in choice of management practices

Vulnerability classes relate to soil properties only and do not take into account climate or management

Soil structure integrity

Structural vulnerability	Moderate (0.52)
Pugging vulnerability	not available yet

Water management

Water logging vulnerability	High
Drought vulnerability - if not irrigated	Low
Bypass flow	High
Hydrological soil group	C/D
Irrigability	Flat to very gently undulating land with severe drainage/permeability restrictions and soils with high to very high PAW

Contaminant management

N leaching vulnerability	Very Low
P leaching vulnerability	not available yet
Bypass flow	High
Dairy effluent (FDE) risk category	B
Relative Runoff Potential	Low

Additional information

Soil classification	Typic Acid Gley Soils
Family	Ohineangaagaf
Sibling number	1
Profile texture group	Loamy
Soil profile material	Tephric soil
Rock class of stones/rocks	From Rhyolitic Rock
Rock origin of fine earth	From Rhyolitic Rock
Parent material origin	Alluvium

Characteristics of functional horizons in order from top to base of profile:

Functional Horizon	Thickness	Stones	Clay*	Sand*
Loamy Fine Slightly Firm, Acidic Tephric	16 - 20 cm	0 %	20 - 30 %	60 - 65 %
Loamy Fine Slightly Firm, Acidic Tephric	8 - 10 cm	0 %	10 - 12 %	75 - 80 %
Loamy Fine Firm, Acidic Tephric	12 - 15 cm	0 - 10 %	10 - 15 %	75 - 80 %
Stony (lapilli) Sandy Loose, Acidic Tephric	8 - 15 cm	5 - 20 %	1 - 5 %	85 - 90 %
Loamy Fine Slightly Firm, Acidic Tephric	30 - 40 cm	0 %	8 - 10 %	75 - 80 %
Loamy Weak, Acidic Tephric	0 - 25 cm	0 %	8 - 10 %	60 - 75 %

* clay and sand percent values are for the mineral fines (excludes stones). Silt = 100 - (clay + sand)



© Landcare Research New Zealand Limited 2019. Licensed under Creative Commons Attribution - NonCommercial - No Derivative Works 3.0 New Zealand License (BY-NC-ND)



Figure A3.6 Ohin_1 soil report–part 2 (Landcare Research 2019).

Report generated: 12-Jun-2019 from <https://smap.landcareresearch.co.nz>

S-map maps soils at a nominal scale of 1:50,000. At this scale it is common to identify two or more soil siblings that are likely to be present at the selected location. A more detailed resolution is needed to produce map units comprising a single soil sibling. Therefore, it is recommended that users consider the characteristics of each of the identified siblings, the expected proportion of each, and select the S-map sibling that best matches their field observations of the paddock. If no local information is available then it is common practice to select the dominant S-map sibling, i.e. the first listed sibling.

This information sheet describes the typical average properties of the specified soil to a depth of 1 metre, and should not be the primary source of data when making land use decisions on individual farms and paddocks.

Ailsaf

Acid Mesic Organic Soil

Ails_3a.1 (100% of the mapunit at location (1892584, 5815416), Confidence: High)

Key physical properties

Depth class (diggability)	Deep (> 1 m)
Texture profile	Loam Over Peat
Potential rooting depth	30 - 50 (cm)
Rooting barrier	Anoxic conditions
Topsoil stoniness	Stoneless
Topsoil clay range	10 - 15 %
Drainage class	Poorly drained
Aeration in root zone	Limited
Permeability profile	Moderate
Depth to slowly permeable horizon	No slowly permeable horizon
Permeability of slowest horizon	Moderate (4 - 72 mm/h)
Profile available water	(0 - 100cm or root barrier) Very high (258 mm) (0 - 60cm or root barrier) Very high (178 mm) (0 - 30cm or root barrier) Very high (83 mm)
Dry bulk density, topsoil	g/cm ³
Dry bulk density, subsoil	1.42 g/cm ³
Depth to hard rock	No hard rock within 1 m
Depth to soft rock	No soft rock within 1 m
Depth to stony layer class	No significant stony layer within 1 m

Key chemical properties

Topsoil P retention	Medium (37%)
---------------------	--------------

About this publication

- This information sheet describes the *typical average properties* of the specified soil to a depth of 1 metre.
- For further information on individual soils, contact Landcare Research New Zealand Ltd: www.landcareresearch.co.nz
- Advice should be sought from soil and land use experts before making decisions on individual farms and paddocks.
- The information has been derived from numerous sources. It may not be complete, correct or up to date.
- This information sheet is licensed by Landcare Research on an "as is" and "as available" basis and without any warranty of any kind, either express or implied.
- Landcare Research shall not be liable on any legal basis (including without limitation negligence) and expressly excludes all liability for loss or damage howsoever and whenever caused to a user of this factsheet.

Figure A3.7 Ails_3 soil report—part 1 (Landcare Research 2019).

Ailsaf

S-map ref: Ails_3a.1

Ails_3a.1 (100% of the mapunit at location (1892584, 5815416), Confidence: High)

Additional factors to consider in choice of management practices

Vulnerability classes relate to soil properties only and do not take into account climate or management

Soil structure integrity

Structural vulnerability	Low (0.49)
Pugging vulnerability	not available yet

Water management

Water logging vulnerability	High
Drought vulnerability - if not irrigated	Low
Bypass flow	High
Hydrological soil group	B/D
Irrigability	Flat to very gently undulating land with moderate drainage/permeability restrictions and soils with high to very high PAW

Contaminant management

N leaching vulnerability	Very Low
P leaching vulnerability	not available yet
Bypass flow	High
Dairy effluent (FDE) risk category	B
Relative Runoff Potential	Low

Additional information

Soil classification	Acid Mesic Organic Soils
Family	Ailsaf
Sibling number	3
Profile texture group	Peaty
Soil profile material	Organic layered or stony
Rock class of stones/rocks	Not Applicable
Rock origin of fine earth	From Rhyolitic Rock
Parent material origin	Tephra on Peat

Characteristics of functional horizons in order from top to base of profile:

Functional Horizon	Thickness	Stones	Clay*	Sand*
Loamy Weak, Acidic Tephric	14 - 16 cm	0 %	10 - 15 %	40 - 50 %
Sandy SI Firm, Acidic Tephric	8 - 10 cm	0 %	1 - 5 %	75 - 85 %
Organic Humic	4 - 7 cm	0 %	1 - 5 %	40 - 50 %
Stony (lapilli) Loamy Weak, Acidic Tephric	4 - 5 cm	10 - 30 %	10 - 15 %	40 - 45 %
Organic Humic	10 - 12 cm	0 %	0 - 15 %	5 - 20 %
Organic Fibric	50 - 60 cm	0 %	0 %	0 %

* clay and sand percent values are for the mineral fines (excludes stones). Silt = 100 - (clay + sand)



© Landcare Research New Zealand Limited 2019. Licensed under Creative Commons Attribution - NonCommercial - No Derivative Works 3.0 New Zealand License (BY-NC-ND)



Figure A3.8 Ails_3 soil report–part 2 (Landcare Research 2019).

Report generated: 12-Jun-2019 from <https://smap.landcareresearch.co.nz>

S-map maps soils at a nominal scale of 1:50,000. At this scale it is common to identify two or more soil siblings that are likely to be present at the selected location. A more detailed resolution is needed to produce map units comprising a single soil sibling. Therefore, it is recommended that users consider the characteristics of each of the identified siblings, the expected proportion of each, and select the S-map sibling that best matches their field observations of the paddock. If no local information is available then it is common practice to select the dominant S-map sibling, i.e. the first listed sibling.

This information sheet describes the typical average properties of the specified soil to a depth of 1 metre, and should not be the primary source of data when making land use decisions on individual farms and paddocks.

Omeheuf

Acidic Orthic Gley Soil

Omeh_6a.1 (100% of the mapunit at location (1891832, 5815379), Confidence: High)

Key physical properties

Depth class (diggability)	Deep (> 1 m)
Texture profile	Loam
Potential rooting depth	30 - 50 (cm)
Rooting barrier	Anoxic conditions
Topsoil stoniness	Slightly stony
Topsoil clay range	15 - 25 %
Drainage class	Poorly drained
Aeration in root zone	Limited
Permeability profile	Moderate
Depth to slowly permeable horizon	No slowly permeable horizon
Permeability of slowest horizon	Moderate (4 - 72 mm/h)
Profile available water	(0 - 100cm or root barrier) High (245 mm)
	(0 - 60cm or root barrier) Very high (147 mm)
	(0 - 30cm or root barrier) High (74 mm)
Dry bulk density, topsoil	0.94 g/cm ³
Dry bulk density, subsoil	1.38 g/cm ³
Depth to hard rock	No hard rock within 1 m
Depth to soft rock	No soft rock within 1 m
Depth to stony layer class	No significant stony layer within 1 m

Key chemical properties

Topsoil P retention	Medium (38%)
----------------------------	--------------

About this publication

- This information sheet describes the *typical average properties* of the specified soil to a depth of 1 metre.
- For further information on individual soils, contact Landcare Research New Zealand Ltd: www.landcareresearch.co.nz
- Advice should be sought from soil and land use experts before making decisions on individual farms and paddocks.
- The information has been derived from numerous sources. It may not be complete, correct or up to date.
- This information sheet is licensed by Landcare Research on an "as is" and "as available" basis and without any warranty of any kind, either express or implied.
- Landcare Research shall not be liable on any legal basis (including without limitation negligence) and expressly excludes all liability for loss or damage howsoever and whenever caused to a user of this factsheet.

Figure A3.9 Omeh_6 soil report–part 1 (Landcare Research 2019).

Omeheuf

S-map ref: Omeh_6a.1

Omeh_6a.1 (100% of the mapunit at location (1891832, 5815379), Confidence: High)

Additional factors to consider in choice of management practices

Vulnerability classes relate to soil properties only and do not take into account climate or management

Soil structure integrity

Structural vulnerability	High (0.65)
Pugging vulnerability	not available yet

Water management

Water logging vulnerability	High
Drought vulnerability - if not irrigated	Low
Bypass flow	High
Hydrological soil group	B/D
Irrigability	Flat to very gently undulating land with moderate drainage/permeability restrictions and soils with high to very high PAW

Contaminant management

N leaching vulnerability	Very Low
P leaching vulnerability	not available yet
Bypass flow	High
Dairy effluent (FDE) risk category	B
Relative Runoff Potential	Low

Additional information

Soil classification	Acidic Orthic Gley Soils
Family	Omeheuf
Sibling number	6
Profile texture group	Loamy
Soil profile material	Tephric soil
Rock class of stones/rocks	Not Applicable
Rock origin of fine earth	From Rhyolitic Rock
Parent material origin	Tephra

Characteristics of functional horizons in order from top to base of profile:

Functional Horizon	Thickness	Stones	Clay*	Sand*
Loamy Weak, Acidic Tephric	13 - 15 cm	0 %	15 - 25 %	25 - 35 %
Stony (lapilli) Sandy Slightly Firm, Acidic Tephric	12 - 16 cm	5 - 15 %	4 - 5 %	75 - 90 %
Loamy Weak, Acidic Tephric	70 - 75 cm	0 %	20 - 28 %	15 - 23 %

* clay and sand percent values are for the mineral fines (excludes stones). Silt = 100 - (clay + sand)



© Landcare Research New Zealand Limited 2019. Licensed under Creative Commons Attribution - NonCommercial - No Derivative Works 3.0 New Zealand License (BY-NC-ND)



Figure A3.10 Omeh_6 soil report—part 2 (Landcare Research 2019).

Report generated: 12-Jun-2019 from <https://smap.landcareresearch.co.nz>

S-map maps soils at a nominal scale of 1:50,000. At this scale it is common to identify two or more soil siblings that are likely to be present at the selected location. A more detailed resolution is needed to produce map units comprising a single soil sibling. Therefore, it is recommended that users consider the characteristics of each of the identified siblings, the expected proportion of each, and select the S-map sibling that best matches their field observations of the paddock. If no local information is available then it is common practice to select the dominant S-map sibling, i.e. the first listed sibling.

This information sheet describes the typical average properties of the specified soil to a depth of 1 metre, and should not be the primary source of data when making land use decisions on individual farms and paddocks.

Ngakuraf

Typic Orthic Allophanic Soil

Ngak_2a.1 (100% of the mapunit at location (1892024, 5815290), Confidence: High)

Key physical properties

Depth class (diggability)	Deep (> 1 m)
Texture profile	Loam
Potential rooting depth	Unlimited
Rooting barrier	No significant barrier within 1 m
Topsoil stoniness	Slightly stony
Topsoil clay range	8 - 9 %
Drainage class	Well drained
Aeration in root zone	Unlimited
Permeability profile	Rapid
Depth to slowly permeable horizon	No slowly permeable horizon
Permeability of slowest horizon	Rapid (> 72 mm/h)
Profile available water	(0 - 100cm or root barrier) Very high (260 mm)
	(0 - 60cm or root barrier) Very high (158 mm)
	(0 - 30cm or root barrier) Very high (82 mm)
Dry bulk density, topsoil	0.78 g/cm ³
Dry bulk density, subsoil	0.86 g/cm ³
Depth to hard rock	No hard rock within 1 m
Depth to soft rock	No soft rock within 1 m
Depth to stony layer class	No significant stony layer within 1 m

Key chemical properties

Topsoil P retention	High (83%)
---------------------	------------

About this publication

- This information sheet describes the *typical average properties* of the specified soil to a depth of 1 metre.
- For further information on individual soils, contact Landcare Research New Zealand Ltd: www.landcareresearch.co.nz
- Advice should be sought from soil and land use experts before making decisions on individual farms and paddocks.
- The information has been derived from numerous sources. It may not be complete, correct or up to date.
- This information sheet is licensed by Landcare Research on an "as is" and "as available" basis and without any warranty of any kind, either express or implied.
- Landcare Research shall not be liable on any legal basis (including without limitation negligence) and expressly excludes all liability for loss or damage howsoever and whenever caused to a user of this factsheet.

Figure A3.11 Ngak_2 soil report–part 1 (Landcare Research 2019).

Ngakuraf

S-map ref: Ngak_2a.1

Ngak_2a.1 (100% of the mapunit at location (1892024, 5815290), Confidence: High)

Additional factors to consider in choice of management practices

Vulnerability classes relate to soil properties only and do not take into account climate or management

Soil structure integrity

Structural vulnerability	Very low (0.34)
Pugging vulnerability	not available yet

Water management

Water logging vulnerability	Very low
Drought vulnerability - if not irrigated	Low
Bypass flow	Low
Hydrological soil group	A
Irrigability	Rolling land with good drainage/permeability and soils with high to very high PAW

Contaminant management

N leaching vulnerability	Low
P leaching vulnerability	not available yet
Bypass flow	Low
Dairy effluent (FDE) risk category	C
Relative Runoff Potential	Very Low

Additional information

Soil classification	Typic Orthic Allophanic Soils
Family	Ngakuraf
Sibling number	2
Profile texture group	Loamy
Soil profile material	Tephric soil
Rock class of stones/rocks	From Rhyolitic Rock
Rock origin of fine earth	From Rhyolitic Rock
Parent material origin	Tephra

Characteristics of functional horizons in order from top to base of profile:

Functional Horizon	Thickness	Stones	Clay*	Sand*
Loamy Weak, Acidic Tephric	18 - 20 cm	0 %	8 - 9 %	63 - 76 %
Stony (lapilli) Loamy Fine Slightly Firm, Acidic Tephric	70 - 75 cm	20 - 35 %	10 - 16 %	54 - 58 %
Loamy Fine Slightly Firm, Acidic Tephric	5 - 12 cm	0 - 10 %	16 - 17 %	50 - 53 %

* clay and sand percent values are for the mineral fines (excludes stones). Silt = 100 - (clay + sand)



© Landcare Research New Zealand Limited 2019. Licensed under Creative Commons Attribution - NonCommercial - No Derivative Works 3.0 New Zealand License (BY-NC-ND)



Figure A3.12 Ngak_2 soil report-part 2 (Landcare Research 2019).

APPENDIX 4 LYSIMETER SITES PHOTOGRAPHS

A4.1 Substation Site

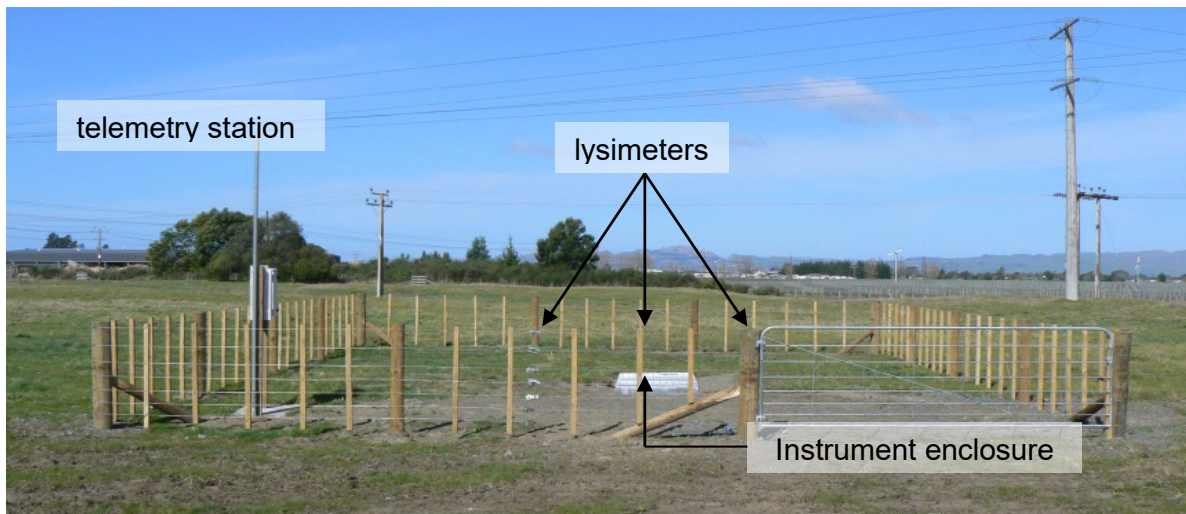


Figure A4.1 Substation lysimeter site in 2013 (White et al. 2014).



Figure A4.2 Substation lysimeter site in April 2019.


A4.2 Collins Lane Site



Figure A4.3 Collins Lane lysimeter site on 09/04/2019.

APPENDIX 5 BORE LITHOLOGICAL LOGS, BOREHEAD PHOTOGRAPHS AND BORE HYDROGRAPHS

A5.1 Substation Site

		<h1>Well 10371</h1>
IDENTIFICATION		WELL INFORMATION
WQ site:	375	Drill date: 18-Nov-74
Easting:	2832439	Driller: Hill Well Drillers Ltd
Northing:	6171204	Casing diameter (mm): 150
Method:	Differential GPS	Bore depth (m): 13.20 Water level access
Owner:	DELEGAT'S WINE ESTATE LTD - Bala	Well depth (m): 13.40 Yes
Address:	P O BOX 305, BLENHEIM	Screen top (m):
		Screen bottom (m):
		Open hole top (m):
		Open hole bottom (m):
Comment:	General remarks : WELL SUB-STATION Measuring point: top of casing Do not confuse with well 10340 Postal "Delegat's Wine Estate Ltd, Cf- Aden Brock, P O Box 305, Blenheim". Phone 03 572 6308. Email aden.brock@delegates.co.nz. Fax 03 5791292 - Contact address verified from christmas mail out feedback form. (20110114)) H&S Review (14/4/10 MD) Vineyard, watch for foot and vehicle traffic.No other obvious hazards were identified.	
CONSENT INFORMATION		
Bore consent:		
Ground-water consent:		
AQUIFER INFORMATION		
Aquifer lithology:	Gravels	Aquifer condition: Unconfined Initial water level (m): 0.00
AQUIFER TEST		
Test date:	18-Nov-74	
Report number:		
Maximum pumping rate (l/s):		
Maximum drawdown (m):		
Duration (hours):		
Number of pumping steps:		
Aquifer thickness (m):		
Transmissivity (m²/d):		
Storativity:		
Hydraulic conductivity (m/d):		
Specific capacity ((l/s)/m):		
Test reliability:	Unreliable	

Disclaimer: Data should be used with caution. Well records are typically from external sources and unverified.

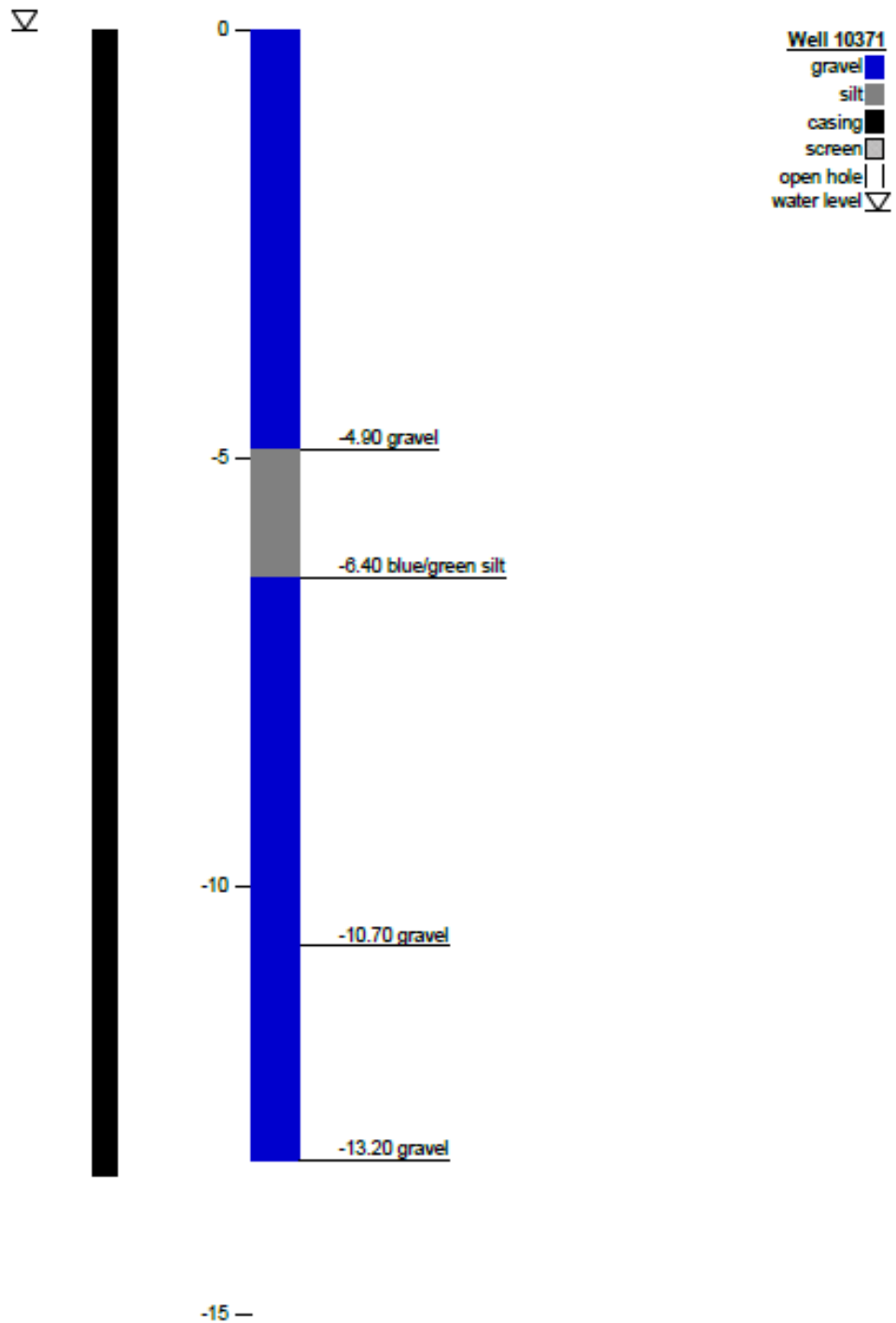




Figure A5.1 Photograph of Well 10371.



Figure A5.2 Hydrograph of Well 10371.

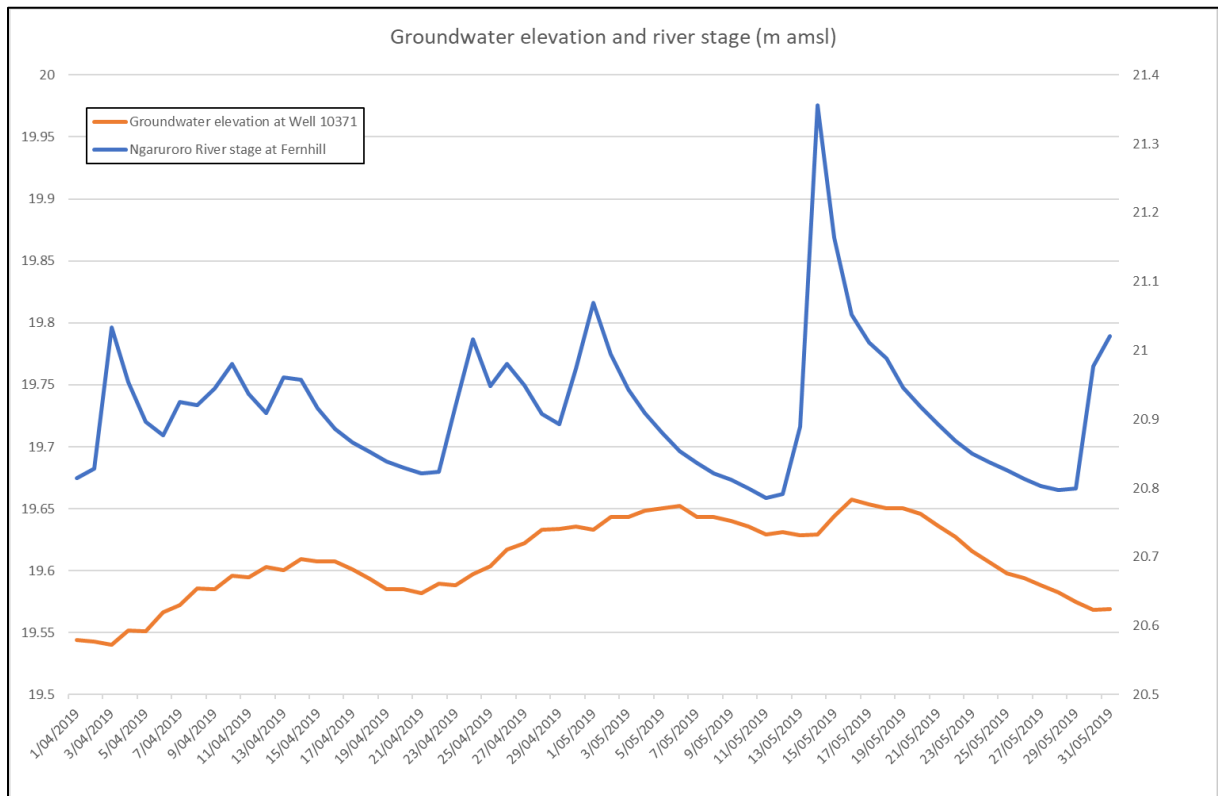


Figure A5.3 Hydrographs of Well 10371 and Ngaruroro River at Fernhill stage site.

A5.2 Collins Lane Site

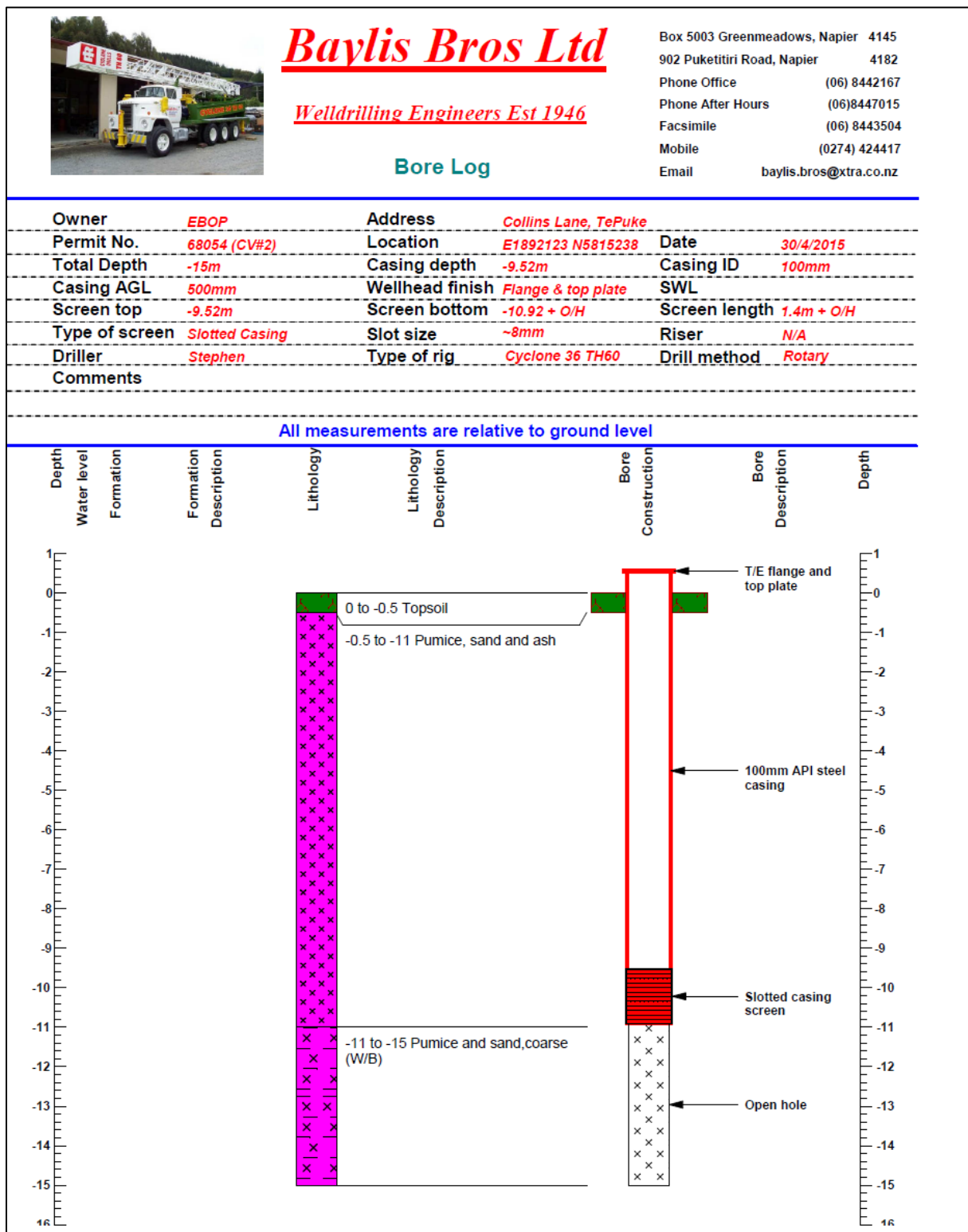




Figure A5.4 Photograph of Bore 1001284.

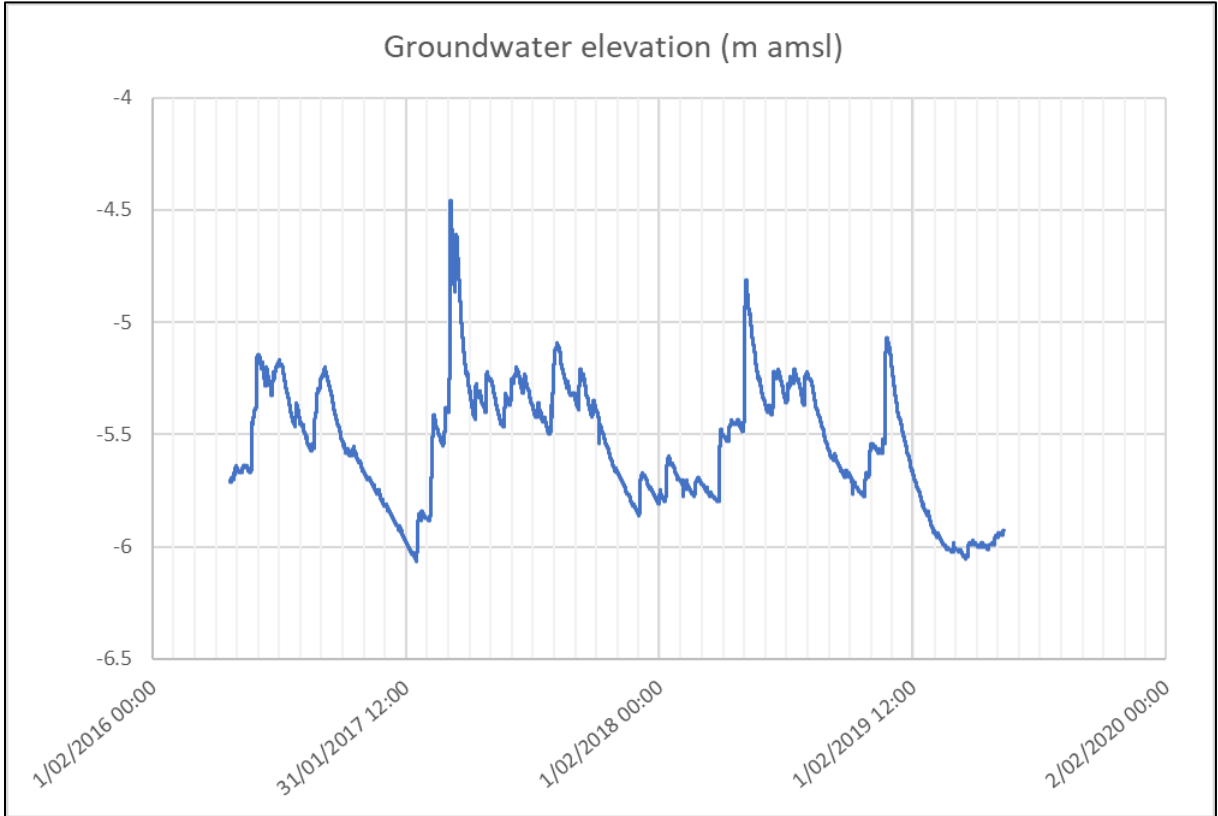


Figure A5.5 Hydrograph of Bore 1001284.

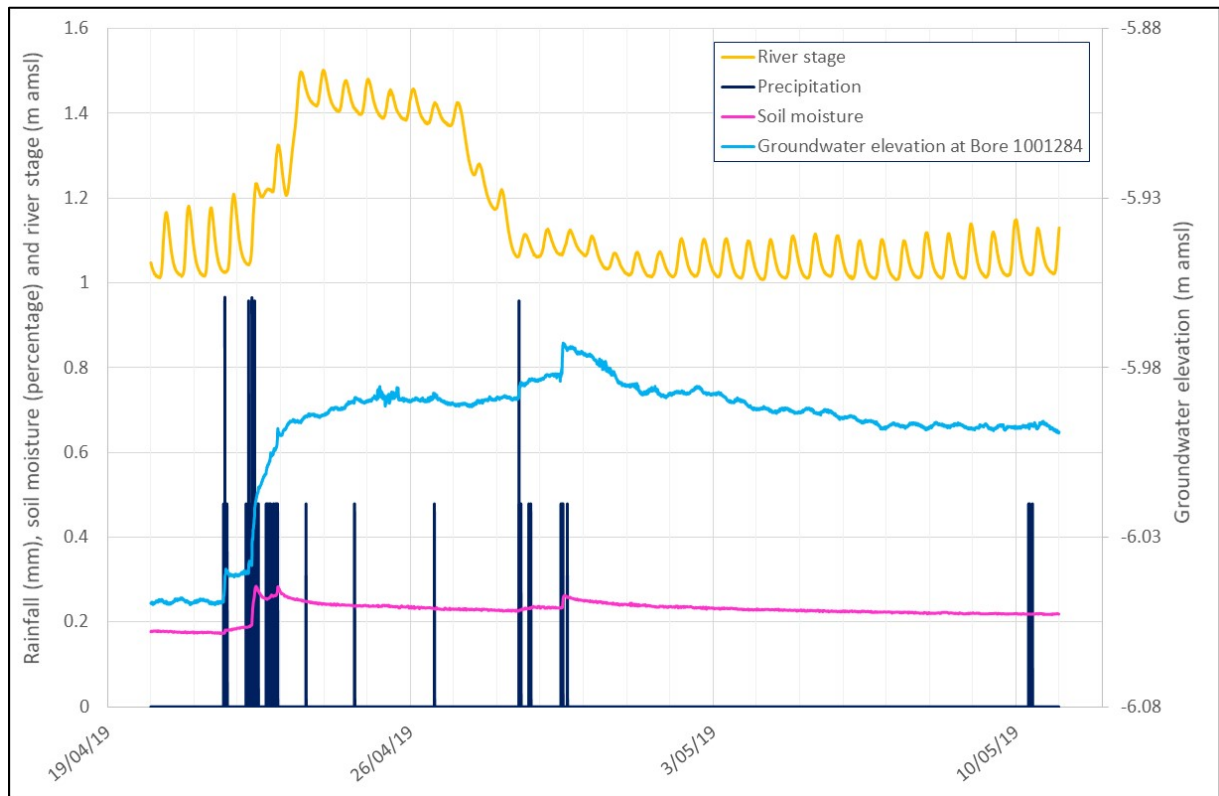


Figure A5.6 Hydrograph of Bore 1001284, Kaituna River at Te Matai stage site, rainfall and soil moisture at Te Puke lysimeter site.

APPENDIX 6 PHOTOGRAPHS OF MATERIAL USED FOR THE UAV IMAGERY COLLECTION

A6.1 Altus LRX UAV and Ground Control Unit



A6.2 Micasense Rededge 3 Multispectral Camera, Attached to an Altus LRX UAV



A6.3 Workswell WIRIS 2nd Gen Thermal Camera, Attached to an Altus LRX UAV



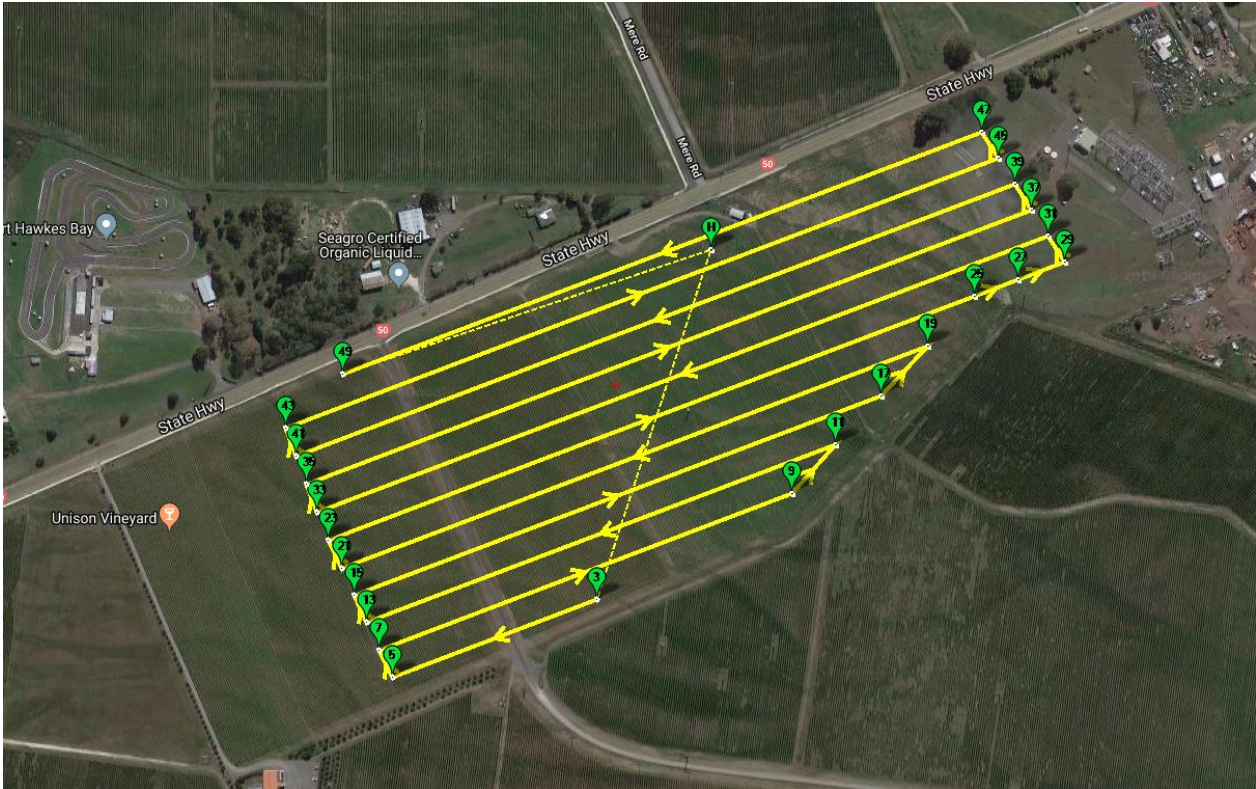
APPENDIX 7 UAV FLIGHT LINES

A7.1 Substation Site

Northern Area



Southern Area



A7.2 Collins Lane Site





www.gns.cri.nz

Principal Location

1 Fairway Drive
Avalon
PO Box 30368
Lower Hutt
New Zealand
T +64-4-570 1444
F +64-4-570 4600

Other Locations

Dunedin Research Centre
764 Cumberland Street
Private Bag 1930
Dunedin
New Zealand
T +64-3-477 4050
F +64-3-477 5232

Wairakei Research Centre
114 Karetoto Road
Wairakei
Private Bag 2000, Taupo
New Zealand
T +64-7-374 8211
F +64-7-374 8199

National Isotope Centre
30 Gracefield Road
PO Box 31312
Lower Hutt
New Zealand
T +64-4-570 1444
F +64-4-570 4657